Transition Metal Manganese and Main Group Gallium Complexes as Catalysts for Alkene Epoxidation

by

Wenchan Jiang

A dissertation submitted to the Graduate Faculty of
Auburn University
in partial fulfillment of the
requirements for the Degree of
Doctor of Philosophy

Auburn, Alabama
May 04, 2012

Approved by

Christian R. Goldsmith, Assistant Professor
David M. Stanbury, Professor
Anne E. V. Gorden, Associate Professor
Eduardus C. Duin, Associate Professor

Department of Chemistry and Biochemistry

Abstract

Epoxides are important organic synthesis precursors and widely used in industry. Alkene epoxidation has been under extensive investigation over decades. Synthetic models have been established for catalytic epoxidations, employing transition and main group metals. Epoxidation proceeds either through high valent metal-oxo species and/or a Lewis acid mechanism for oxygen transfer to substrate. Specifically, by high valent metal-oxo species, Jacobsen's catalyst (Mn^{III}-salen) and non-porphyrin Mn^{II} complexes can catalyze enantioselective epoxidation and electron-rich terminal alkene epoxidation respectively. Sharpless catalyst (Ti^{IV}-tartrate) and Al^{3+} centered complexes catalyze epoxidation through Lewis acid mechanisms.

Manganese complexes with phenanthroline derivatives ([Mn(*R*-phen)$_2$Cl$_2$]Cl, *R* = NH_2, Me, H, Cl, NO_2) as catalysts are reported. The Mn^{II} complexes catalyze epoxidation of a variety of substrates with electron-rich alkenes being favored. The installation of functional groups on the 5-position of phenanthroline ligand plays important roles in influencing catalyst reactivity. The more electron-donating the functional group is, the more reactive it is. The reactivities with different substituent groups on the ligand have been correlated with Hammett constant, which showed a good linear relationship. EPR and spectroscopic studies indicated possible involvement of high valent Mn^{IV}-oxo species which decays quickly under experimental conditions.

Gallium complexes are effective catalysts as well. [Ga(phen)$_2$Cl$_2$]Cl is reported to be the first homogeneous gallium catalyst for alkene epoxidation with peracetic acid. Compared with other group 13 metals, the activity of [Ga(phen)$_2$Cl$_2$]Cl is high with low loading of 1%. The epoxide is the only product, indicating good selectivity. Furthermore, six gallium(III) complexes with N-donor ligands were synthesized to study the mechanism of Ga(III)-catalyzed olefin epoxidation by peracetic acid. Although the complexes with relatively electron-poor phenanthroline derivatives display faster initial reactivity, the Ga(III) complexes with the polydentate pyridylamine ligands appear to be more robust, with less noticeable decreases in their catalytic activity over time. The more highly chelating trispicen and tpen are associated with markedly decreased activity.

Acknowledgement

This dissertation is completed under the supervision of Prof. Christian Goldsmith. I am very grateful for his help all through these years. As my advisor, he has set up an example for me about how to pursue science achievement in a hard working and intellectual way. I leant a lot from his expertise in chemistry. I owe thanks to Prof. David Stanbury, who taught me in two advanced inorganic courses and shared his profound knowledge in helpful research discussion. I extend my thanks to Prof. Anne Gorden, who taught me organic chemistry in my first year and gave me suggestions in my oral defense. I also want to thank Dr. John Gorden who guided me through all of my crystal data collection and analysis. I am indebted to Prof. Evert Duin who taught me biochemistry and helped with EPR experiments and data analysis, and Dr. Yonnie Wu for his assistance with MS experiments and interpretation. I am thankful to Prof. William Robert Ashurst for spending his precious time serving on the committee and providing advice on this dissertation. I appreciate their help and care. I will always remember the friendship I got in my lab with all lab mates Roger (Yu) He, Qiao Zhang, and Meng Yu.

I would like to thank my fiancée Wenting (Lucia) Wang, who moved from Boston to be with me in Auburn and has been supportive all through even during my toughest time. Last but not least, I dedicate this dissertation to my parents, without their support and encouragement I wouldn't even have arrived in the United States to pursue my Ph.D. degree.

Table of Contents

List of Tables

List of Figures

List of Schemes

Chapter 1

Review of Alkene Epoxidation Catalyzed by Main Group and Transition Metal Complexes

1.1 Value and Industrial Production of Epoxides

Epoxides are valuable for their capacity to be converted into a wide range of useful functional groups. Ethylene oxide and propylene oxide are particularly vital to industry. Ethylene oxide is a key precursor for ethylene glycol and surface-active agents.[1] Further polymerization of ethylene glycol leads to polyethylene glycol for detergent use.[2] Propylene oxide is used in the preparation of polyurethane-based plastics. Certain medicinal compounds are either prepared via epoxide intermediates or are themselves epoxides. The HIV protease inhibitor *indinavir* is made from 3,4-epoxytetrahydrofuran.[3] The antibiotic (1*R*,2*S*)-(-)-(1,2)-epoxypropyl phosphonic acid is prepared by the epoxidation of *cis*-1-propenylphosphonic acid.[4-5]

Industrial epoxidation relies heavily on heterogeneous catalysts to accelerate the oxidation of alkenes by dioxygen or other oxidants. In the industrial preparation of ethylene oxide, ethylene is directly oxidized with air or pure oxygen at 230-280 ^{o}C under 10-35 atm in a packed-bed, multitubular reactor.[6-7] Generally, these systems use cesium as a promoter and silver supported on α-Al_2O_3 as a catalyst.[8-9] The activity relies on silver's ability to rapidly adsorb and desorb oxygen.[10-11] Gold has also been used as a catalyst, albeit on different solid supports such as titanium/silicon.[12] Propylene oxide is often produced using a gold catalyst supported on a titanium-containing silicate mesoporous material, with barium serving as a promoter.[13] These reactions have several disadvantages, including the cost of the catalysts, the necessity of high reaction temperatures and pressures, and substantial side-reactivity. The high reaction temperatures, in particular, preclude the use of these systems for the production of more thermally sensitive epoxides.

1.2 Development of Alternative Catalysts for Alkene Epoxidation

Much recent research in the catalysis of olefin epoxidation reactions is directed at identifying and developing cheaper alternatives to the aforementioned silver and gold species that can speed the oxidation of alkenes under milder conditions. Recently investigated

catalysts are remarkably diverse and include both main group and transition metal complexes. Boron,[14] arsenic,[15-16] selenium,[17-19] silicon,[20] and aluminum[21] compounds have been reported to catalyze the epoxidation of alkenes by H_2O_2.

Transition metal complexes have been explored more thoroughly. The successful catalysts can be further classified into two categories, based on whether they contain early or late transition metal ions. In the catalysts that contain early transition metals, such as molybdenum,[22-25] vanadium,[26-29] zirconium,[30] and titanium,[31-34] the metal ions are believed to remain in their highest possible oxidation states during the alkene epoxidation. The metals are believed to accelerate oxygen atom transfer from a metal-oxidant adduct to the substrate by acting as Lewis acids. Late transition metal species used to promote the oxidation of alkenes to epoxides include manganese[35-42] and iron complexes.[43-45] The proposed mechanisms for alkene epoxidation involving these more redox-active metals generally posit higher valent intermediates, such as Mn^{V}=O species, as the active oxidant.[46]

Although O_2 is the most desirable oxygen source due to its ready availability and low cost, it isn't commonly used in specialty epoxidation reactions because of the high free energy barrier for its activation and its involvement in autoxidation-related radical side-reactions.[47] Because of these drawbacks, two-electron terminal oxidants, such as hydrogen peroxide (H_2O_2), isodosylbenzene (PhIO), sodium hypochlorite (NaOCl), *meta*-chloroperoxybenzoic acid (*m*-CPBA), *N*-methyl-morpholine-*N*-oxide,[38] dimethyldioxirane,[48] or peracetic acid (PAA),[42] are used instead.

The remainder of this Chapter will focus on five specific classes of homogeneous catalysts for alkene epoxidation. These have been chosen due to their relevance to the material presented in Chapters 2-4.

1.2.1 Jacobsen's Catalyst

Jacobsen's catalyst consists of a Mn^{III}-salen compound (Figure 1.1) and promotes the enantioselective epoxidation of non-functionalized olefins by either PhIO or NaOCl.[49-51] Sample illustrative reactions are summarized in Table 1.1.

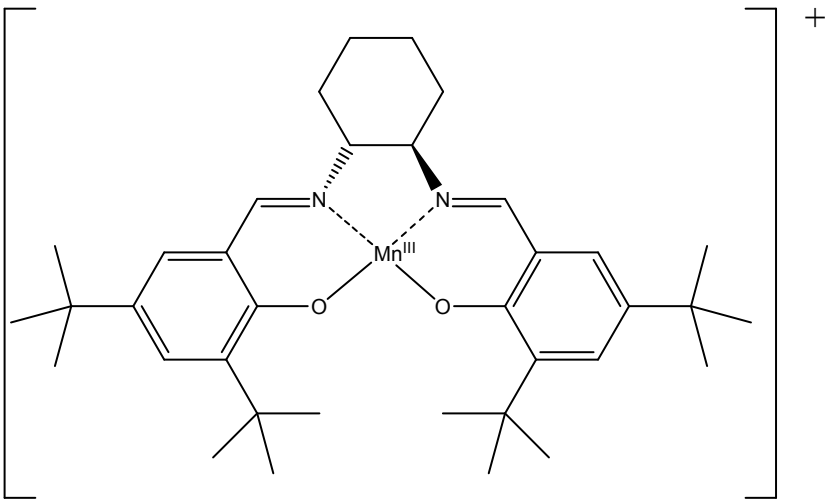

Figure 1.1 Structure of the prototypical Jacobsen catalyst[37]

Table 1.1 Asymmetric epoxidation of representative olefins by Jacobsen's catalyst[a]

entry	olefin substrate	yield (%)[b]	ee (%)[c]	equiv of catalyst required for complete reaction
1	Ph, Me	84	92	0.04
2	*p*-ClC$_6$H$_4$, Me	67	92	0.04
3	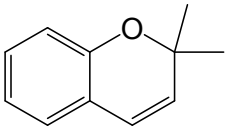	72	98	0.02
4	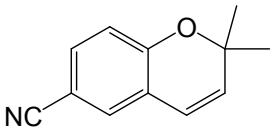	96	97	0.03
5	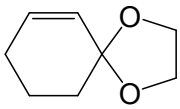	63	94	0.15
6[d]	Ph, CO_2Me	65[e]	89	0.10

[a]Reactions were run at 4 °C in CH_2Cl_2 with 0.25 mmol catalyst and 12.5 mmol substrate. [b]Isolated yield based on olefin. [c]Enantiomeric excess. [d]Reaction carried out in the presence of 0.4 equiv of 4-phenylpyridine N-oxide. [e]Yield determined by GC. All data are from reference 35.

Several trends were noted in the studies of Jacobsen's catalyst and its close derivatives. First, electron-donating and withdrawing substituents on substrates influence both the *cis*/*trans* selectivity and the rate of the reaction, as summarized in Scheme 1.1. With the more electron-rich alkenes, the *cis*-epoxide product forms preferentially. It is hypothesized that electron-withdrawing groups stabilize radical intermediates that can form when the substrate binds to the Mn^{V}-oxo center. This facilitates C-C bond rotation necessary for the formation of *trans*-epoxides (Scheme 1.2).

R = Me X	*cis*-epoxide/ *trans*-epoxide
OCH_3	11.7
CH_3	7.0
H	5.7
CF_3	0.80
NO_2	0.27

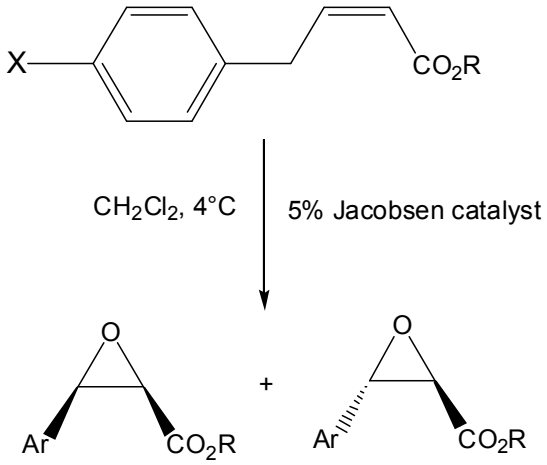

Scheme 1.1 Substituent effects on stereoselectivity

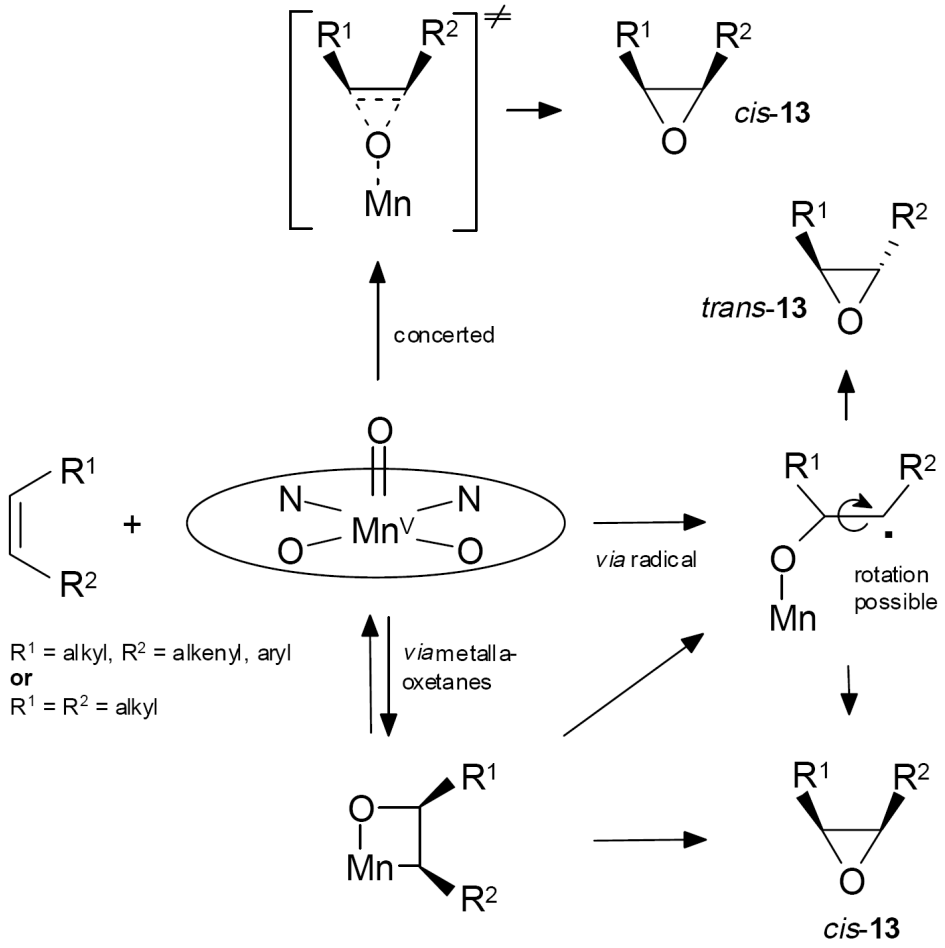

Scheme 1.2 Possible pathways for epoxidation catalyzed by Jacobsen's compound[46]

The *cis*/*trans* ratios of the stilbene oxides produced by the oxidation to stilbene by various iodosylbenzene derivatives were found to be dependent on the terminal oxidant.[52] The results suggest at least partial coordination of an equiv of terminal oxidant in the active oxidant, as opposed to the sole agency of a Mn^{V}=O species.

The counterion also modulates the *cis*/*trans* ratio of the epoxide products.[53] In the epoxidation of *cis*-stilbene, $[Mn(salen)]^{+}$ catalysts with strongly coordinating counteranions favor *trans*-stilbene oxide as the major product, whereas non-ligating couteranions are associated with the preferential formation of *cis*-stilbene oxide.[54] Computational studies suggest the involvement of different Mn^{V}=O spin-states, which are stabilized by coordinating ligands to varying degrees.[55-56]

The salen ligand in Jacobsen's first epoxidation catalyst is chiral, opening the possibility for chiral epoxide products from prochiral alkenes. The enantioselectivity of Mn^{III}(salen)-catalyzed asymmetric epoxidation is directly correlated to the electronic character of the ligand, with more strongly electron-donating ligands resulting in higher enantiomeric excesses. The ratio of enantiomers for the epoxidation of 2,2-dimethylchromene and *cis*-β-methylstyrene can be fit to a Hammett plot (Scheme 1.3).[36] Jacobsen and co-workers proposed that the ligand's electron-withdrawing groups enable the Mn(V) oxo to react with the substrate in an earlier transition state, which reduces the selectivity. Electron-donating groups, conversely, stabilize the Mn(V) oxidant, allowing a later transition state and higher enantioselectivity.[57]

Much effort has been spent towards evaluating the mechanism of the Jacobsen epoxidation. Four mechanisms have been proposed (Scheme 1.2 and Scheme 1.4). In the first proposed mechanism, the olefin substrate reacts directly with the Mn^{V}-oxo oxidant, proceeding through a transition state resembling a manganese-bound epoxide. Due to the concerted nature of this pathway, the oxygen atom transfer results in exclusively *cis*-epoxides. In the second proposed mechanism, metallaoxetane species result from the reaction between the alkene and the Mn(V) species. The subsequent release of the product from the organometallic intermediate can either occur in a single concerted step, resulting in *cis*-epoxides, or in two steps, which can allow the formation of *trans*-epoxides. In the third pathway, the Mn^{V}-oxo oxidant adds to the alkene as a radical species. The alkyl radical can rotate freely around the former C=C bond, allowing both *cis*- and *trans*-epoxides. The fourth pathway (pathway 2 in Scheme 1.4) differs from the previous three in that it does not involve oxidation or reduction of the manganese center.[54] Instead, the manganese serves as a Lewis acid, analogous to what has been proposed for early transition metal-containing catalysts for olefin epoxidation. The relevant oxidant in this pathway is a Mn^{III} adduct with the terminal oxidant (OLG in Scheme 1.4).

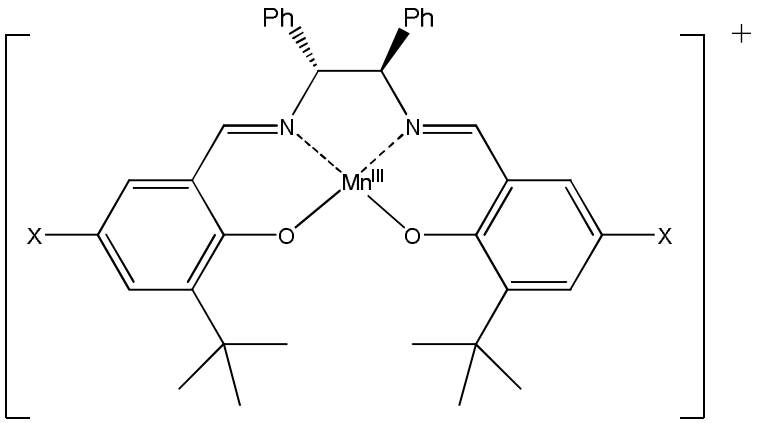

a: X = OMe
b: X = Me
c: X = H
d: X = Cl
e: X = NO_2

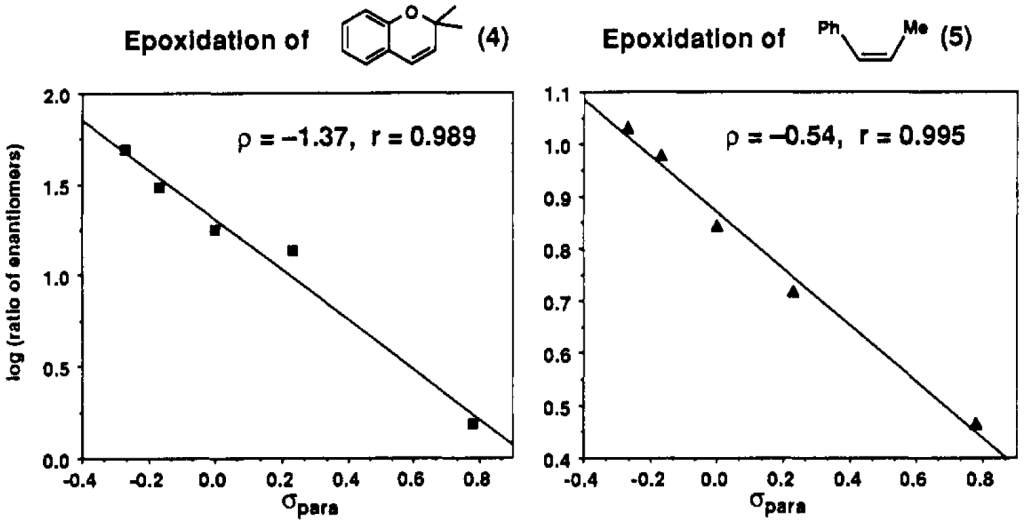

Scheme 1.3 Hammett plots depicting enantiomeric ratios of epoxides generated with catalysts with various electronically modified ligands. Data from reference 34.

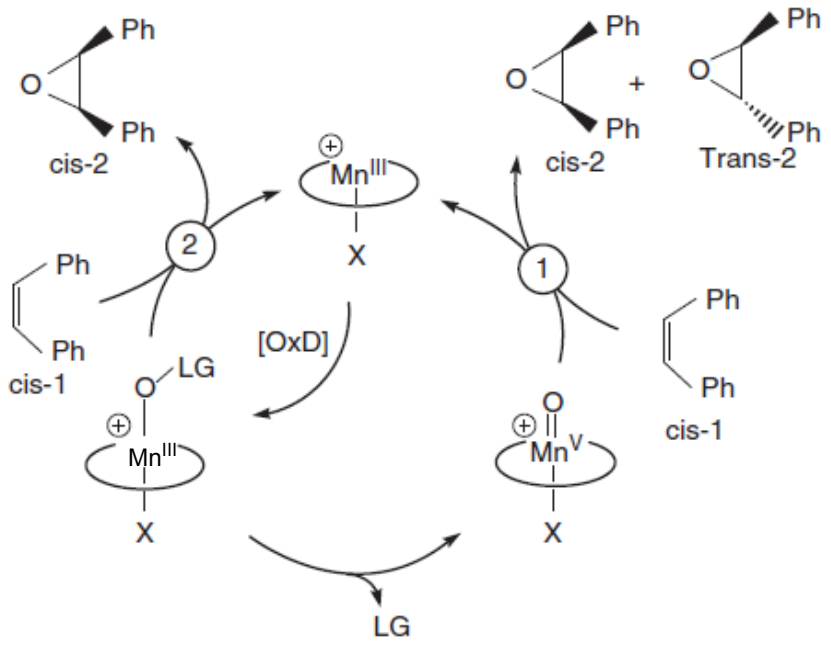

Scheme 1.4 Parallel Lewis acid and redox pathways for $[Mn(salen)]^+$ catalyzed epoxidations.

1.2.2 Manganese Complexes with Neutral, Polydentate N-Donors

Manganese can also catalyze alkene epoxidation when bound to neutral N-donor ligands. Unlike the aforementioned salen complexes, the metal starts in the +2, rather than +3, oxidation state. Another key difference from the aforementioned salen complexes is that the tetradentate ligand does not coordinate the metal in a square planar fashion.

Stack *et al* evaluated the epoxidation performance of a variety of Mn^{II} complexes, finding $[Mn^{II}(R,R\text{-mcp})(CF_3SO_3)_2]$ to be the most active catalyst (Figure 1.2).[41] Within 5 min, $[Mn^{II}(R,R\text{-mcp})(CF_3SO_3)_2]$ efficiently catalyzes the epoxidation of a wide range of terminal olefins by PAA (Table 1.2), with turnover frequencies as high as 250 min^{-1}. The reactivity proceeds with a catalyst loading as low as 0.1 mol%.[41] Although terminal alkenes can be oxidize, electron-rich olefins are preferentially oxidized.

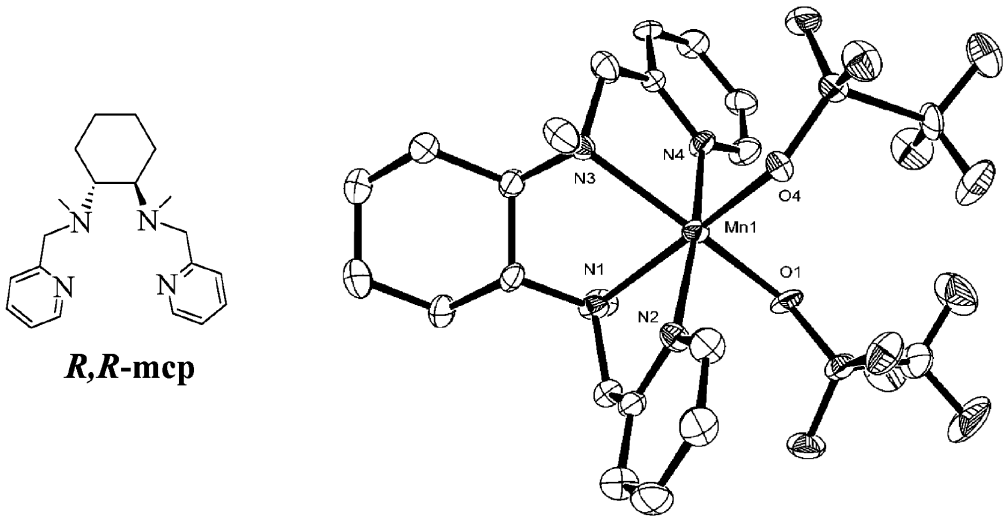

Figure 1.2 The molecular structure of the *R,R*-mcp ligand and the crystal structure of $[Mn^{II}(R,R\text{-mcp})(CF_3SO_3)_2]$.[41]

Table 1.2 Epoxidations catalyzed by $[Mn^{II}(R,R\text{-mcp})(CF_3SO_3)_2]$ with PAA[a]

	alkene	mol % **1**	oxidant (equiv)	GC yield[b]	isolated yield[c]
1	cyclooctene	0.1	1.2	99 (1)	90 (4)[d]
2	cyclohexene	0.1	1.2	98 (2)	85 (2)
3	1-methyl-cyclohexene	0.1	2	92 (3)	
4	*cis*-2-heptene	0.1	1.2	99 (1)[e]	
5	*trans*-2-heptene	0.1	1.2	99 (1)[f]	
6	2-methyl-1-pentene	0.1	1.2	97 (1)	
7	1-heptene	0.1	1.2	95 (3)	89 (3)
8	vinyl cyclohexane	0.1	1.2	99 (1)	90 (2)
9	allyl acetate	0.1	2	89 (3)	
10	methyl methacrylate	0.2	1.2	98 (1)	86 (6)
11	2-cyclohexen-1-one	0.5	1.2	97 (4)	88 (2)
12	ethyl sorbate[g]	0.1	1.2	94 (4)[h]	
13	*cis*-β-methylstyrene	1.0	1.2	90 (1)	
14	*trans*-β-methylstyrene	1.0	1.2	97 (1)	
15a	*R*-(−)-carvone	0.5	3	98 (1)[i]	88 (2)[i]
15b	*R*-(−)-carvone	0.5	1	97 (2)[j]	91 (2)[j]

[a]General reaction conditions: $[olefin]_o$ = 0.50 M, MeCN, 25 °C. Yields measured at 5 min. [b]Yields determined by GC. The numbers in parentheses represent a standard deviation of a minimum of three experiments. [c]Isolated yields, 1 g scale. [d]0.25-mol scale, 88% yield. [e]98% *cis*-epoxide, 2% *trans*-epoxide. [f]97% *trans*-epoxide, 3% *cis*-epoxide. [g]*trans,trans*-$CH_3CH_2{=}CH_2CH_2{=}CH_2\text{-}CO_2CH_2CH_3$. [h]4:1 mixture of 4,5-monoepoxide and 2,3-monoepoxide. [i]0 °C, diepoxide product, 20% disastereoselectivity. [j]-20 °C, *R*-carvone-8,9-monoepoxide, 15% disastereoselectivity. All data are from reference 41.

In subsequent research, the influence of the solvent's acidity and the catalyst's ligand structure were further explored.[40, 42] The pH greatly impacts the catalyst reactivity, and the addition of $HClO_4$ slows the initial reaction rate. Conversely, the use of a less acidic grade of PAA results in faster reactivity and higher turnover numbers. The inhibitory effect of acid is attributed to the protonation of the N-donor ligand, which promotes its dissociation from the metal center. Various Mn^{II} salts (e.g. $MnCl_2$, $Mn(CF_3SO_3)_2$) are not competent catalysts for olefin epoxidation in the absence of the N-donor ligand. Neutral, tetradentate N-donor ligands capable of binding Mn(II) in a *cis*-α conformation best support the reactivity. The availability of *cis* vacant coordination sites associated with this conformation is believed to facilitate activation of the PAA.[40]

Electron paramagnetic resonance (EPR) studies were unable to identify high valent manganese species during the catalysis; the EPR spectrum appears unchanged from the Mn(II) starting material after the addition of oxidant. However, this does not necessarily preclude the possible involvement of such high valent intermediates, which simply may not accumulate to detectable levels. The possible contribution of a Lewis acid mechanism was tested by analyzing the reactivity of the redox-inactive $[Zn^{II}(R,R\text{-mcp})]^{2+}$. The Zn(II) complex could not catalyze the oxidation of alkenes, suggesting that the manganese is accelerating the reactivity through alternative pathways, at least for the *R,R*-mcp system.[41]

As with the manganese-salen complexes, multiple mechanistic pathways have been proposed for the Mn(II)-catalyzed olefin epoxidations (Scheme 1.5).[58] The leftmost pathway has the manganese remaining in the +2 oxidation state, with a Mn(II)-oxidant adduct transferring an oxygen atom to the substrate. Here, the Mn(II) is simply acting as a Lewis acid. The middle pathway features the Mn(II) being oxidized to a Mn^{IV}=oxo intermediate that oxidizes the substrate. Upon the oxygen atom transfer, the manganese gets reduced back to the +2 oxidation state. The oxygen atom transfer can occur in either a single concerted step or in two steps, analogous to that depicted for the manganese salen complexes in Scheme 1.2. In the rightmost pathway, the Mn^{IV}=oxo intermediate acts as a Lewis acid activator, binding an additional equiv of oxidant, which provides the transferred oxygen atom. The high-valent manganese oxo species does not change its +4 oxidation state during the actual catalysis.

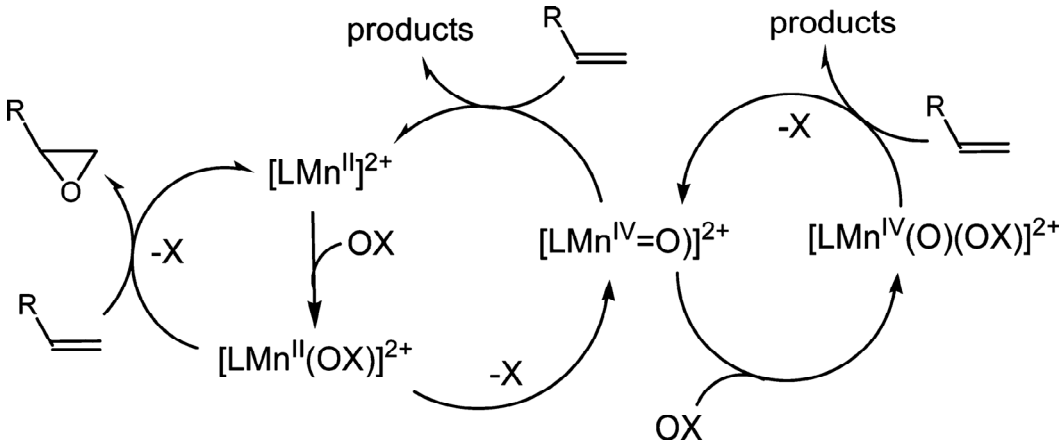

Scheme 1.5 Possible mechanistic pathways for Mn(II)-catalyzed olefin epoxidation.[58]

1.2.3 Non-Heme Iron Complexes

Many non-heme iron complexes have been found to accelerate the epoxidation of alkenes by H_2O_2. White et al., for instance, found that the complex of Fe(II) with the tetradentate ligand *N,N'*-dimethyl-*N,N'*-bis(2-pyridylmethyl)-ethane-1,2-diamine (mep, Figure 1.3) could catalyze the epoxidation of a wide variety of substrates, including terminal olefins, in under 5 min with isolated yields ranging from 60-90% (Table 1.3).[45] They crystallized a μ-oxo, carboxylate bridged diiron(III) complex (Figure 1.3) from the reaction between the Fe^{II}-mep precursor, H_2O_2, and acetic acid. Whether this species is catalytically relevant remains unresolved .

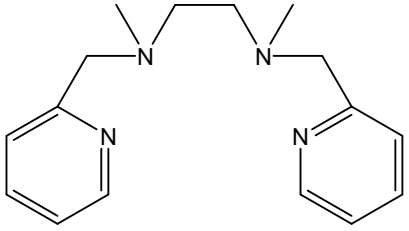

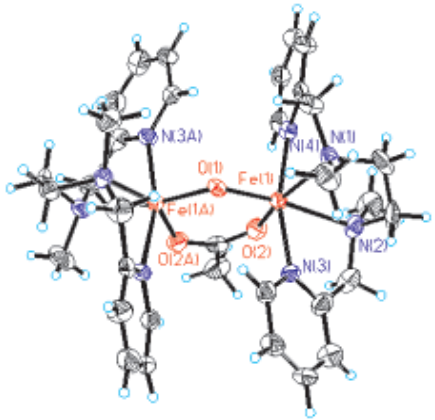

Figure 1.3 Illustration of the mep ligand (left) and the crystal structure of dinuclear $[Fe_2(\mu\text{-}O)(\mu\text{-}CH_3CO_2)(mep)_2]^{3+}$ cation.[45]

Table 1.3 Epoxidations catalyzed by $[Fe(mep)(CF_3SO_3)_2]$[a]

Entry	Substrate	Isolated Yields[b] (GC yield)[c]
1	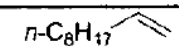	85%
2	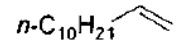	90%[d]
3	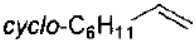	76%[e]
4		63%[f]
5		61%[g]
6	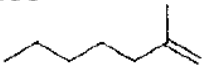	77%
7	cyclooctene	86%
8		87%
9	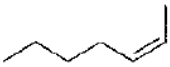	80% (90%)
10		85% (90%)

[a]Reaction conditions: olefin (2.0 mmol, 0.16 M in MeCN), mononuclear precursor (3.0 mol %), CH_3CO_2H, H_2O_2 (aqueous 50 wt %, 3.0 mmol, 1.5 M in MeCN, added dropwise over 2 min), 4 °C, 5 min. [b]Isolated yields based on an average of 3 runs. [c]GC yields were determined using nitrobenzene as an internal standard for especially volatile substrates. [d]Reaction carried out at $[olefin]_o$ = 0.13 M due to poor solubility in MeCN. [e]5 mol % mononuclear precursor. [f]1.5 mol % mononuclear precursor/1.5 mol % CH_3CO_2H. [g]6 mol % CH_3CO_2H. Data from Reference 45.

Beller et al. prepared a catalyst *in situ* using $FeCl_3 \cdot 6H_2O$ as the iron source and a protonated pyridine-2,6-dicarboxylate (H_2Pydic) ligand which was proposed to mimic the carboxylate and histidine groups in the coordination sphere of a non-heme dioxygenase.[59] Their system showed excellent reactivity and selectivity towards terminal and 1,2-disubstituted aromatic olefins and moderate reactivity towards 1,3-dienes at room temperature (Table 1.4).

Table 1.4 Summary of epoxidation scope catalyzed by Beller's *in situ* Fe^{III} complex[a]

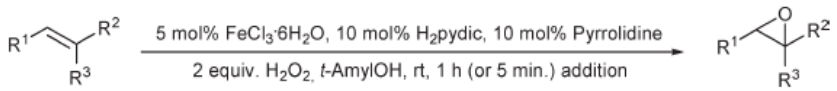

Entry	Substrate	Conv. (%)[a,b]	Yield (%)[b]	Selectivity (%)[c]
1	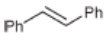	100	97	97
2		98[d]	96[d]	98[d]
3	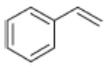	94	93	99
4		88[d]	69[d]	78[d]
5	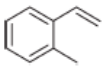	100	97	97
6		88[d]	87[d]	99[d]
7	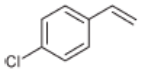	100	77	77
8		100[d]	79[d]	79[d]
9	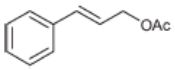	71	69	97
10	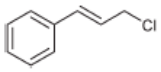	77	63	82
11	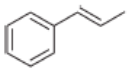	100	95	95
12	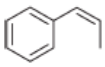	75	56[e]	75
13	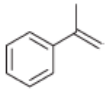	93	64	69
14		77	65	84

[a]Reaction procedure: in a 25 mL Schlenk tube, $FeCl_3.6H_2O$ (0.025 mmol), H_2pydic (0.025 mmol), tert-amyl alcohol (9 mL), pyrrolidine (0.05 mmol), olefin (0.5 mmol) and dodecane (GC internal standard, 100 mL) were added in sequence at RT in air. To this mixture, a solution of 30% H_2O_2 (114 mL, 1.0 mmol) in tert-amyl alcohol (886 mL) was added over a period of 1 h (or 5 min) at RT by a syringe pump. [b]Conversion and yield were determined by GC analysis. [c]Selectivity refers to the ratio of yield to conversion as percentage. [d]The oxidant was added over a period of 5 min. [e]19% trans-β-methylstyrene oxide was observed. Data from Reference 59.

The coordination geometry of the ligand strongly impacts the activity of iron catalysts. Catalysts with pentadentate ligands are found to have inferior stereoselectivity and epoxidation efficiency,[60] whereas systems containing tetradentate ligands with a proclivity for binding metal ions in *trans* conformations generally lead to better reactivity.[61-62] The counteranions on the metal salt also influence the activity, similar to what was observed for the manganese-salen systems. In a study of iron compounds with tetradentate N-donor ligands, increasing the amount of chloride present in solution decreases the alkene

epoxidation.[62] Weakly coordinating anions like triflate and hexafluoroantimonate, conversely, lead to enhanced activity.

In the epoxidation catalyzed by non-heme Fe(II) catalysts, two high-valent iron-oxo oxidants have been proposed: Fe^{V}=O and Fe^{IV}=O. The agency of Fe^{V}=O species was suggested as a means to explain how ^{18}O atoms from added $H_2{}^{18}O$ were incorporated into the epoxide products.[62-63] Such species have not, however, been isolated and spectroscopically characterized. Fe^{IV}=O species, conversely, are stable enough to be structurally and spectroscopically studied.[64-66] Consequently, Fe(IV) species are currently believed to be more plausible intermediates (Scheme 1.6).

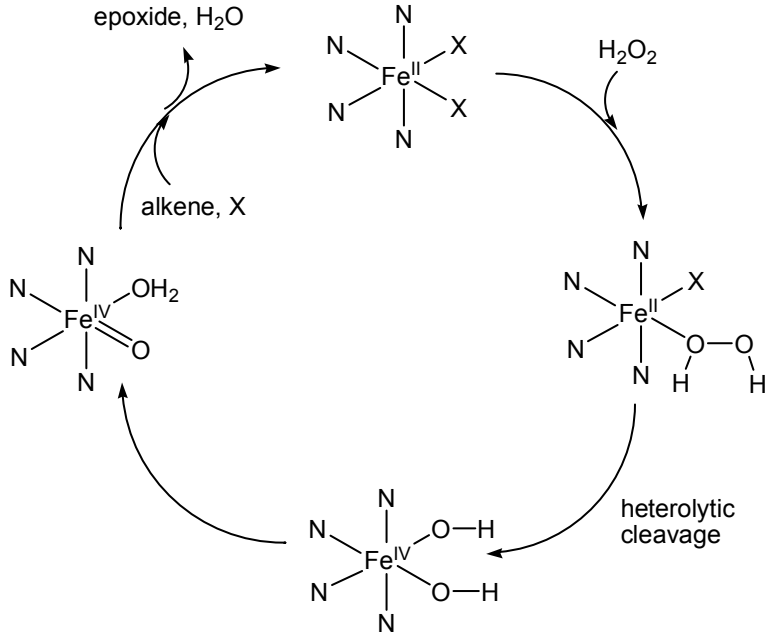

Scheme 1.6 Proposed catalytic cycle for non-heme iron catalyzed epoxidation.

1.2.4 The Sharpless Catalyst

Sharpless used a mixture of titanium(IV) tetraisopropoxide (Ti(O*i*-Pr)$_4$), (+/-)diethyl tartrate, and *t*-BuOOH to catalyze the asymmetric epoxidation of olefins.[31-32] The major species in the titanium-tartrate mixture is a dimeric species (Figure 1.4), as supported by mass spectrometry, NMR, and IR measurements.[33]

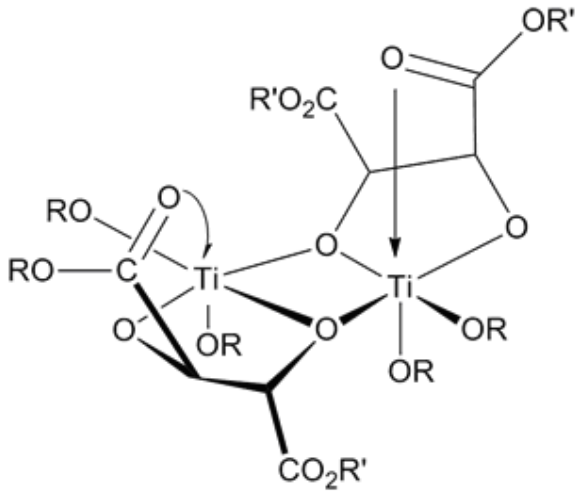

Figure 1.4 The dimeric structure of the Sharpless catalyst.[33]

The Ti(IV) complex catalyzes the oxidation of a variety of substrates by *t*-BuOOH. (Table 1.5).[31] The enantioselectivity is determined by the given tartrate enantiomer and is not dependent on the substituents on the allylic alcohol skeleton.

The proposed mechanism of the Sharpless epoxidation is shown on Scheme 1.7. There are several key features about this route: 1) both the substrate and terminal oxidant bind to the Ti(IV) as ligands; 2) the tartrates direct the bound oxidant towards the face of the C=C bond, accounting for the observed enantioselectivity; 3) the epoxide and *t*-BuO group dissociate from Ti(IV) center to complete the catalytic cycle; 4) the titanium remains in the +4 oxidation state, and the redox-activity is limited to the two transiently bound ligands.

Table 1.5 Selected asymmetric epoxidation of allylic alcohols[a]

Allylic Alcohol	Epoxyalcohol	% yield[b]	% e.e.[c]	Configuration
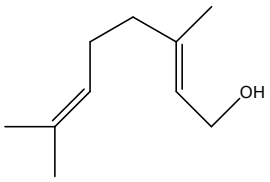	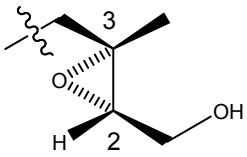	77	95	2 (*S*), 3 (*S*)
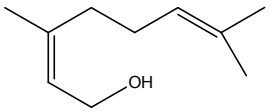	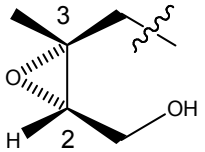	79	94	2 (*S*), 3 (*R*)
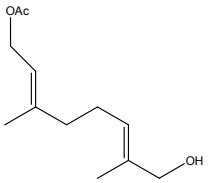	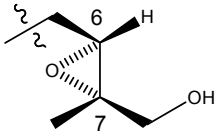	70	>95	6 (*S*), 7 (*S*)
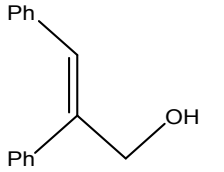	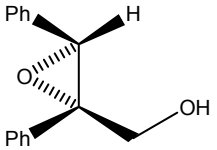	87	>95	2 (*S*), 3 (*S*)
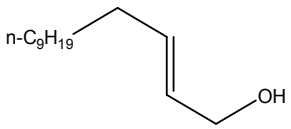	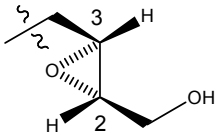	79	>95	2 (*S*), 3 (*S*)
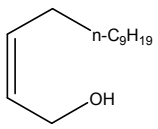	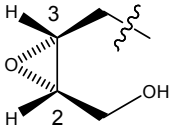	82	90	2 (*S*), 3 (*R*)
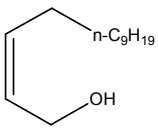	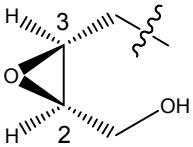	80	90	2 (*R*), 3 (*S*)
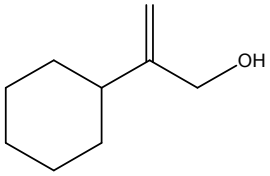	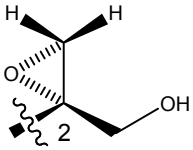	81	>95	2 (*S*)

[a]5%-10% catalyst loading, -20 °C. [b]Isolated yield. [c]Enantiomeric excess determined by ^{1}H NMR on the corresponding epoxy acetates. Data from Reference 31.

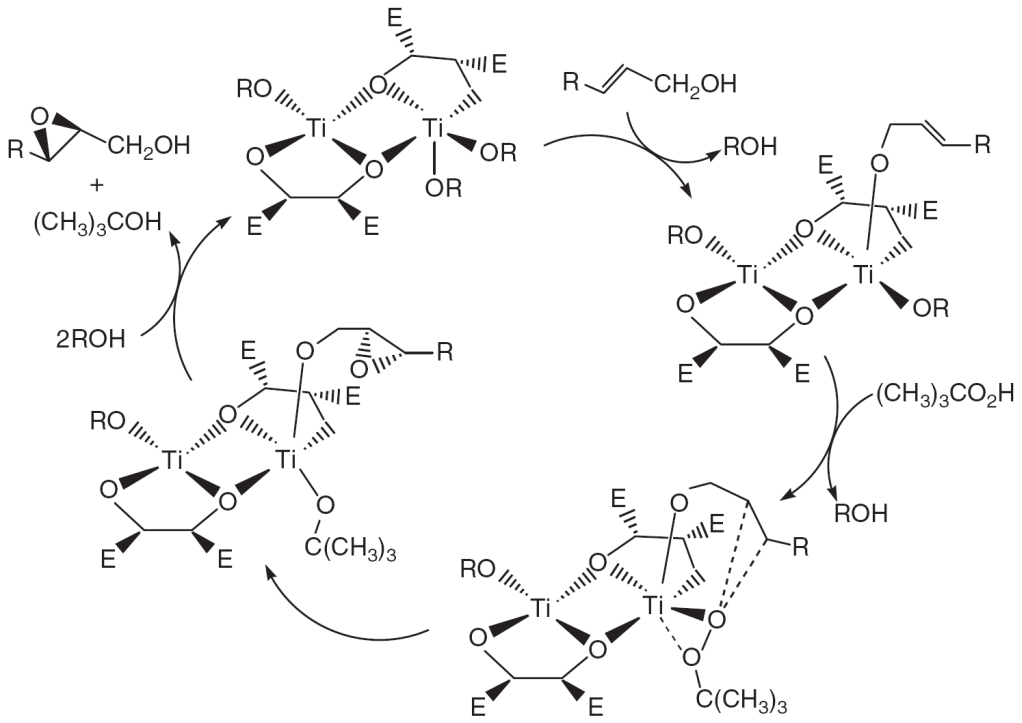

Scheme 1.7 Proposed mechanism for Sharpless epoxidation (E refers to ester group).[67]

1.2.5 Homogenous Aluminum Catalysts

Although aluminum is typically not redox-active, it can support modest alkene epoxidation catalysis. Valentine used [Al^{III}(porphyrin)]Cl to promote the epoxidation of stilbene and cyclohexene by PhIO, with up to 9.3 turnovers.[61] More recently, mixtures of $[Al(H_2O)_6]^{3+}$ and H_2O_2 in MeCN-H_2O were reported to catalyze the epoxidation of α, β-unsaturated ketones (Table 1.6).[68] Much like the aforementioned Sharpless epoxidation, Al(III) catalysis is proposed to proceed through pathways that do not involve metal-centered redox or high-valent metal oxo intermediates.

Table 1.6 Epoxidation of α, β-unsaturated ketones by $[Al(H_2O)_6]^{3+}/H_2O_2$

Substrate	Main product	T (°C)	Oxid.	5 h		24 h	
				C (%)	S (%)	C (%)	S (%)
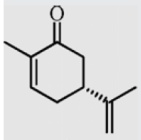 1	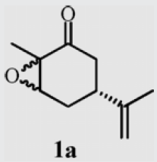 1a	80	H_2O_2 30%	21	74	75	45
			H_2O_2 70%	78	81	93	56
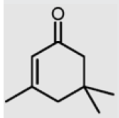 2	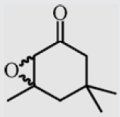 2a	60	H_2O_2 30%	13	13	21	3
			H_2O_2 70%	38	30	49	29
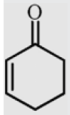 3	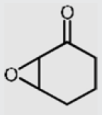 3a	25	H_2O_2 30%	29	33	79	22
			H_2O_2 70%	82	22	88	1

C: conversion, S: selectivity. Reaction conditions: substrate (25 mmol), di-n-butylether (internal standard, 12.5 mmol), 70 wt.% H_2O_2 (56 mmol), $Al(ClO_4)_3 \cdot 9H_2O$ (0.5 mmol), THF (solvent), at the temperature indicated in this table. Data from Reference 68.

The reactivity of (*R*)-carvone (compound 1 in Table 1.6) is used to assess the electronic character of the active oxidant. (*R*)-Carvone has two C=C bond sites. The external C=C bond is most nucleophilic, whereas the ring olefin is more electrophilic, as supported by DFT calculations. Epoxidation exclusively occurs at the ring C=C bond site, suggesting a nucleophilic oxidant, e.g. HOO^- derived from H_2O_2. This differs from most transition metal-based systems, which prefer to oxidize more electron-rich olefins.

A Sharpless-type mechanism is proposed, based on DFT calculations (Scheme 1.8).[21] Much like the aforementioned Ti(IV) catalysis, the oxidant binds to the Al(III) center as a ligand, and the Al(III) serves to activate the oxidant through its Lewis acidity. The substrate is subsequently oxidized by the bound H_2O_2, generating the epoxide and H_2O as a by-product. The $[Al(H_2O)_6]^{3+}/H_2O_2$/MeCN-H_2O system requires elevated temperatures and long reaction times, particularly relative to the aforementioned transition metal catalysts. Additionally, the reactivity becomes less selective as the catalyst degrades, leading to increasingly large amounts of side-products such as diols.

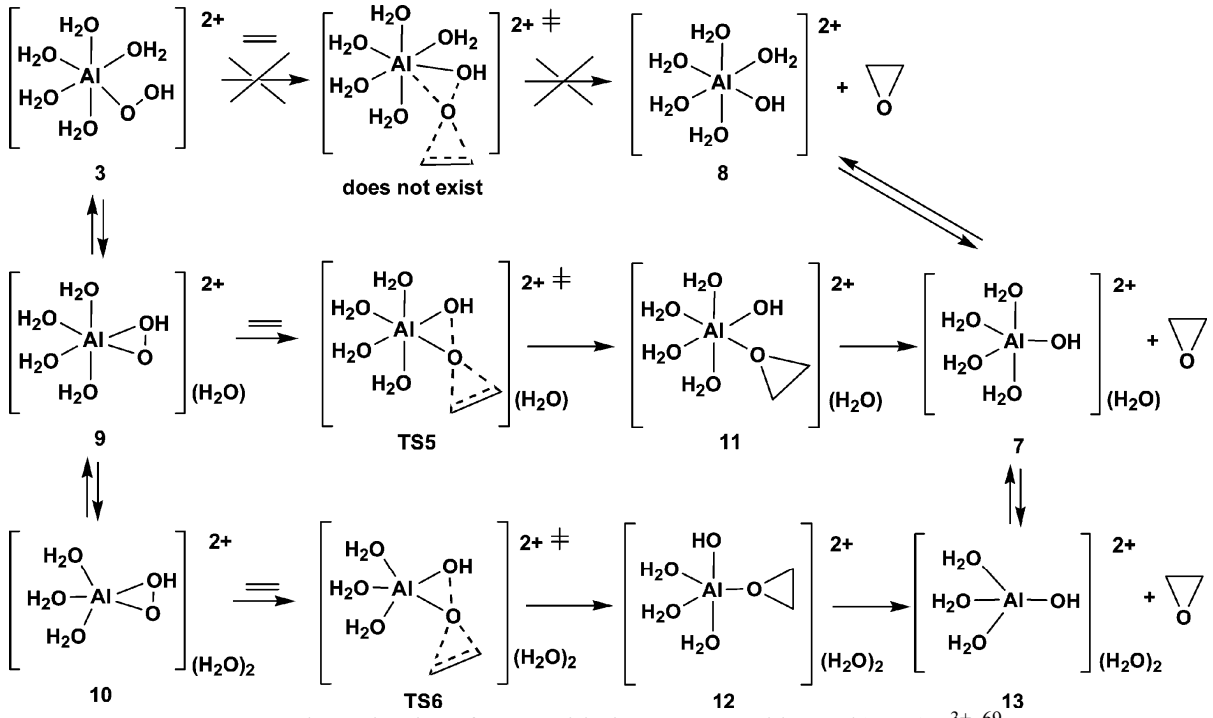

Scheme 1.8 Proposed mechanism for epoxidation promoted by $[Al(H_2O)_6]^{3+}$.[69]

1.3 Summary

In Chapter 2 of this thesis, we use Mn(II) complexes with phenanthroline derivatives to assess the influence of the ligand's electronic character on Mn(II)-catalyzed alkene epoxidation. We also study the impact of acidity on the epoxidation reactivity. In Chapters 3 and 4, we study olefin epoxidation catalyzed by Ga(III) complexes with various N-donor ligands. We systematically explore how the ligand influences the reactivity in Chapter 4.

References

(1) Ullmann's Encyclopedia of Industrial Chemistry, Sixth Edition, John Wiley & Sons, Inc., **2003**, Vol 12, *Ethylene Glycol*, 597.

(2) Ullmann's Encyclopedia of Industrial Chemistry, Sixth Edition, John Wiley & Sons, Inc., **2003**, Vol 28, *Polyoxalkylenes*, 497.

(3) Senanayake, C. H., Roberts, F. E., DiMichele, L. M., Ryan, K. M., Liu, J., Fredenburgh, L. E., Foster, B. S., Douglas, A. W., Larsen, R. D., Verhoeven, T. R. and Reider, P. J., *Tetrahedron Lett.* **1995**, *36*, 3993-3996.

(4) Wang, X.-Y., Shi, H.-C., Sun, C. and Zhang, Z.-G., *Tetrahedron* **2004**, *60*, 10993-10998.

(5) Hendlin, D., Stapley, E. O., Jackson, M., Wallick, H., Miller, A. K., Wolf, F. J., Miller, T. W., Chaiet, L., Kahan, F. M., Foltz, E. L., Woodruff, H. B., Mata, J. M., Hernandez, S. and Mochales, S., *Science* **1969**, *166*, 122-123.

(6) Mao, C.-F. and Albert Vannice, M., *Appl. Catal., A* **1995**, *122*, 61-76.

(7) Ayame, A., Uchida, Y., Ono, H., Miyamoto, M., Sato, T. and Hayasaka, H., *Appl. Catal., A* **2003**, *244*, 59-70.

(8) Linic, S. and Barteau, M. A., *J. Catal.* **2003**, *214*, 200-212.

(9) Atkins, M., Couves, J., Hague, M., Sakakini, B. H. and Waugh, K. C., *J. Catal.* **2005**, *235*, 103-113.

(10) Linic, S. and Barteau, M. A., *J. Am. Chem. Soc.* **2001**, *124*, 310-317.

(11) Linic, S. and Barteau, M. A., *J. Am. Chem. Soc.* **2003**, *125*, 4034-4035.

(12) Taylor, B., Lauterbach, J. and Delgass, W. N., *Appl. Catal., A* **2005**, *291*, 188-198.

(13) Lu, J., Zhang, X., Bravo-Suárez, J. J., Bando, K. K., Fujitani, T. and Oyama, S. T., *J. Catal.* **2007**, *250*, 350-359.

(14) Wolf, P. F. and Barnes, R. K., *J. Org. Chem.* **1969**, *34*, 3441-3445.

(15) Tosaki, S.-y., Tsuji, R., Ohshima, T. and Shibasaki, M., *J. Am. Chem. Soc.* **2005**, *127*, 2147-2155.

(16) van Vliet, M. C. A., Arends, I. W. C. E. and Sheldon, R. A., *Tetrahedron Lett.* **1999**, *40*, 5239-5242.

(17) Hori, T. and Sharpless, K. B., *J. Org. Chem.* **1978**, *43*, 1689-1697.

(18) Jacobson, S. E., Mares, F. and Zambri, P. M., *J. Am. Chem. Soc.* **1979**, *101*, 6946-6950.

(19) ten Brink, G.-J., Fernandes, B. C. M., van Vliet, M. C. A., Arends, I. W. C. E. and Sheldon, R. A., *J. Chem. Soc., Perkin Trans. 1* **2001**, 224-228.

(20) Rebek, J. and McCready, R., *Tetrahedron Lett.* **1979**, *20*, 4337-4338.

(21) Kuznetsov, M. L., Kozlov, Y. N., Mandelli, D., Pombeiro, A. J. L. and Shul'pin, G. B., *Inorg. Chem.* **2011**, *50*, 3996-4005.

(22) Sobczak, J. and Ziółkowski, J. J., *J. Mol. Catal.* **1977**, *3*, 165-172.

(23) Sharpless, K. B., Townsend, J. M. and Williams, D. R., *J. Am. Chem. Soc.* **1972**, *94*, 295-296.

(24) Ledon, H. J., Durbut, P. and Varescon, F., *J. Am. Chem. Soc.* **1981**, *103*, 3601-3603.

(25) Mitchell, J. M. and Finney, N. S., *J. Am. Chem. Soc.* **2001**, *123*, 862-869.

(26) Chong, A. O. and Sharpless, K. B., *J. Org. Chem.* **1977**, *42*, 1587-1590.

(27) Itoh, T., Jitsukawa, K., Kaneda, K. and Teranishi, S., *J. Am. Chem. Soc.* **1979**, *101*, 159-169.

(28) Mimoun, H., Mignard, M., Brechot, P. and Saussine, L., *J. Am. Chem. Soc.* **1986**, *108*, 3711-3718.

(29) Murase, N., Hoshino, Y., Oishi, M. and Yamamoto, H., *J. Org. Chem.* **1999**, *64*, 338-339.

(30) Li, Z. and Yamamoto, H., *J. Am. Chem. Soc.* **2010**, *132*, 7878-7880.

(31) Katsuki, T. and Sharpless, K. B., *J. Am. Chem. Soc.* **1980**, *102*, 5974-5976.

(32) Woodard, S. S., Finn, M. G. and Sharpless, K. B., *J. Am. Chem. Soc.* **1991**, *113*, 106-113.

(33) Finn, M. G. and Sharpless, K. B., *J. Am. Chem. Soc.* **1991**, *113*, 113-126.

(34) Corey, E. J., *J. Org. Chem.* **1990**, *55*, 1693-1694.

(35) Jacobsen, E. N., Deng, L., Furukawa, Y. and Martínez, L. E., *Tetrahedron* **1994**, *50*, 4323-4334.

(36) Jacobsen, E. N., Zhang, W. and Guler, M. L., *J. Am. Chem. Soc.* **1991**, *113*, 6703-6704.

(37) Jacobsen, E. N., Zhang, W., Muci, A. R., Ecker, J. R. and Deng, L., *J. Am. Chem. Soc.* **1991**, *113*, 7063-7064.

(38) Palucki, M., Pospisil, P. J., Zhang, W. and Jacobsen, E. N., *J. Am. Chem. Soc.* **1994**, *116*, 9333-9334.

(39) Terry, T. J. and Stack, T. D. P., *J. Am. Chem. Soc.* **2008**, *130*, 4945-4953.

(40) Murphy, A. and Stack, T. D. P., *J. Mol. Catal. A: Chem.* **2006**, *251*, 78-88.

(41) Murphy, A., Dubois, G. and Stack, T. D. P., *J. Am. Chem. Soc.* **2003**, *125*, 5250-5251.

(42) Murphy, A., Pace, A. and Stack, T. D. P., *Org. Lett.* **2004**, *6*, 3119-3122.

(43) Dubois, G., Murphy, A. and Stack, T. D. P., *Org. Lett.* **2003**, *5*, 2469-2472.

(44) Chen, K., Costas, M., Kim, J., Tipton, A. K. and Que, L., *J. Am. Chem. Soc.* **2002**, *124*, 3026-3035.

(45) White, M. C., Doyle, A. G. and Jacobsen, E. N., *J. Am. Chem. Soc.* **2001**, *123*, 7194-7195.

(46) Flessner, T. and Doye, S., *J. Prakt. Chem.* **1999**, *341*, 436-444.

(47) Pozzi, G. and Cinato, F., *Chem. Commun.* **1998**, 877-878.

(48) Kass, S. R. and DePuy, C. H., *J. Org. Chem.* **1985**, *50*, 2874-2877.

(49) Linker, T., *Angew. Chem. Int. Ed.* **1997**, *36*, 2060-2062.

(50) Feichtinger, D. and Plattner, D. A., *Angew. Chem. Int. Ed.* **1997**, *36*, 1718-1719.

(51) Feichtinger, D. and Plattner, D. A., *Chem. Eur. J.* **2001**, *7*, 591-599.

(52) Collman, J. P., Zeng, L. and Brauman, J. I., *Inorg. Chem.* **2004**, *43*, 2672-2679.

(53) Adam, W., Roschmann, Konrad J. and Saha-Möller, Chantu R., *Eur. J. Org. Chem.* **2000**, *2000*, 3519-3521.

(54) Adam, W., Roschmann, K. J., Saha-Möller, C. R. and Seebach, D., *J. Am. Chem. Soc.* **2002**, *124*, 5068-5073.

(55) Schröder, D., Shaik, S. and Schwarz, H., *Acc. Chem. Res.* **2000**, *33*, 139-145.

(56) Abashkin, Y. G. and Burt, S. K., *Org. Lett.* **2003**, *6*, 59-62.

(57) Palucki, M., Finney, N. S., Pospisil, P. J., Güler, M. L., Ishida, T. and Jacobsen, E. N., *J. Am. Chem. Soc.* **1998**, *120*, 948-954.

(58) Ottenbacher, R. V., Bryliakov, K. P. and Talsi, E. P., *Inorg. Chem.* **2010**, *49*, 8620-8628.

(59) Anilkumar, G., Bitterlich, B., Gelalcha, F. G., Tse, M. K. and Beller, M., *Chem. Commun.* **2007**, *0*, 289-291.

(60) Bukowski, M. R., Comba, P., Lienke, A., Limberg, C., Lopez de Laorden, C., Mas-Ballesté, R., Merz, M. and Que, L., *Angew. Chem. Int. Ed.* **2006**, *45*, 3446-3449.

(61) Nam, W., Ho, R. and Valentine, J. S., *J. Am. Chem. Soc.* **1991**, *113*, 7052-7054.

(62) Mas-Ballesté, R., Costas, M., van den Berg, T. and Que, L., *Chem. Eur. J.* **2006**, *12*, 7489-7500.

(63) Oldenburg, P. D., Shteinman, A. A. and Que, L., *J. Am. Chem. Soc.* **2005**, *127*, 15672-15673.

(64) Rohde, J.-U., In, J.-H., Lim, M. H., Brennessel, W. W., Bukowski, M. R., Stubna, A., Münck, E., Nam, W. and Que, L., *Science* **2003**, *299*, 1037-1039.

(65) Klinker, E. J., Kaizer, J., Brennessel, W. W., Woodrum, N. L., Cramer, C. J. and Que, L., *Angew. Chem.* **2005**, *117*, 3756-3760.

(66) Costas, M., Mehn, M. P., Jensen, M. P. and Que, L., *Chem. Rev.* **2004**, *104*, 939-986.

(67) Katsuki, T. and Martin, V. *Asymmetric Epoxidation of Allylic Alcohols: the Katsuki–Sharpless Epoxidation Reaction*, *Org. React.*, **1996**, *48*, 1-299.

(68) Rinaldi, R., de Oliveira, H. F. N., Schumann, H. and Schuchardt, U., *J. Mol. Catal. A: Chem.* **2009**, *307*, 1-8.

(69) Kuznetsov, M. L., Kozlov, Y. N., Mandelli, D., Pombeiro, A. J. L. and Shul'pin, G. B., *Inorg. Chem.* **2011**, *50*, 3996-4005.

Chapter 2

Alkene Epoxidation Catalyzed by Manganese Complexes with Electronically Modified 1,10-Phenanthroline Ligands*

* This chapter is a revision of a published paper: Christian R. Goldsmith, Wenchan Jiang, *Inorg. Chim. Acta*, **2012**, 384, 340-344. Reprinted with permission.

2.1 Introduction

The epoxidation of terminal and electron-deficient olefins remains a challenging task in synthetic chemistry. Although many alkenes react directly with peracids, these uncatalyzed reactions often require extended reactions times and/or elevated temperatures, both of which can reduce selectivity. The use of transition metal catalysts can enhance the selectivity, reduce reaction times, and allow reactivity at ambient temperatures [1-21]. Many homogeneous and heterogeneous catalysts for epoxidation reactions employ manganese as the active metal.[1-13]

Electron-rich olefins are generally more reactive, to the extent that the development of catalysts capable of activating more electron-deficient olefins, such as terminal alkenes, remains an intense area of research.[1-4, 21] The terminal oxidant and the acidity of the reaction also strongly influence the activity.[1-2, 13, 22] Systematic studies on the influence of the electronic nature of the catalyst, as opposed to that of the substrate,[23] on alkene epoxidation are comparatively rare.[24-25] In studies involving manganese–salen catalysts, the addition of electron-donating substituents onto the catalyst's ligand were found to slow the rate and improve the stereoselectivity of olefin oxidation.[10, 24] This has been attributed to the ability of the electron donors to stabilize the Mn=O bond in the Mn(V) oxo species that is believed to be the active oxidant.[25]

We report three novel monomeric manganese complexes with electronically modified derivatives of 1,10-phenanthroline (phen) that are related to two highly active catalysts reported by Murphy and Stack.[2] 1,10-phenanthroline is chosen as the ligand backbone based on the facts that with versatile derivatives it has strong chelating ability and is relatively oxidative robust during catalysis. The electronic perturbations are installed on the 5-position of the phen ligands in order to minimize the influence of steric effects on the alkene epoxidation. Scheme 2.1 shows the molecular structure of the phen derivatives and a sketch of the anticipated coordination around the Mn(II) ion.[26-27] Each of the $[Mn(R\text{-}phen)_2Cl_2]$ compounds (R = NH_2, CH_3, H, NO_2) can catalyze the oxygenation of alkenes by peracetic acid (Scheme 2.2). The yields of the reactions are correlated with the electron-donating capacity of the substituent on the 5-position, with electron-withdrawing groups impeding, not hastening, the alkene epoxidation.

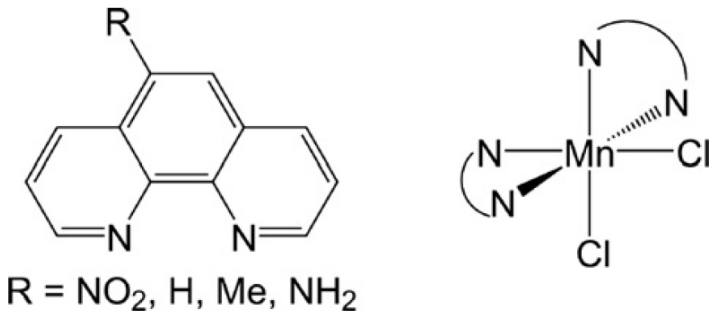

Scheme 2.1 Illustration of Mn(*R*-phen)$_2$Cl$_2$ complexes

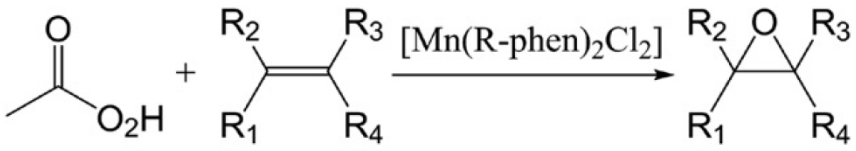

Scheme 2.2 Mn(*R*-phen)$_2$Cl$_2$ catalyzed epoxidation reaction

2.2 Experimental

Materials

Acetonitrile (MeCN), manganese(II) chloride ($MnCl_2$), 1,10-phenanthroline (phen), 5-nitro-1,10-phenanthroline (NO_2-phen), 5-chloro-1,10-phenanthroline (Cl-phen), cyclohexene, cyclohexene oxide, 3-cyclohexenol, 3-cyclohexenone, cyclooctene, 1-octene, 2,4-hexadienoic acid (sorbic acid), peracetic acid (32% in acetic acid, PAA), and 1,2-dichlorobenzene were purchased from Sigma–Aldrich and used as received. 5-Amino-1,10-phenanthroline (NH_2-phen) and 5-methyl-1,10-phenanthroline (Me-phen) were acquired from Acros. Anhydrous ethanol (EtOH) and anhydrous diethyl ether (ether) were bought from Pharmco-Aaper and Fisher Scientific, respectively. Deuterated acetonitrile (CD_3CN) was purchased from Cambridge Isotopes.

Instrumentation

All ^{1}H magnetic resonance (NMR) spectra were acquired on a 400 MHz AV Bruker NMR spectrometer at 294 K. All NMR resonances were referenced to internal standards. A Shimadzu IR Prestige-21 FT-IR spectrophotometer was used to record infrared spectra on samples that were prepared as KBr pellets. All samples that were submitted for elemental analysis were powdered and dried before shipment; Atlantic Microlabs (Norcross, GA) performed all elemental analysis. The magnetic susceptibilities of solid samples were measured

on a Johnson Matthey balance (model MK I#7967). The diamagnetic contribution to each magnetic susceptibility was estimated using Pascal's constants.[28] Electron paramagnetic resonance (EPR) spectra were collected on a Bruker EMX-6/1 X-band EPR spectrometer operated in the perpendicular mode. Each EPR sample was run as a frozen 3:2 MeCN/$CHCl_3$ solution in a quartz tube, and the program EasySpin was used to analyze the acquired EPR data. Gas chromatography (GC) was obtained on a ThermoScientific Trace GC Ultra spectrometer with a flame ionization detector (FID).

Syntheses

Dichloro(bis(5-nitro-1,10-phenanthroline))manganese(II), [Mn(NO_2-phen)$_2$$Cl_2$]

A solution of NO_2-phen (0.105 g, 0.47 mmol) in 10 mL of EtOH was added to 0.046 g of $MnCl_2$ (0.23 mmol). The resultant slurry was heated until the residual manganese salt had dissolved. The solution was filtered and cooled to precipitate the product as a yellow powder (0.113 g, 85%). Solid-state magnetic susceptibility (294 K): μ_{eff} = 5.7 μB. Elemental Anal. Calc. for $C_{24}H_{14}Cl_2MnN_6O_4$: C, 50.02; H, 2.45; N, 14.58. Found: C, 49.80; H, 2.51; N, 14.54%. FT-IR (KBr, cm^{-1}): 3422 (m), 3325 (m), 3226 (m), 3051 (m), 2951 (m), 2922 (m), 2852 (m), 2729 (w), 2694 (w), 1634 (s), 1628 (s), 1501 (s), 1480 (s), 1378 (m).

Dichloro(bis(1,10-phenanthroline))manganese(II), [Mn(phen)$_2$$Cl_2$]

The synthesis of this compound has been reported previously [17]. Solid-state magnetic susceptibility (294 K): μ_{eff} = 5.8 μB. Elemental Anal. Calc. for $C_{24}H_{16}Cl_2MnN_4$: C, 59.28; H, 3.32; N, 11.52. Found: C, 58.41; H, 3.25; N, 11.35.FT-IR% (KBr, cm^{-1}): 2951 (w), 2922 (w), 2852 (w), 2727 (w), 2673 (w), 1635 (m), 1544 (m), 1494 (m), 1300 (m).

Dichloro(bis(5-methyl-1,10-phenanthroline))manganese(II), [Mn(Me-phen)$_2$$Cl_2$]

Me-phen (0.100 g, 0.52 mmol) and $MnCl_2$ (0.051 g, 0.26 mmol) were added to 10 mL of EtOH. The resultant slurry was refluxed until the solids had completely dissolved. The solution was filtered and cooled to precipitate the product as a yellow powder (0.106 g, 79%). Solid-state magnetic susceptibility (294 K): μ_{eff} = 5.6 μB. Elemental Anal. Calc. for $C_{26}H_{20}Cl_2MnN_4 \cdot H_2O$: C, 58.66; H, 4.17; N, 10.53. Found: C, 58.83; H, 3.83; N, 10.52%. FT-IR (KBr, cm^{-1}): 3043 (w), 2951 (s), 2922 (s), 2852 (s), 2725 (w), 2673 (w), 1462 (m), 1377 (m).

Dichloro(bis(5-amino-1,10-phenanthroline))manganese(II), [Mn(NH_2-phen)$_2$$Cl_2$]

NH_2-phen (0.103 g, 0.51 mmol) was dissolved in 10 mL of EtOH. The resultant solution was added to 0.051 g of $MnCl_2$ (0.25 mmol) and heated to dissolve as much of the residual manganese salt as possible. The hot solution was filtered, then cooled to deposit the product

as a yellow powder (0.112 g, 87%). Solid-state magnetic susceptibility (294 K): μ_{eff} = 5.7 μB. Elemental Anal. Calc. for $C_{24}H_{18}Cl_2MnN_6$: C, 55.83; H, 3.51; N, 16.28. Found: C, 55.24; H, 3.60; N, 15.97%. FT-IR (KBr, cm^{-1}): 3385 (w), 2922 (s), 2854 (s), 2725 (w), 2671 (w), 1529 (m), 1514 (m), 1462 (m), 1377 (m), 1350 (m).

Reactivity studies

All reactions were run in MeCN at 0 ^oC under N_2. The initial concentrations of the catalyst, olefin substrate, and terminal oxidant (PAA) were 0.010, 1.00, and 2.00 mM, respectively. The reaction mixtures were stirred for 1 h, at which point excess ether was added to precipitate the manganese compounds. With all substrates except sorbic acid, the quenched reaction mixtures were sequentially filtered through plugs of neutral alumina, basic alumina, and silica gel to remove the remaining PAA and metal salts. For these substrates, the preceding workup did not remove organic starting materials or products from the reaction mixture. For reactions using sorbic acid as the substrate, the reaction mixtures were not run through the basic alumina plug; the workup was otherwise identical to that previously described. All products were identified by both GC and NMR. The yields of the products were quantified relative to both an internal standard of 1,2-dichlorobenzene, which does not react under these conditions, and the remaining alkene starting material. All reactions were run at least six times to ensure reproducibility; the yields were averaged to provide the values listed on Table 2.1.

Table 2.1 Yields of epoxides for Mn(II)-catalyzed olefin oxidation by PAA.

Substrate	R = NH_2	R = Me	R = H	R= NO_2	Control[a]
Cyclohexene	41 (±7)	40 (±7)	36 (±7)	24 (±5)	5 (±3)
1-Octene	39 (±4)	36 (±6)	29 (±7)	23 (±7)	0[b]
Cyclooctene	87 (±6)	78 (±7)	76 (±7)	69 (±9)	20 (±3)
Sorbic acid	30 (±3)	25 (±3)	23 (±5)	16 (±5)	0

Initial concentrations in MeCN: [substrate] = 1.00 mM, [PAA] = 2.00 mM, [Mn(R-phen)$_2$Cl$_2$] = 0.010 mM. Reactions ran at 0 ^oC for 1 h under N_2.

a: Experiments were run in the absence of Mn(II) with identical concentrations of substrate and PAA.

b: No epoxide products were detected above the limit of detection.

2.3 Results

Syntheses and characterization of the manganese complexes

All four organic ligands are commercially available (Scheme 2.1), and the syntheses of the associated Mn(II) complexes are straightforward. The complex $[Mn(phen)_2Cl_2]$ had been reported previously;[29] the other three Mn(II) compounds can prepared through the same fundamental procedure. The yields for the metal complex syntheses range from 70% to 83%, with no correlation between the yield and the identity of the substituent on the 5 -position of the phen. Spectroscopically, the four compounds are typical Mn(II) complexes. Each is pale yellow, with no ligand-to-metal charge transfer bands past 300 nm. The magnetic moments of the compounds range from 5.6 to 5.8 μB and are most consistent with high-spin d^5 metal centers. The electronic modifications to the ligand are not great enough to force a change in the spin-state.

Reactivity studies with manganese compounds

The abilities of the four manganese compounds to act as catalysts for olefin epoxidation were tested with four olefin substrates: cyclohexene, cyclooctene, 1-octene, and sorbic acid (Scheme 2.3, Table 2.1). The latter two are relatively electron-deficient and resistant to epoxidation. In the absence of a metal catalyst, no epoxidation above the detection limit of the GC is observed over the course of 1 h for sorbic acid and 1-octene. The more electron-rich cyclohexene and cyclooctene, conversely, will react directly with PAA, with non-negligible amounts of products observable at 1 h. With all four olefin substrates, the yield of the manganese-catalyzed epoxidation dwarfs that of the uncatalyzed reaction. As shown in Figure 2.1, the epoxidation reaction is mostly finished at 1 h. The yield continues to increase past this point, but this additional activity can be attributed to the uncatalyzed reaction between the residual olefin and the peracid.

Only epoxides and unreacted alkene starting materials are observed in the product mixtures. Cyclohexene is often oxidized at the allylic position to 3-cyclohexenol and 3-cyclohexenone,[11-12, 30] but neither of these side-products is observed. Diols, which have been observed as products in some transition metal-catalyzed epoxidation reactions,[19-20, 31-33] are likewise not seen above the limit of detection. The diene sorbic acid is oxygenated at the more electron-rich alkene farther from the carboxylic acid functional group, yielding 4,5-sorbic acid oxide as the sole organic product.

EPR spectroscopy of [Mn(NO$_2$-phen)$_2$Cl$_2$]

The reaction between [Mn(NO$_2$-phen)$_2$Cl$_2$] and PAA was followed by EPR (Figure 2.2). The addition of PAA to a solution of the Mn(II) compound in 3:2 MeCN/CHCl$_3$ does not generate Mn(IV) species above the limit of detection, as had been observed by Ottenbacher et al. in a recent study of manganese complexes with neutral N-donor ligands.[13] The spectra of the solutions with 0, 2, 4, and 8 equiv of PAA are nearly identical, with integrated signal intensities that are within error of each other. Although the solvent and the concentrations of PAA in these samples are different than those used in the catalytic epoxidation reactions, they were sufficient to generate Mn(IV) species in the aforementioned studies of Mn(II) complexes with aminopyridyl ligands.[13] When 50 equiv of PAA are added, the integrated signal intensity decreases by 15%. This is accompanied by a noticeable browning of the solution, which is typical of oxidation to either Mn(III) or Mn(IV) [34]. Monitoring the reaction by optical spectroscopy reveals that the brown color is due to an absorption band at 365 nm.

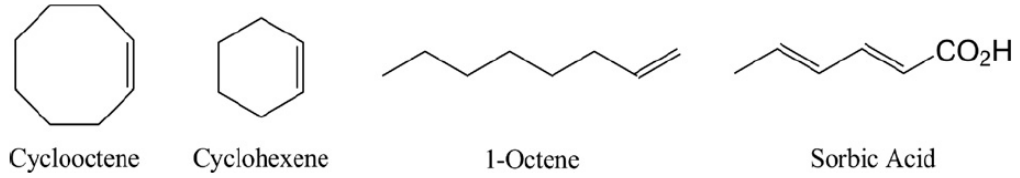

Scheme 2.3 Substrates used in this study

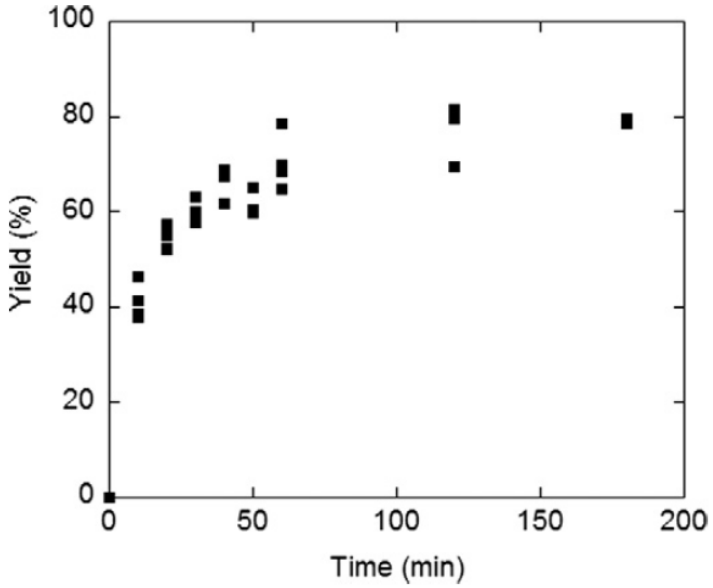

Figure 2.1 Epoxidation of cyclooctene by peracetic acid catalyzed by [Mn(NO$_2$-phen)$_2$Cl$_2$] in MeCN at 0 ^{o}C under N$_2$. The results from four independent kinetic runs are superimposed.

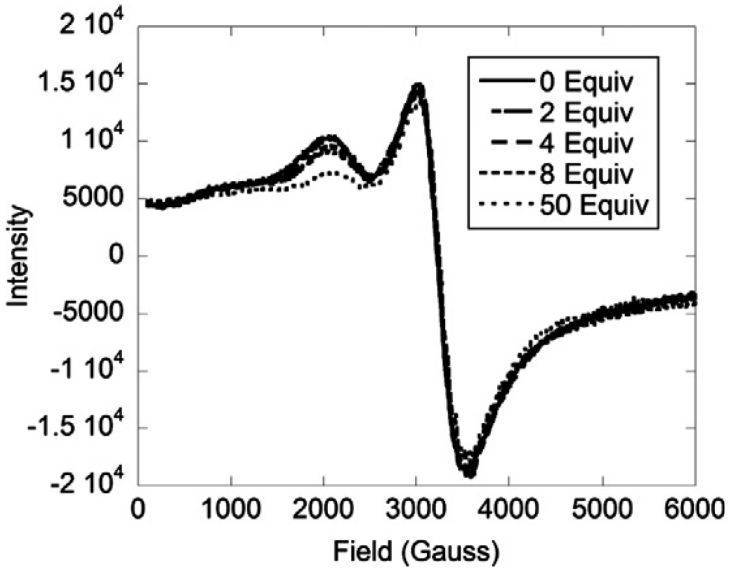

Figure 2.2 X-band EPR spectra of a solution of 1.1 mM [$Mn(NO_2$-phen$)_2Cl_2$] in 3:2 MeCN/$CHCl_3$ (solid). To this solution was added 2, 4, 8, and 50 equiv of peracetic acid. The following signal intensities were calculated through the double integration of the first-derivative spectra with subsequent normalization to the intensity of the 0 Equiv spectrum: 1.00 (0 Equiv), 0.99 (2 Equiv), 0.97 (4 Equiv), 1.01 (8 Equiv), 0.85 (50 Equiv). The temperature of all samples was 77 K.

2.4 Discussion

Installing electronic modifications on organic ligands has been shown to impact the reactivity of transition metal catalysts. In the current work, Mn(II) complexes with electronically modified phenanthroline (phen) ligands are prepared and used to catalyze the epoxidation of alkenes by peracetic acid (PAA). The electronic perturbations are installed on the 5-position of the phen heterocycle (Scheme 1); this placement minimizes the ability of the added functional groups to modulate the chemistry through steric effects. Previously, it was found that Mn(II) complexes with 2-derivatized phen ligands displayed severely curtailed oxidative catalysis.[2] The functional groups present on the 2-position either block the access of substrate and/or terminal oxidant to the metal center or weaken the Mn-N bonds enough to promote the dissociation of the ligands from the manganous ions.[2] Either of these events would account for the diminished reactivity.

The reactivity was tested using commercially available PAA as the terminal oxidant. Commercially available PAA is not as effective as a previously reported, less concentrated grade of PAA;[35] consequently, the yields (Table 2.1) and reaction times (Figure 2.1) of the

reported olefin epoxidations compare poorly to previously reported epoxidation catalyzed by Mn(II)-phen species.[2] The greatest number of catalytic turnovers is 87, corresponding to the epoxidation of cyclooctene to cyclooctene oxide by [Mn(NH_2-phen)$_2$$Cl_2$], and 20 of those turnovers can be accounted for by the background reactivity (Table 2.1). The oxidative efficiency, defined as the yield with respect to the terminal oxidant, is also inferior, reaching a maximum of 44% in the aforementioned cyclooctene reaction. The selectivities of the catalyzed reactions for the epoxide, however, are retained,[2] and no products corresponding to allylic oxidation or dihydroxylation are observed.

The less extensive reactivity offers an advantage in that it allows us to differentiate the oxygenating activities of the four manganese catalysts. Murphy and Stack had previously compared the reactivity of manganese complexes with 1,10-phenanthroline and 5-chloro--1,10-phenanthroline. With a 5 min reaction time, they did not observe a meaningful difference in the epoxidation activity using either commercial or custom-made PAA.[2] Using a less efficient terminal oxidant and extending the reaction times to 1 h reveal the impact of such electronic modifications. When an electron-withdrawing substituent (NO_2) is used, the yields of all four alkene epoxidation reactions decrease (Figure 2.3). Conversely, electron-donating substituents (NH_2, Me) increase the yields of the reactions measured at 1 h. The decrease in the yield going from R = NH_2 to NO_2 is approximately 15% for each substrate, with a strong linear correlation between the yield at 1 h and the σ_P parameter for the substituent on the 5-position of the phen. With cyclohexene, 1-octene, and sorbic acid, the reactivity is approximately halved upon switching the ligand from NH_2-phen to NO_2-phen. The R values for the fits in Figure 2.3 range from 0.95 (cyclohexene) to 0.98 (cyclooctene). These results differ from the manganese–salen chemistry developed by Jacobsen, in which electron-withdrawing substituents were found to increase the rate of epoxidation.[10, 24-25] As with other reported systems, more electron-rich olefins (cyclohexene, cyclooctene) are oxygenated to a greater extent than more electron-deficient ones (sorbic acid, 1-octene),[1, 13, 24, 30, 36] and the diene sorbic acid is oxygenated at the more electron-rich 4,5-alkene.

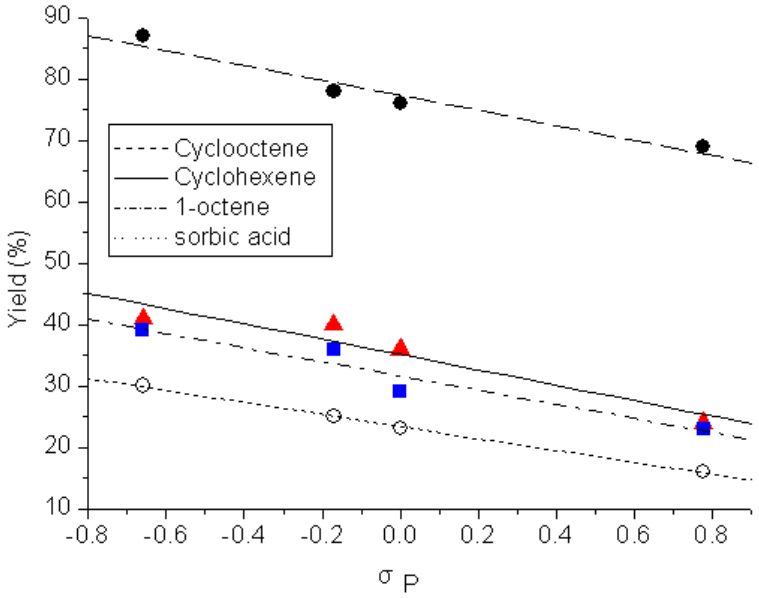

Figure 2.3 Plot of the reaction yields (as assessed at 1 h) for the oxygenation of each alkene as a function of the σ_P value of the 5-substituent on the catalyst's phenanthroline ligands.

There is compelling evidence that Jacobsen's system proceeds through a Mn(V) oxo species,[10, 37] which installs the oxygen atom onto the alkene through either a single two-electron or two one-electron steps.[23] A study of Mn(II) complexes with aminopyridyl ligands also implicates higher-valent oxidants in epoxidation, specifically Mn(IV) oxo adducts with the terminal oxidant.[13] The presence of electron-withdrawing groups would further destabilize these already electron-deficient metal centers and provide a greater thermodynamic impetus for the reduction of the manganese oxidant, with concomitant oxidation of the alkene.[24-25] That we see the opposite effect may indicate either a different rate-determining step or a fundamentally different mechanism.

The greater negative charge on the salens used in the aforementioned work would be anticipated to better stabilize more positively charged metal centers (e.g. Mn(V)) relative to neutral ligands. The EPR spectra of [Mn(NO_2-phen)$_2$$Cl_2$] and the [Mn ($NO_2$-phen)$_2$$Cl_2$]/PAA mixtures differ only slightly, and we observe no unambiguous evidence for Mn(IV) even with a 50-fold excess of terminal oxidant. Parallel experiments monitored by NMR did not reveal any paramagnetic resonances that would be indicative of Mn(III). The EPR signal intensity of the Mn(II), however, does decrease 15% when a 50-fold excess of PAA is added. This loss of signal intensity and the concurrent browning of the solution under these circumstances suggest that the manganese is being oxidized. The data suggest that [Mn(R-phen)$_2$$Cl_2$]

complexes may be more difficult to oxidize than related salen and aminopyridyl manganese complexes but certainly cannot preclude higher-valent oxidants in the catalytic cycle. One mechanistic possibility is that the reactivity proceeds through a Mn(IV) oxo species but with the rate-limiting step being the oxidation of the Mn(II) rather than the oxygen atom transfer from the oxidized manganese species to the alkene. This would prevent the accumulation of Mn(IV) above the detection threshold of EPR and would explain the decreased activity with more electron-withdrawing ligands.

In their analysis of non-porphyrin manganese catalysts, Murphy and Stack proposed that the acid in many epoxidation reactions quenches the reactivity by protonating the phenanthroline, which facilitates their removal from the manganese ions.[1] In their control studies, these unbound manganese ions were found to be unproductive as catalysts for epoxidation. The more electron-deficient phen derivatives are anticipated to bind to the metal ions less avidly and [Mn(R-phen)$_2$Cl$_2$] complexes with these ligands may be more susceptible to acid-induced deactivation. Although we do not observe any of the ^{1}H NMR features associated with dissociated phenanthroline ligands in mixtures of the [Mn(R-phen)$_2$Cl$_2$] species with either acetic acid or peracetic acid, this remains a plausible alternative explanation for the reduced activity of [Mn(NO$_2$-phen)$_2$Cl$_2$].

Another possibility consistent with the EPR data is that the active oxidant is a Mn(II)–PAA adduct and that higher-valent manganese species are not relevant to the hydrocarbon oxidation. Similar low-valent metal species have been mentioned as potential oxidants in other transition metal-based epoxidations.[13, 38] Furthermore, complexes with metals that generally do not exhibit much redox activity (e.g. Ti(IV), Al(III), Zn(II)) have been found to act as competent catalysts for alkene epoxidation.[30, 39-41] If the metal ion were merely acting as a Lewis acid, however, more strongly electron-withdrawing ligands would be anticipated to amplify the reactivity, which is contrary to what we observe.

2.5 Conclusions

A series of Mn(II) complexes with electronically modified phenanthroline ligands has been prepared. The three novel compounds catalyze the epoxidation of alkenes by commercially available peracetic acid. Unexpectedly, the more electron-rich ligands lead to faster reactivity with all alkenes investigated, as assessed by the yields of the olefin oxidations measured at 1

h. The results may suggest that $[Mn(phen)_2Cl_2]$ and related complexes may oxidize alkenes to epoxides through a fundamentally different free energy pathway than Mn(III)–salen catalysts. Further experimental and theoretical work is needed to fully elucidate these differences.

References

(1) Murphy, A., Pace, A. and Stack, T. D. P., *Org. Lett.* **2004**, *6*, 3119-3122.

(2) Murphy, A. and Stack, T. D. P., *J. Mol. Catal. A: Chem.* **2006**, *251*, 78-88.

(3) Murphy, A., Dubois, G. and Stack, T. D. P., *J. Am. Chem. Soc.* **2003**, *125*, 5250-5251.

(4) Ho, K.-P., Wong, W.-L., Lam, K.-M., Lai, C.-P., Chan, T. H. and Wong, K.-Y., *Chem. Eur. J.* **2008**, *14*, 7988-7996.

(5) Jacobsen, E. N., Zhang, W., Muci, A. R., Ecker, J. R. and Deng, L., *J. Am. Chem. Soc.* **1991**, *113*, 7063-7064.

(6) Terry, T. J. and Stack, T. D. P., *J. Am. Chem. Soc.* **2008**, *130*, 4945-4953.

(7) Wu, M., Wang, B., Wang, S., Xia, C. and Sun, W., *Org. Lett.* **2009**, *11*, 3622-3625.

(8) Fujii, Y., Ebina, F., Yanagisawa, M., Matsuoka, H. and Kato, T., *J. Inorg. Organomet. P.* **1994**, *4*, 273-288.

(9) Collman, J. P., Lee, V. J., Kellen-Yuen, C. J., Zhang, X., Ibers, J. A. and Brauman, J. I., *J. Am. Chem. Soc.* **1995**, *117*, 692-703.

(10) McGarrigle, E. M. and Gilheany, D. G., *Chem. Rev.* **2005**, *105*, 1563-1602.

(11) Nehru, K., Kim, S. J., Kim, I. Y., Seo, M. S., Kim, Y., Kim, S.-J., Kim, J. and Nam, W., *Chem. Commun*. **2007**, 4623-4625.

(12) Yin, G., Buchalova, M., Danby, A. M., Perkins, C. M., Kitko, D., Carter, J. D., Scheper, W. M. and Busch, D. H., *J. Am. Chem. Soc.* **2005**, *127*, 17170-17171.

(13) Ottenbacher, R. V., Bryliakov, K. P. and Talsi, E. P., *Inorg. Chem.* **2010**, *49*, 8620-8628.

(14) Sharpless, K. B. and Michaelson, R. C., *J. Am. Chem. Soc.* **1973**, *95*, 6136-6137.

(15) White, M. C., Doyle, A. G. and Jacobsen, E. N., *J. Am. Chem. Soc.* **2001**, *123*, 7194-7195.

(16) Kamata, K., Yonehara, K., Sumida, Y., Yamaguchi, K., Hikichi, S. and Mizuno, N., *Science* **2003**, *300*, 964-966.

(17) Gelalcha, F. G., Anilkumar, G., Tse, M. K., Brückner, A. and Beller, M., *Chem. Eur. J.* **2008**, *14*, 7687-7698.

(18) Bühl, M., Schurhammer, R. and Imhof, P., *J. Am. Chem. Soc.* **2004**, *126*, 3310-3320.

(19) Chen, K., Costas, M., Kim, J., Tipton, A. K. and Que, L., *J. Am. Chem. Soc.* **2002**, *124*, 3026-3035.

(20) Mas-Ballesté, R. and Que, L., *J. Am. Chem. Soc.* **2007**, *129*, 15964-15972.

(21) Dubois, G., Murphy, A. and Stack, T. D. P., *Org. Lett.* **2003**, *5*, 2469-2472.

(22) Zhang, J.-L. and Che, C.-M., *Chem. Eur. J.* **2005**, *11*, 3899-3914.

(23) Linde, C., Koliaï, N., Norrby, P.-O. and Åkermark, B., *Chem. Eur. J.* **2002**, *8*, 2568-2573.

(24) Jacobsen, E. N., Zhang, W. and Guler, M. L., *J. Am. Chem. Soc.* **1991**, *113*, 6703-6704.

(25) Cavallo, L. and Jacobsen, H., *J. Org. Chem.* **2003**, *68*, 6202-6207.

(26) Malinowski, T. J., Kravtsov, V. C., Simonov, Y. A., Lipkowski, J. and Bologa, O. A., *J. Coord. Chem.* **1996**, *37*, 187-193.

(27) McCann, M., Casey, M. T., Devereux, M., Curran, M. and McKee, V., *Polyhedron* **1997**, *16*, 2741-2748.

(28) Bain, G. A. and Berry, J. F., *J. Chem. Educ.* **2008**, *85*, 532.

(29) Morcom, R. E. and Bell, C. F., *J. Inorg. Nucl. Chem.* **1973**, *35*, 1865-1874.

(30) Nam, W. and Valentine, J. S., *J. Am. Chem. Soc.* **1990**, *112*, 4977-4979.

(31) Matsumoto, T., Furutachi, H., Kobino, M., Tomii, M., Nagatomo, S., Tosha, T., Osako, T., Fujinami, S., Itoh, S., Kitagawa, T. and Suzuki, M., *J. Am. Chem. Soc.* **2006**, *128*, 3874-3875.

(32) Mas-Ballesté, R., Costas, M., van den Berg, T. and Que, L., *Chem. Eur. J.* **2006**, *12*, 7489-7500.

(33) Quiñonero, D., Musaev, D. G. and Morokuma, K., *Inorg. Chem.* **2003**, *42*, 8449-8455.

(34) Cotton, F. A., Wilkinson, G., Advanced Inorganic Chemistry, 5th Edition, *John Wiley & Sons, New York* **1988**.

(35) Hawkinson, A.T., Schmitz, W. R., E.I. du Pont de Nemours & Co., US 2910504, **1959**.

(36) Indictor, N., *J. Org. Chem.* **1965**, *30*, 2074-2075.

(37) Hamada, T., Fukuda, T., Imanishi, H. and Katsuki, T., *Tetrahedron* **1996**, *52*, 515-530.

(38) Collman, J. P., Chien, A. S., Eberspacher, T. A. and Brauman, J. I., *J. Am. Chem. Soc.* **2000**, *122*, 11098-11100.

(39) Katsuki, T. and Sharpless, K. B., *J. Am. Chem. Soc.* **1980**, *102*, 5974-5976.

(40) Kuznetsov, M. L., Kozlov, Y. N., Mandelli, D., Pombeiro, A. J. L. and Shul'pin, G. B., *Inorg. Chem.* **2011**, *50*, 3996-4005.

(41) Pescarmona, P. P., Janssen, K. P. F. and Jacobs, P. A., *Chem. Eur. J.* **2007**, *13*, 6562-6572.

Chapter 3

A Homogeneous Gallium(III) Compound Selectively Catalyzes the Epoxidation of Alkenes*

* This chapter is a revision of a published paper: Wenchan Jiang, John D. Gorden, and Christian R. Goldsmith, *Inorg. Chem.*, **2012**, 51, 2725-2727. Reprinted with permission.

3.1 Introduction

Group 13 elements have been explored intensively as catalysts for many reactions because of their low cost and ability to be readily extracted and recovered from reaction mixtures.[1] The overwhelming majority of their catalytic capability derives from their strong Lewis acidity.[2-6] Alkyl and hydrido complexes with these elements are also well-known for their ability to stoichiometrically reduce various functional groups, with the metal complex donating a carbanion or hydride, respectively.[2-3, 7-9] Because of the limited redox activity exhibited by these elements, there are comparatively few reports of group 13 catalyzed oxidation−reduction reactions; notable examples include Meerwein−Verley−Ponndorf carbonyl reduction and Oppenauer oxidation.[5, 10-19] The hydrocarbon oxidation catalysis that has been reported tends to be unselective; the documented olefin epoxidation, for instance, is accompanied by substantial allylic oxidation.[12-17, 20]

Reported here is the selective epoxidation of olefins by the previously described $[Ga(phen)_2Cl_2]Cl$ (phen = 1,10-phenanthroline).[14, 17, 20-22] To the best of our knowledge, this is the first instance of a gallium(III) compound serving as a homogeneous catalyst in alkene epoxidation (Scheme 3.1), although this metal ion has previously been a component in heterogeneous catalysts for such reactions.[14, 17]

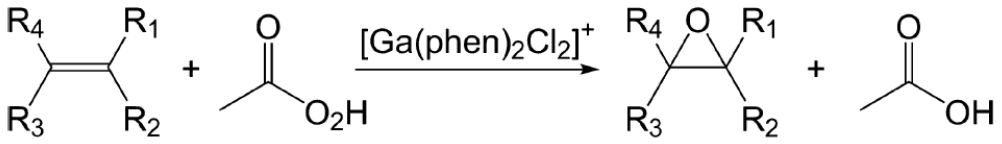

Scheme 3.1 Illustration of epoxidation catalyzed by $[Ga(phen)_2Cl_2]Cl$

3.2 Experimental

Materials

Unless stated otherwise, all chemicals were purchased from Sigma-Aldrich and used as received. Anhydrous ethanol and diethyl ether (ether) were bought from Pharmco-Aaper and

Fisher Scientific, respectively. Deuterated acetonitrile (CD_3CN) was purchased from Cambridge Isotopes. $[Ga(phen)_2C1_2]Cl$ was prepared and characterized as previously described.[20-22] The Ga(III) complex crystallized upon adding ether to a saturated solution of the compound in acetonitrile (MeCN). The identity and purity of the Ga(III) catalyst were confirmed by nuclear magnetic resonance (NMR).

Preparation of Custom-Made Peracetic Acid (PAA_R)

The more basic grade of peracetic acid (PAA_R) was prepared through a slightly modified version of a reported procedure.[4] 17 g of 50% H_2O_2 (0.25 mol) was slowly added to glacial acetic acid (150 g, 2.5 mol), which was stirred in a polyethylene bottle at room temperature. After 5 min, 5.0 g of Amberlite IR-120 was added. The resultant mixture was allowed to stir behind a blast shield for 24 h. After this duration, the solution was filtered, and the molar concentration of PAA was determined by its integrated ^{13}C NMR resonance relative to that of acetic acid. The solution was stored in a standard -20 ^oC freezer when not in use. The content of PAA was determined to be 7.1% (molar) by ^{13}C NMR analysis; this molar concentration was replicated in multiple batches.

CAUTION: Peracids and mixtures of peroxides and organic solvents are potentially explosive and should be handled with care. The dangers can be minimized by using minimal amounts of these materials, using proper protective equipment including blast shields, and working at lower temperatures.

Instrumentation

Proton and carbon-13 nuclear magnetic resonance (^1H NMR, ^{13}C NMR) spectra were acquired on a 400 MHz AV Bruker NMR spectrometer at 294 K. All resonances were referenced to internal standards. Gas chromatography (GC) was obtained on a ThermoScientific Trace GC Ultra spectrometer with a flame ionization detector (FID).

Mass spectrometry was performed on an Ultra Performance LC System (ACQUITY, Waters Corporation, Milford, MA) coupled to a quadrupole time-of-flight mass spectrometer (QS2 TOF Premier, Waters Corporation, Milford, MA) via direct probe analysis operated in the positive ion mode. All samples were run as MeCN solutions.

Inductively coupled plasma optical emission spectrometry (ICP-OES) was performed on a

SPECTRO CIROS ICP-OES spectrometer in Auburn University's Department of Agronomy and Soils. All samples were prepared and run as solutions in 10% (by volume) aqueous HCl.

X-Ray Crystallography

The crystal was mounted in paratone oil on a glass fiber and aligned on a Bruker SMART APEX CCD X-ray diffractometer. Intensity measurements were performed using graphite monochromated Mo Kα radiation (λ = 0.71073 Å) from a sealed tube and monocapillary collimator. SMART (v 5.624) was used to determine the preliminary cell constants and control the data acquisition. The intensities of reflections of a sphere were collected through the compilation of three sets of exposures (frames). Each set had a different ϕ angle for the crystal, with each exposure spanning 0.3^{o} in ω. A total of 1800 frames were collected with exposure times of 40 s per frame. After the data were corrected for Lorentz and polarization effects, the structure was solved using direct methods and expanded using Fourier techniques. All non-hydrogen atoms were refined anisotropically. Hydrogen atoms were included at idealized positions 0.95 Å from their parent atoms prior to the final refinement. Details regarding the data acquisition and analysis are included in Table 3.1.

Table 3.1. Selected crystallographic data for $[Ga(phen)_2Cl_2]Cl$.

Parameter	$[Ga(phen)_2Cl_2]Cl \cdot 0.5MeCN \cdot H_2O$
Formula	$C_{50}H_{39}Cl_6Ga_2N_9O_2$
Mw	1150.04
Crystal System	Orthorhombic
Space group	P_{bcn} (#60)
a (Å)	12.7377 (11)
b (Å)	23.275 (2)
c (Å)	16.5439 (15)
α (deg)	90
β (deg)	90
γ (deg)	90
V ($Å^3$)	4904.8 (8)
Z	4
Crystal color	Yellow
T (K)	183
Reflns collected	47811
Unique reflns	4661
R1 (F, $I > 2\sigma(I)$)	0.0476
wR2 (F^2, all data)	0.121

$R1 = \Sigma \big| |F_o| - |F_c| \big| / \Sigma |F_o|$; $wR2 = [\Sigma w(F_o^2 - F_c^2)^2 / \Sigma w(F_o^2)^2]^{1/2}$

Reactivity studies

All reactions were run in acetonitrile (MeCN) at 0 ^oC under N_2. The reaction mixtures were stirred for 1 h, at which point excess ether was added to precipitate the gallium compounds. With all substrates, the quenched reaction mixtures were sequentially filtered through plugs of neutral alumina, basic alumina, and silica gel to remove the remaining PAA and metal salts. The workup did not remove organic starting materials or products from the reaction mixture, as assessed by analyzing control mixtures of alkenes and epoxides that were subjected to the

same protocol. All products were identified by their GC retention times and NMR. The yields of the products were quantified relative to an internal standard of 1,2-dichlorobenzene, which was found to be unreactive under these conditions. All reactions were run at least four times to ensure reproducibility. The results were also found to be reproducible with different batches of both $[Ga(phen)_2Cl_2]Cl$ and PAA_R.

Isolated Yields

Isolated yields were obtained for cyclohexene, cyclooctene, and 1-octene.

Cyclohexene oxide. $[Ga(phen)_2C1_2]Cl$ (0.054 g, 0.10 mmol) and cyclohexene (0.842 g, 10.0 mmol) were dissolved in 2 mL of MeCN. After the solution was put under N_2 and cooled to 0 ^oC, PAA_R solution (11.4 g, 20.0 mmol) was added dropwise. After 1 h, the reaction solution was filtered through plugs of silica gel and K_2CO_3. Cyclohexene oxide was isolated from the filtrate through distillation, yielding 0.38 g of product (39% vs. 46% GC yield).

Cyclooctene oxide. $[Ga(phen)_2C1_2]Cl$ (0.0540 g, 0.10 mmol) and cyclooctene (1.18 g, 10.0 mmol) were dissolved in 2 mL of MeCN. The solution was put under N_2 through nitrogen bubbling and cooled to 0 ^oC. Subsequently, PAA_R solution (11.4 g, 20.0 mmol) was added slowly. After 1 h, the reaction mixture was filtered through silica gel and K_2CO_3. Cyclooctene oxide was distilled from the filtrate (0.97 g, 77% vs. 87% GC yield).

1-Octene oxide. $[Ga(phen)_2C1_2]Cl$ (0.054 g, 0.10 mmol) and 1-octene (1.14 g, 10.0 mmol) were dissolved in 2 mL of MeCN. The reaction mixture was put under N_2 and cooled to 0 ^oC. Once the temperature equilibrated, 11.4 g of PAA_R solution (20.0 mmol) was added dropwise. 1 h after the addition was completed, the reaction mixture was filtered through plugs of silica gel and K_2CO_3. 1-Octene oxide was distilled from the filtrate (0.47 g, 37% vs. 41% GC yield).

3.3 Results and Discussion

The $[Ga(phen)_2Cl_2]Cl$ complex was crystallized from ethanol (Figure 3.1). The structural data confirm the compositions of the inner and outer spheres, with the outer-sphere chloride

located 5.57 Å away from the Ga^{III} ion. The halides are terminal rather than bridging, analogous to what is observed in the structure of $[Ga(phen)_2Br_2]Br$.[23] The structure is a rare example of a hexacoordinate dihalide gallium(III) complex.[23-25] The chlorides are *cis* to each other, as has been observed in other hexacoordinate dihalide gallium(III) complexes with bidentate ligands.[23-25]

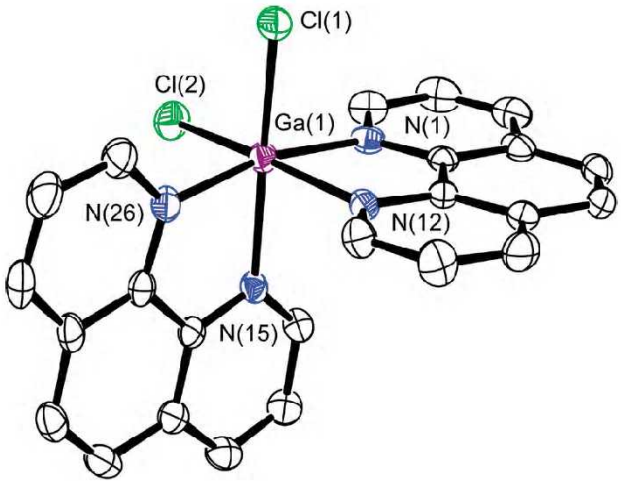

Figure 3.1 ORTEP representation of the cation $[Ga(phen)_2Cl_2]^+$. The counterion, H atoms, and outer-sphere solvent molecules have been removed for clarity. All thermal ellipsoids are drawn at 50% probability. A fuller description of the structure, including a table of metrical parameters, is included in Table 3.2.

Table 3.2 Bond lengths (Å) and bond angles (°) for $[Ga(phen)_2Cl_2]^+$.

Bond Length		Angle	
Ga-N (1)	2.085 (2)	N(1)-Ga-Cl(1)	94.19 (6)
Ga-N (12)	2.127 (2)	N(1)-Ga-Cl(2)	95.09 (7)
Ga-N (15)	2.134 (2)	N(12)-Ga-Cl(1)	88.16 (6)
Ga-N (26)	2.084 (2)	N(12)-Ga-Cl(2)	171.58 (6)
Ga-Cl (1)	2.2849 (7)	N(15)-Ga-N(26)	78.57 (9)
Ga-Cl (2)	2.2642 (8)	N(15)-Ga-Cl(1)	169.26 (6)
Angle		N(15)-Ga-Cl(2)	90.47 (6)
N(1)-Ga-N(12)	78.73 (8)	N(26)-Ga-Cl(1)	94.32 (7)
N(1)-Ga-N(15)	91.51 (8)	N(26)-Ga-Cl(2)	93.61 (7)
N(1)-Ga-N(26)	166.86 (9)	Cl(1)-Ga-Cl(1)	98.07 (3)

The Ga(III)-N bond distances and the L-Ga(III)-L bond angles are similar to those reported for $[Ga(phen)_2Br_2]^+$.[23] The major difference between the two structures is that the bonds between the Ga(III) and the nitrogen atoms on the 10-positions of the phenanthroline ligands are slightly longer in the chloride structure, averaging 2.13 Å as opposed to the 2.10 Å average for the bromide structure.

The ability of $[Ga(phen)_2Cl_2]Cl$ to catalyze the epoxidation of alkenes in acetonitrile (MeCN) was initially tested using H_2O_2. Although H_2O_2 served as a competent terminal oxidant in aluminum(III)-catalyzed alkene epoxidation,[12, 15] it did not lead to any epoxidation with the gallium(III) catalyst. Speculating that the poor binding affinity of H_2O_2 to Ga^{III} was responsible for the lack of activity,[26] we investigated two grades of peracetic acid (PAA). In addition to commercially available PAA (PAA_C, pH ~ 1), we prepared and investigated a less acidic, custom-made grade (PAA_R, pH ~ 4)[27] that previously led to excellent activity in manganese-catalyzed epoxidation.[28-29] PAA_R was prepared by reacting acetic acid and H_2O_2 in the presence of a highly acidic resin (Amberlite IR 120); PAA_R lacks the ~1% H_2SO_4 additive that is used as the catalyst for the commercial preparation of PAA. The peracids should ligate metal ions more readily than H_2O_2, particularly under more basic conditions.

Using PAA_C as the terminal oxidant led to modest epoxidation at 0 °C, but PAA_R was

much more effective, particularly with electron-deficient substrates (Table 3.3). As is commonly observed, the more electron-deficient olefins tend to react less readily. The two substrates with two alkene groups, ethyl sorbate and 4-vinylcyclohexene, are oxidized exclusively at the more electron-rich site. These results parallel those found for the aforementioned manganese(II)-catalyzed alkene epoxidation.[28-29] Although the yields of the epoxide do increase when more PAA_R is added, the reactions become noticeably less efficient. Adding one additional equiv of PAA_R to the cyclooctene reaction, for instance, only raises the yield of the epoxide from 64% to 87%, with a concomitant drop in the oxidative efficiency from 64% to 44%.

Table 3.3 Yields/Turnover Numbers of Gallium(III) Catalyzed Alkene Epoxidation Reactions by Various Grades and Amounts of PAA[a]

Substrate	Product	2 equiv PAA_C[b]	2 equiv PAA_R[b]	1 equiv PAA_R[b]
	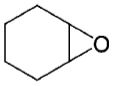	17 (±4)	46 (±8)[c]	31 (±4)
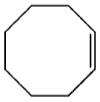	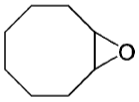	40 (±3)	87 (±4)[c]	64 (±4)
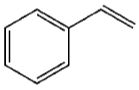	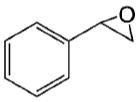	0	11 (±2)	8 (±2)
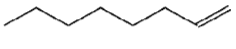	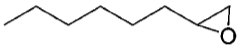	15 (±4)	41 (±3)[c]	30 (±3)
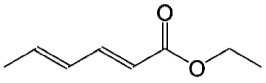	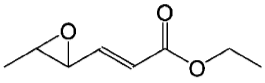	0	11 (±2)	8 (±2)
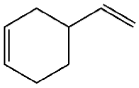	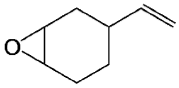	33 (±8)	61 (±6)	48 (±5)

[a] Sandard reaction conditions: MeCN, 0 °C, initial concentrations of 5.0 mM $[Ga(phen)_2Cl_2]Cl$ and 500 mM alkene. The yields, defined as the percentage of alkene converted to the epoxide, were measured at 1 h via gas chromatography. The yields also serve as the turnover numbers because the substrate is present in a 100-fold excess relative to the gallium(III).

[b] The ratio of $[Ga(phen)_2Cl_2]Cl$/alkene/PAA was 1:100:200 when 2 equiv of PAA was used and 1:100:100 when 1 equiv of terminal oxidant was added.

[c] Isolated yields for cyclohexene oxide (39%), cyclooctene oxide (77%), and 1-octene oxide (37%).

The control studies confirm that both the phen ligands and the Ga^{III} ions are essential for the observed catalysis. $GaCl_3$ by itself does not catalyze epoxidation to an appreciably greater extent than the metal-free controls. The summary of control experiments is in Table 3.4. We hypothesize that the electron-withdrawing nature of the phen ligands[30] amplifies the Lewis acidity of the Ga^{III} metal center relative to that in the chloride salt.

Table 3.4 Yields of Epoxide Products (%) in Control Reactions.

Substrate	Product	Catalyst	2 PAA_C	2 PAA_R
	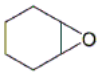	None	2	4
	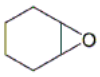	5.0 mM $GaCl_3$	3	4
	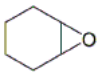	0.1 mM $[Mn(phen)_2Cl_2]$	13 (±3)	14 (±2)
		None	12 (±3)	15 (±3)
	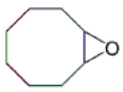	5.0 mM $GaCl_3$	12 (±3)	16 (±3)
		0.1 mM $[Mn(phen)_2Cl_2]$	22 (±3)	26 (±4)
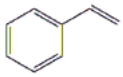	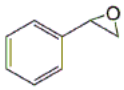	None	0	0
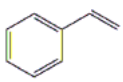	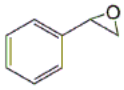	5.0 mM $GaCl_3$	0	0.3
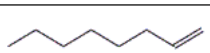	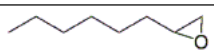	None	0	0
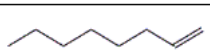	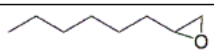	5.0 mM $GaCl_3$	1	2
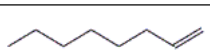	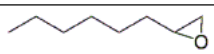	0.1 mM $[Mn(phen)_2Cl_2]$	10 (±3)	13 (±4)
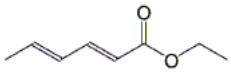	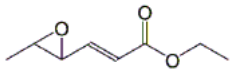	None	0	0
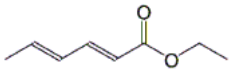	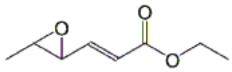	5.0 mM $GaCl_3$	0	0
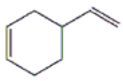	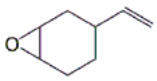	None	3	7
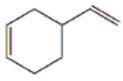	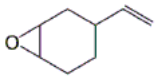	5.0 mM $GaCl_3$	4	7

The conditions are identical to those described for the reactions in Table 3.3, with the exceptions of the identity and concentration of the catalyst. For the above reactions, the ratio of alkene/PAA was 1:2 when 2 equiv. of PAA were used and 1:1 when 1 equiv. of terminal oxidant was added, with the concentration of alkene set at 500 mM. All reactions were run in MeCN at 0 °C under N_2. The yields, defined here as the percentage of alkene converted to the epoxide, were measured at 1 h through a comparison of the GC integration of the epoxide peak to that of an internal standard, 1,2-dichlorobenzene. No other organic products were observed in the above reactions.

In order to exclude the mechanistic possibility of a highly active transition-metal contaminant, we assessed the catalytic activity of 0.1 mM $[Mn(phen)_2Cl_2]$ and found it to be inferior to that of 5.0 mM $[Ga(phen)_2Cl_2]^+$. The loading of the manganese(II) complex, which is known to catalyze olefin epoxidation,[29] is meant to mimic an active 2% molar impurity. The 2% value is a conservative upper limit, given the high purities of the available gallium(III) salts and the crystallinity of the $[Ga(phen)_2Cl_2]^+$ catalyst (Figure 3.1). The purity of the gallium(III) complex is further confirmed by inductively coupled plasma optical emission spectrometry (ICP-OES), which found that the iron and manganese contents were equal within error to those of a blank sample. The results of ICP-OES are summarized in Table 3.5. That the reactivity cannot be fully accounted for by a highly active transition-metal contaminant demonstrates that a gallium(III) species is indeed catalyzing olefin epoxidation.

Table 3.5 Summary of ICP-OES Analysis

Analyte	Blank Sample Conc. [ppm]	28 ppm $[Ga(phen)_2Cl_2]Cl$ [ppm]	122 ppm $[Ga(phen)_2Cl_2]Cl$ [ppm]
Ag	<0.002[a]	<0.001	<0.001
Al	<0.019	<0.030	<0.040
As	<0.010	<0.003	<0.000
B	0.013	0.579	0.653
Ba	<0.001	<0.000	0.001
Ca	0.265	0.402	0.457
Cd	<0.000	<0.000	<0.000
Co	<0.000	<0.001	<0.002
Cr	<0.001	<0.002	<0.001
Cu	<0.000	<0.002	<0.000
Fe	**0.041**	**0.033**	**0.034**
K	4.658	2.697	1.640
Mg	0.143	0.175	0.182
Mn	**<0.009**	**<0.008**	**0.014[b]**
Mo	**0.029**	**0.014**	**<0.004**
Na	3.382	3.844	3.613
Ni	**<0.002**	**<0.012**	**<0.007**
P	<0.037	<0.029	<0.027
Pb	<0.001	<0.001	<0.005
S	0.895	0.975	0.882
Se	0.067	0.069	0.061
Si	0.032	0.268	0.265
Ti	**0.004**	**<0.002**	**<0.001**
Zn	0.007	0.125	0.049
Zr	<0.015	<0.008	<0.003

a The "<" means the given value is below the limit of accurate detection for that analyte. *b* Corresponds to a 0.01% impurity in the 122 ppm sample.

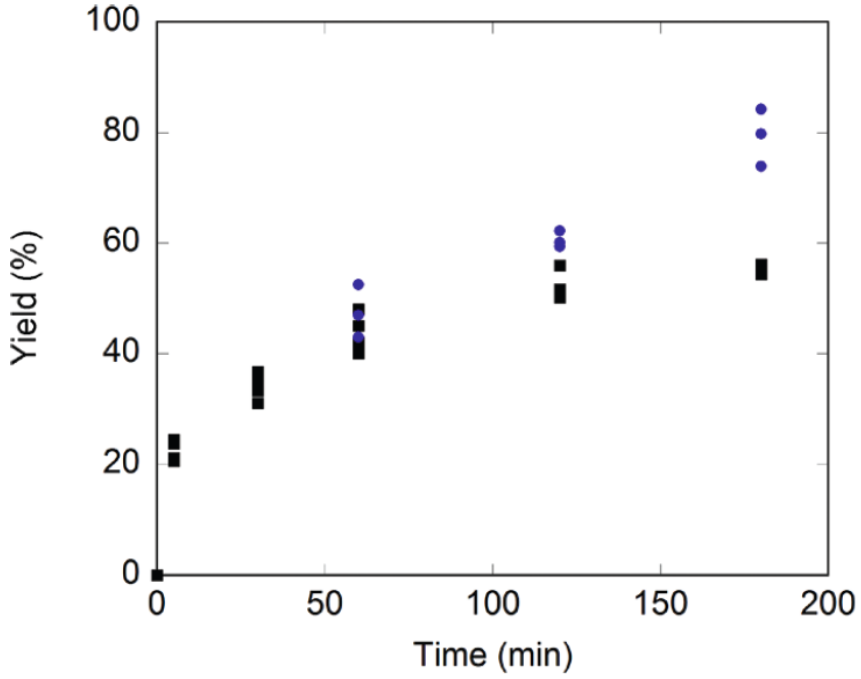

Figure 3.2 Yield of cyclohexene oxidation by 2 equiv of PAA_R as a function of time. The blue data points (round dot) correspond to the reactivity observed in the presence of 10 equiv of additional phen. Otherwise, the reaction conditions are identical with those in Table 3.3.

Monitoring the yield of several epoxidation reactions over time reveals that the reactivity persists for approximately 2 h at 0 °C (Figure 3.2). Mass spectrometric (MS) analysis of the reaction suggests that the chloride ligands are displaced by acetate almost immediately; by mass balance, this would generate HCl. MS analysis (Figure 3.3) also reveals that the phen ligands dissociate from the Ga^{III} ions over the period of the reaction, with noticeably fewer Ga^{III}phen adducts remaining at 1 h. Because the gallium(III) salts by themselves are not competent catalysts for olefin epoxidation, dissociation of the phen ligands is a plausible explanation for the loss of activity. The speculation that the resultant greater concentration of H^+ will more effectively compete with the Ga^{III} ions for the N-donor atoms of the phen ligands has been proved to be wrong after a careful calculation. Under current experimental conditions, the pH value in the reaction solutions will not change too much even after all PAA_R have been converted to acetic acid. The lifetime of the catalytic activity and the ultimate yield of the epoxide can be increased by adding free phen ligand to the initial reaction mixture (Figure 3.2). With the shown cyclohexene epoxidation, the yield at 3 h

increased from 55% to 79% when 10 equiv of additional phen were present. Attempts to further increase the yield by running the reaction in a solution of 50 mM HEPES in H_2O buffered to pH 7.0 were unsuccessful. The yield measured at 3 h was 68% in the HEPES buffer, as opposed to 79% in MeCN. We attribute this lesser activity to the immiscibility of the alkene substrate with water.

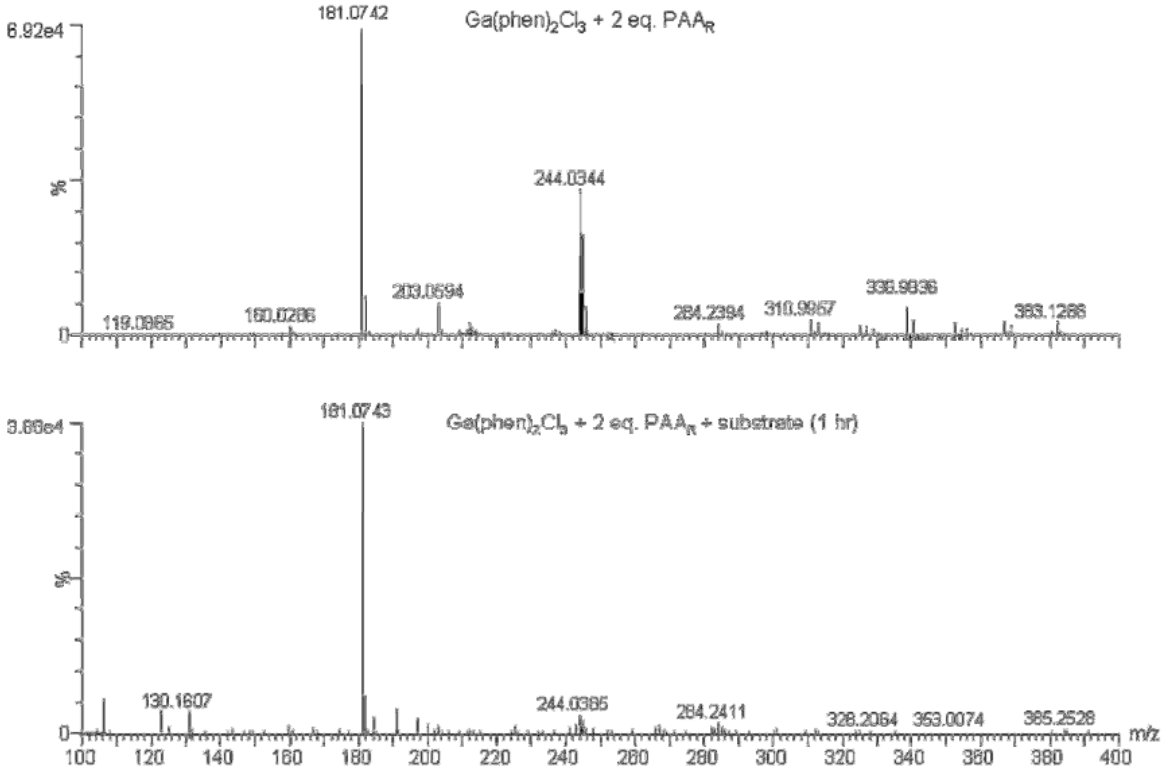

Figure 3.3. Mass spectrometric analysis of the reaction between cyclooctene and two equiv. of PAA_R at t = 5 s (top) and t = 60 min (bottom). The reaction conditions are identical to those listed under Table 3.3 (0 °C, MeCN, 5.0 mM $[Ga(phen)_2Cl_2]Cl$, 500 mM cyclooctene, 1000 mM PAA_R). The *m/z* feature at 244.0344 was assigned to $[Ga(phen)_2(CH_3CO_2)]^{2+}$, indicating that the chlorides are displaced almost instantaneously by the acetic acid in solution. At t = 60 min, this feature has almost completely disappeared; the major feature of this spectrum has *m/z* = 181.0743, which corresponds to protonated phen. Since the $GaCl_3$ salt by itself is unable to catalyze significant alkene epoxidation (Table 3.5), we propose that the oxidation of the phen ligands by PAA_R promotes the dissociation of the ligands from the Ga(III), halting the catalytic activity.

The $[Ga(phen)_2Cl_2]^+$/PAA mixtures oxidize olefins quickly relative to other group 13 metal-containing systems. Previously reported homogeneous and heterogeneous aluminum(III) and gallium(III) catalysts for these reactions have been reported to turn over

up to ~50 times.[13-15, 17] The most successful of these alkene epoxidations were run at a relatively high temperature (80 °C) and required 4−5 h to reach this level of activity.[14-15] In contrast, the turnover number of 87 for the best cyclooctene epoxidation in Table 3.3 was measured at 1 h and corresponded to reactions run at 0 °C. Increasing the reaction temperature to 25 °C did not have a substantial impact on the yield. When cyclohexene epoxidation (MeCN, 10 equiv of additional phen) was run at this temperature, the yield at 3 h only increased from 79% to 82%. Although the time and temperature required for the reactions are both lower than those reported for other group 13 mediated epoxidations, it should be noted that the gallium(III)-promoted epoxidations proceed much more slowly than those catalyzed by Mn^{II}phen complexes and other transition-metal compounds.[28-29, 31-32]

Notably, the only oxidized organic products with the 1% catalyst loading are epoxides. This again contrasts with other reported group 13 catalyzed alkene epoxidations, which produce sizable amounts of alcohols and ketones/aldehydes.[12-15] This selectivity is lost as the catalyst loading is lowered. With a gallium(III) loading of 0.1%, the major products are 3-cyclohexenol (39%) and 1,2-cyclohexanediol (51%); the yield of cyclohexene oxide is only 8%. The new products do not result from further chemical transformation of the epoxide; epoxides do not react with the Ga^{III}/PAA mixtures when used as substrates. The inability of the system to oxidize epoxides suggests that different oxidation mechanisms, as opposed to overoxidation, occur with the higher PAA/Ga^{III} ratio.

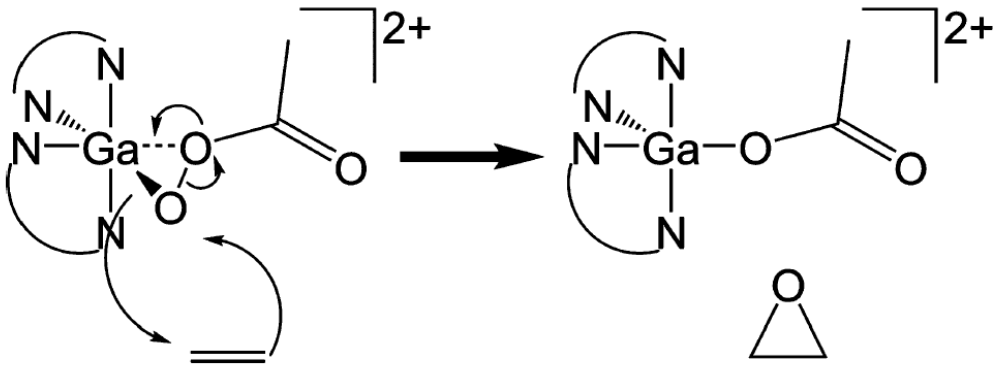

Scheme 3.2 Proposed Sharpless type mechanism

On the basis of our observations, we speculate that the olefin epoxidation proceeds through a Sharpless-type mechanism (Scheme 3.2),[33] as has been proposed for a $[Al(H_2O)_6]^{3+}/H_2O_2$

system.[12] The competitive C−H activation observed in the aluminum(III) system was attributed to the formation of $[Al(H_2O)_4(H_2O_2)(O_2H)]^{2+}$ species.[12] The bidenticity of the phen ligands would be anticipated to hinder similar chemistry in the $[Ga(phen)_2Cl_2]^+$ reactions by better blocking the coordination of a second equiv of terminal oxidant. When the concentration of PAA is much higher, the formation of such species should be more likely. The higher levels of 2:1 PAA/ adducts associated with the 0.1% catalyst loading would account for the observed allylic oxidation.

3.4 Conclusions

In summary, we report the first homogeneous gallium(III) catalyst for olefin epoxidation. Relative to other group 13 catalysts, the activity of $[Ga(phen)_2Cl_2]^+$ is both fast and, with a 1% catalyst loading, exquisitely selective for the epoxide product. We attribute the greater activity and selectivity to the presence of the electron-withdrawing and bidentate 1,10 phenanthroline ligands. Although Ga^{III} is widely perceived to be less Lewis acidic than Al^{III}, the greater affinity of Ga^{III} for these π-accepting N-donor ligands compensates for this deficiency. The results suggest that the full potential of group 13 metals for hydrocarbon oxidation reactions has not yet been realized, and the $[Ga(phen)_2Cl_2]^+$ complex may be a promising lead to other homogeneous, non-transition-metal catalysts.

References

(1) Moskalyk, R. R., *Miner. Eng.* **2003**, *16*, 921-929.

(2) Dagorne, S. and Atwood, D. A., *Chem. Rev.* **2008**, *108*, 4037-4071.

(3) Yamaguchi, M. and Nishimura, Y., *Chem. Commun.* **2008**, 35-48.

(4) Kilyanek, S. M., Fang, X. and Jordan, R. F., *Organometallics.* **2008**, *28*, 300-305.

(5) Fricke, R., Kosslick, H., Lischke, G. and Richter, M., *Chem. Rev.* **2000**, *100*, 2303-2406.

(6) Balskus, E. P. and Jacobsen, E. N., *Science* **2007**, *317*, 1736-1740.

(7) Tewari, B. B., Shekar, S., Huang, L., Gorrell, C. E., Murphy, T. P., Warren, K., Nesnas, N. and Wehmschulte, R. J., *Inorg. Chem.* **2006**, *45*, 8807-8811.

(8) Larock, R. C., Comprehensive Organic Transformations, 2nd ed; *Wiley-VCH: New York* **1999**.

(9) Gu, W., Haneline, M. R., Douvris, C. and Ozerov, O. V., *J. Am. Chem. Soc.* **2009**, *131*, 11203-11212.

(10) Oppenauer, R. V., *Recl. Trav. Chim. Pays-Bas* **1937**, *56*, 137-144.

(11) Meerwein, H. and Schmidt, R., *Justus Liebigs Ann. Chem.* **1925**, *444*, 221-238.

(12) Kuznetsov, M. L., Kozlov, Y. N., Mandelli, D., Pombeiro, A. J. L. and Shul'pin, G. B., *Inorg. Chem.* **2011**, *50*, 3996-4005.

(13) Nam, W. and Valentine, J. S., *J. Am. Chem. Soc.* **1990**, *112*, 4977-4979.

(14) Pescarmona, P. P., Janssen, K. P. F. and Jacobs, P. A., *Chem. Eur. J.* **2007**, *13*, 6562-6572.

(15) Rinaldi, R., de Oliveira, H. F. N., Schumann, H. and Schuchardt, U., *J. Mol. Catal. A: Chem.* **2009**, *307*, 1-8.

(16) Rinaldi, R. and Schuchardt, U., *J. Catal.* **2005**, *236*, 335-345.

(17) Stoica, G., Santiago, M., Jacobs, P. A., Pérez-Ramírez, J. and Pescarmona, P. P., *Appl. Catal., A* **2009**, *371*, 43-53.

(18) Verley, A., *Bull. Soc. Chim. Fr.* **1925**, *37*, 537.

(19) Ponndorf, W., *Angew. Chem.* **1926**, *39*, 138-143.

(20) Ivanov-Emin, B. N. N. s., L. A.; Rabovik, Ya. I.; Larionova, L. E., *Russ. J. Inorg. Chem.*

1961, *6*, 1142-1146.

(21) Carty, A. J., Dymock, K. R. and Boorman, P. M., *Can. J. Chem.* **1970**, *48*, 3524-3529.

(22) McPhail, A. T., Miller, R. W., Pitt, C. G., Gupta, G. and Srivastava, S. C., *J. Chem. Soc., Dalton Trans.* **1976**, 1657-1661.

(23) Junk, P. C., Skelton, B. W. and White, A. H., *Aust. J. Chem.* **2006**, *59*, 147-154.

(24) Restivo, R. and Palenik, G. J., *J. Chem. Soc., Dalton Trans.* **1972**, 341-344.

(25) Sofetis, A., Raptopoulou, C. P., Terzis, A. and Zafiropoulos, T. F., *Inorg. Chim. Acta* **2006**, *359*, 3389-3395.

(26) DiPasquale, A. G. and Mayer, J. M., *J. Am. Chem. Soc.* **2008**, *130*, 1812-1813.

(27) E.I. du Pont de Nemours & Co. Hawkinson, U.S. 2,910,504, **1959**.

(28) Murphy, A., Pace, A. and Stack, T. D. P., *Org. Lett.* **2004**, *6*, 3119-3122.

(29) Murphy, A. and Stack, T. D. P., *J. Mol. Catal. A: Chem.* **2006**, *251*, 78-88.

(30) Bencini, A. and Lippolis, V., *Coordin. Chem. Rev.* **2010**, *254*, 2096-2180.

(31) White, M. C., Doyle, A. G. and Jacobsen, E. N., *J. Am. Chem. Soc.* **2001**, *123*, 7194-7195.

(32) Jacobsen, E. N., Zhang, W., Muci, A. R., Ecker, J. R. and Deng, L., *J. Am. Chem. Soc.* **1991**, *113*, 7063-7064.

(33) Sharpless, K. B., Townsend, J. M. and Williams, D. R., *J. Am. Chem. Soc.* **1972**, *94*, 295-296.

Chapter 4

Catalysis of Alkene Epoxidation by a Series of Gallium(III) Complexes with Neutral N-Donor Ligands*

* This chapter derived from a manuscript in preparation to be submitted to a peer-reviewed scientific journal, co-authored by Wenchan Jiang, John D. Gorden, and Christian R. Goldsmith.

4.1 Introduction

The coordination chemistry of gallium has been investigated to serve a number of applications, including the development of volatile precursors for gallium oxide, nitride, selenide, arsenide, and sulfide layers in chemical vapor deposition[1-7] as well as ^{68}Ga-containing radiopharmaceuticals suitable for positron emission tomography.[8-11] Gallium(III) compounds have also garnered attention for their capabilities to act as homogeneous Lewis acid catalysts.[7, 12-16] One trend observed in the aforementioned catalysis is that cationic Ga(III) species tend to promote faster and more extensive reactivity.

Recently, our group reported that the previously known compound $[Ga(phen)_2Cl_2]Cl$ (phen = 1,10-phenanthroline)[17-19] could catalyze the epoxidation of alkenes by peracetic acid.[20] This is a rare example of gallium accelerating an oxidation-reduction reaction[21-24] and to the best of our knowledge, represents the first instance of a homogeneous Ga(III) catalyst for olefin epoxidation. The reactivity proceeded more quickly and at a lower temperature than analogous reactions catalyzed by Al(III) complexes.[25-27] We attributed the activity of $[Ga(phen)_2Cl_2]^+$ to the presence of the neutral and relatively electron-poor phen ligands, which appear to remain bound to the Ga(III) during the catalysis.[20] Without these ligands, the oxidation does not proceed; $GaCl_3$ by itself is not a competent catalyst. Neutral N-donor ligands do not commonly coordinate to Al(III), which instead prefers to ligate harder bases. These ligands' affinities for Ga(III), however, are considerably higher.[28] Although the complexation of Ga(III) to polydentate neutral N-donor ligands could result in enhanced catalytic activity for Group 13 metals, this chemistry has never been systematically studied.

Here, we report the syntheses and characterizations of six Ga(III) complexes with neutral N-donor ligands (Scheme 4.1). The ligands were selected to interrogate the influences of ligand denticity and electronics on the catalytic activity. One noted shortcoming with the $[Ga(phen)_2Cl_2]^+$ system is that its catalysis essentially ends after approximately 1 h.[20] Replacing the two bidentate phen ligands with a single more highly coordinating molecule extends the lifetime of the catalysis and increases the optimum yield of the epoxides, although the activity decreases if the ligand has the capacity to bind in a penta- or

hexadentate fashion. The more electron-poor ligands promote more extensive alkene epoxidation, with the best activity being associated with 5-nitro-1,10-phenanthroline (NO_2-phen).

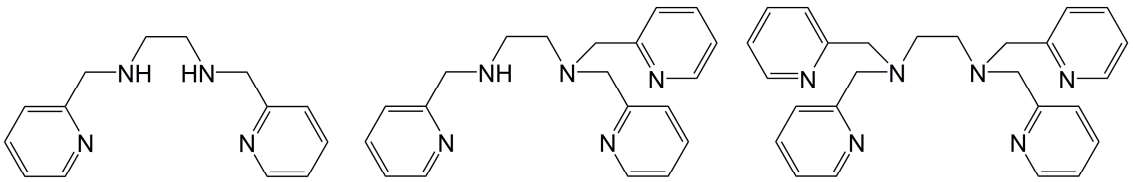

bispicen
[Ga(bispicen)Cl_2]Cl **1**

trispicen
[Ga(trispicen)Cl_2]Cl **2**

tpen
[Ga(tpen)Cl_2]Cl **3**

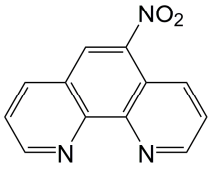

NO_2-phen
[Ga(NO_2-phen)$_2Cl_2$]Cl **4**

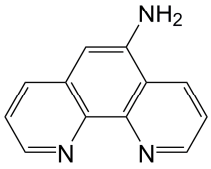

NH_2-phen
[Ga(NH_2-phen)$_2Cl_2$]Cl **5**

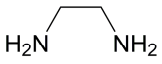

en
[Ga(en)$_2Cl_2$]Cl **6**

Scheme 4.1 Neutral N-donor ligands

4.2 Experimental

Materials

Cyclooctene, cyclohexene, styrene, 1-octene, 4-vinylcyclohexene, 1,2-ethanediamine (en), 5-amino-1,10-phenanthroline (NH_2-phen), 5-nitro-1,10-phenanthroline (NO_2-phen), and gallium trichloride ($GaCl_3$) were purchased from Sigma-Aldrich and used as received. Methylene chloride (CH_2Cl_2) was bought from Macron Chemicals. Anhydrous acetonitrile (MeCN) and methanol (MeOH) were procured from Acros. Diethyl ether (ether) was obtained from J. T. Baker. Deuterated chloroform ($CDCl_3$), acetonitrile (CD_3CN), dimethylsulfoxide (DMSO-*d6*), water (D_2O), and methanol (CD_3OD) were purchased from Cambridge Isotopes.

Peracetic acid (PAA_R) was prepared through a previously described procedure that uses an acidic resin as the catalyst in place of the more commercially used sulfuric acid.[29] 50% H_2O_2 (17 g, 0.25 mol) was slowly added to 150 g of glacial acetic acid (2.5 mol) in a room temperature (RT) polyethylene bottle. After the addition was complete, 5.0 g of Amberlite IR-120 was added, and the reaction mixture was stirred behind a blast shield for 24 h at RT. After this time, the solution was filtered to remove the resin and yield the 7.5% wt PAA_R solution used for the reactivity experiments. The solution was stored in a freezer when not in use. The concentration of PAA_R was determined by comparing the intensities of the ^{13}C NMR resonances of CH_3CO_3H and CH_3CO_2H.

CAUTION: Peracids and their mixtures with organic solvents are potentially explosive and should be handled judiciously. The potential hazards can be minimized by using minimal amounts of these materials at lower temperatures and by using proper protective equipment, such as blast shields.

Instrumentation

All ^1H nuclear magnetic resonance (NMR) spectra were acquired on either a 250, 400, or 600 MHz AV Bruker NMR spectrometer at 294 K. All resonances were referenced to internal standards. Atlantic Microlabs (Norcross, GA) performed all elemental analyses. A Shimadzu IR Prestige-21 FT-IR spectrophotometer was used for the described infrared (IR) spectroscopy. Gas chromatography (GC) data were obtained using a ThermoScientific Trace GC Ultra spectrometer with a flame ionization detector. High-resolution mass spectrometry (HR-MS) data were collected at the Mass Spectrometer Center at Auburn University using a Bruker microflex LT MALDI-TOF mass spectrometer via direct probe analysis operated in the positive ion mode.

X-ray Crystallography

X-ray diffraction data were acquired using a Bruker SMART APEX CCD X-ray diffractometer and Mo Kα radiation. Crystalline samples were mounted in Paratone-N oil on glass fibers. The program SMART (v 5.624) was used for the preliminary determination of cell constants and data collection control. Determination of integrated intensities and global cell refinement were performed with the Bruker SAINT software package using a

narrow-frame integration algorithm. The program suite SHELXTL (v 5.1) was used for space group determination, structure solution, and refinement.[30] Refinement was performed against F^2 by weighted full-matrix least-square, and empirical absorption correction (SADABS) were applied.[31] Hydrogen atoms were placed at calculated positions using suitable riding models with isotropic displacement parameters derived from their carrier atoms. Crystallographic data are provided in Table 4.1.

Syntheses

The ligands *N,N'*-bis(2-pyridylmethyl)-1,2-ethanediamine (bispicen), *N,N,N'*-tris(2-pyridylmethyl)-1,2-ethanediamine (trispicen), and *N,N,N',N'*-tetrakis(2-pyridylmethyl)-1,2-ethanediamine (tpen) were prepared as described previously.[32-34] The identities and purities of these compounds were confirmed by NMR.

***cis*-Dichloro(*N,N'*-Bis(2-pyridylmethyl)-1,2-ethanediamine)gallium(III) chloride (1).** $GaCl_3$ (0.164 g, 0.931 mmol) and bispicen (0.227 g, 0.937 mmol) were dissolved in 10 mL of CH_2Cl_2 and stirred at RT under N_2. After 2 h, ether was added to the cloudy solution, precipitating 0.360 g of the product as a white powder (82%). Colorless crystals were grown from the slow diffusion of ether into a saturated solution of the complex in MeOH. ^{1}H NMR (CD_3OD, 400 MHz): 9.41 (2H, d, J = 5.2 Hz), 8.24 (2H, t, J = 7.6 Hz), 7.77 (2H, t, J = 6.4 Hz), 7.71 (2H, d, J = 7.6 Hz), 4.88 (2H, d, J = 17.2 Hz), 4.18 (2H, d, J = 17.2 Hz), 2.69 (2H, d, J = 9.2 Hz), 2.53 (2H, d, J = 9.2 Hz). ^{13}C NMR (CD_3OD, 150 MHz): 153.7, 147.0, 143.0, 125.8, 124.6, 51.5, 47.0. IR (KBr, cm^{-1}): 3416 (s), 3389 (s), 3100 (s), 3040 (s), 2991 (s), 2914 (s), 2850 (s), 2482 (w), 2395 (w), 2270 (w), 2166 (w), 1665 (w), 1612 (s), 1578 (m), 1481 (s), 1440 (s), 1363 (s), 1300 (s) 1262 (m), 1226 (s), 1160 (m), 1099 (s), 1048 (s), 1033 (s), 980 (m), 906 (w), 849 (m), 821 (w), 777 (s), 723 (m), 649 (m), 567 (m), 506 (m), 480 (m), 425 (m). Elemental Analysis: Calcd for $C_{14}H_{18}N_4GaCl_3 \cdot H_2O$: C, 38.53%; H, 4.62%; N, 12.84%; Found: C, 38.32%; H, 4.53%; N, 12.51%.

Dichloro(*N,N,N'*-tris(2-pyridylmethyl)-1,2-ethanediamine)gallium(III) chloride (2). $GaCl_3$ (0.189 g, 1.074 mmol) and trispicen (0.359 g, 1.079 mmol) were dissolved in 10 mL of CH_2Cl_2 (2 mL). The resultant solution was stirred for 2 h at RT under N_2. The addition of ether deposited the product as a pale yellow powder (0.356 g, 65%). ^{1}H NMR (CD_3OD, 400

MHz): 9.40 (1H, d, J = 4.4 Hz), 9.17 (1H, d, J = 4.4 Hz), 8.45 (1H, d, J = 5.2 Hz), 8.26 (2H, m), 7.96 (2H, m), 7.83 (2H, m), 7.61 (1H, d, J = 5.2 Hz), 7.55 (1H, t, J = 4.4 Hz), 7.16 (1H, d, J = 3.6 Hz), 4.56 (1H, d, J = 15.6 Hz), 4.49 (1H, d, J = 15.6 Hz), 4.08 (1H, d, J = 14.4 Hz), 3.58 (4H, m), 3.20 (1H, m), 2.93 (1H, m), 2.84 (1H, m). ^{13}C NMR (CD_3OD, 150 MHz): 148.5, 147.9, 147.5, 146.0, 144.7, 144.6, 143.5, 128.8, 128.1, 127.9, 127.1, 126.3, 126.2, 124.7, 61.2, 61.1, 56.8, 53.1, 47.5. IR (KBr, cm^{-1}): 3487 (s), 3387 (s), 3334 (s), 3115 (s), 2850 (s), 2657 (s), 2476 (m), 2392 (m), 2271 (m), 2157 (m), 2034 (w), 1936 (w), 1882 (w), 1815 (w), 1747 (w), 1611 (s), 1478 (s), 1438 (s), 1363 (s), 1298 (s), 1230 (s), 1159 (s), 1107 (s), 1040 (s), 1031 (s), 977 (s), 910 (w), 849 (m), 777 (s), 720 (m), 646 (m), 565 (m), 492 (m), 424 (m). Elemental Analysis: Calcd for $C_{20}H_{23}N_5GaCl_3$: C, 47.15%; H, 4.55%; N, 13.75%; Found: C, 47.44%; H, 4.45%; N, 13.36%.

Dichloro(*N,N,N',N'*-tetrakis(2-pyridylmethyl)-1,2-ethanediamine)gallium(III) chloride (3). $GaCl_3$ (0.134 g, 0.761 mmol) and tpen (0.324 g, 0.763 mmol) were dissolved in 10 mL of CH_2Cl_2 under N_2. The resultant solution stirred for 2 h at RT, after which excess ether was added to precipitate 0.388 g of the product as a white powder (85%). ^{1}H NMR ($CDCl_3$, 250 MHz): 9.61 (2H, d, J = 5.4 Hz), 8.64 (2H, d, J = 4.8 Hz), 8.19 (2H, t, J = 8.2 Hz), 7.85 (2H, m), 7.74 (2H, t, J = 6.8 Hz), 7.60 (4H, m), 7.39 (2H, m), 5.09 (2H, d, J = 16.2 Hz), 4.65 (2H, d, J = 13.2 Hz), 4.20 (2H, d, J = 11.4 Hz), 3.60 (4H, m), 3.00 (2H, m). ^{1}H NMR (CD_3CN, 400 MHz): 9.52 (2H, d, J = 5.2 Hz), 8.63 (2H, d, J = 5.6 Hz), 8.21 (2H, t, J = 8.0 Hz), 7.83 (2H, t, J = 5.6 Hz), 7.75 (2H, t, J = 6.4 Hz), 7.62 (4H, d, J = 7.6 Hz), 7.41 (2H, m), 4.93 (2H, d, J = 16.0 Hz), 4.56 (2H, d, J = 13.6 Hz), 3.97 (2H, d, J = 16.4 Hz), 3.61 (2H, d, J = 13.6 Hz), 3.48 (2H, d, J = 5.2 Hz), 3.27 (2H, d, J = 5.2 Hz). ^{13}C NMR ($CDCl_3$, 100 MHz): 151.9, 151.5, 149.9, 147.0, 142.8, 137.5, 127.5, 126.6, 125.6, 124.2, 56.6, 56.4, 46.3. IR (KBr, cm^{-1}): 3045 (m), 3008 (s), 2945 (s), 2907 (s), 2863 (s), 2815 (s), 2800 (s), 2764 (s), 2695 (m), 2550 (w), 2300 (w), 1905 (w), 1859 (w), 1796 (w), 1662 (w), 1588 (s), 1572 (s), 1472 (s), 1433 (s), 1364 (s), 1345 (s), 1298 (s), 1245 (s), 1209 (m), 1170 (s), 1126 (s), 1085 (m), 1045 (m), 1016 (w), 989 (s), 902 (m), 864 (m), 839 (m), 786 (s), 765 (s), 732 (m), 687 (w), 662 (w), 617 (m), 593 (w), 546 (w), 470 (w). MS (ESI): Calcd for $[Ga(tpen)Cl_2]^+$, 563.1008; Found, 563.0988. Elemental Analysis: Calcd for $C_{26}H_{28}N_6GaCl_3$: C, 51.99%; H, 4.70%; N, 13.99%; Found: C,

51.70%; H, 4.65%; N, 14.00%.

Dichlorobis(5-nitro(1,10-phenanthroline)gallium(III) chloride (4). $GaCl_3$ (0.169 g, 0.959 mmol) and NO_2-phen (0.437 g, 1.94 mmol) were combined in 10 mL of CH_2Cl_2 under N_2. After the solution was stirred for 2 h at RT, ether was added, precipitating 0.332 g of the product as a pale yellow powder (51%). ^{1}H NMR (CD_3OD, 600 MHz): 10.35 (2H, m), 9.82 (1H, d, *J* = 12.0 Hz), 9.50 (1H, d, *J* = 8.4 Hz), 9.44 (1H, s), 9.33 (2H, m), 9.03 (1H, d, *J* = 8.4 Hz), 8.67 (2H, m), 8.06 (1H, d, *J* = 3.6 Hz), 8.02 (1H, d, *J* = 3.6 Hz), 7.86 (2H, m). ^{13}C NMR (CD_3OD, 150 MHz): 155.9, 153.4, 151.8, 149.6, 148.0, 147.2, 146.6, 146.3, 146.0, 144.6, 141.4, 140.0, 139.5, 139.0, 133.2, 131.1, 129.6, 129.3, 129.0, 128.4, 128.1, 127.1, 126.8, 124.9, 124.5. IR (KBr, cm^{-1}): 3422 (m), 3113 (w), 3071 (m), 3004 (w), 2970 (w), 2934 (w), 2871 (w), 2337 (w), 1970 (w), 1946 (w), 1841 (w), 1627 (m), 1586 (m), 1540 (s), 1522 (s), 1507 (s), 1490 (m), 1453 (m), 1421 (s), 1388 (m), 1349 (s), 1335 (s), 1261 (w), 1207 (m), 1181 (m), 1153 (m), 1117 (m), 1104 (m), 1038 (w), 992 (w), 974 (w), 920 (m), 838 (s), 823 (s), 810 (m), 751 (m), 734 (s), 721 (s), 652 (m), 619 (w), 541 (w), 507 (w), 429 (w). Elemental Analysis: Calcd for $C_{24}H_{14}N_6GaCl_3 \cdot 3H_2O$: C, 42.34%; H, 2.96%; N, 12.35%; Found: C, 42.56%; H, 2.73%; N, 12.11%.

Dichlorobis(5-amino(1,10-phenanthroline)gallium(III) chloride (5). $GaCl_3$ (0.104 g, 0.589 mmol) and NH_2-phen (0.228 g, 1.18 mmol) were dissolved in 10 mL of MeCN under N_2. The solution was allowed to stir for 2 h at RT. After this time, excess ether was added to precipitate 0.287 g of the product as a yellow powder (87%). ^{1}H NMR (DMSO-*d6*, 250 MHz): 10.00 (1H, t, *J* = 5.2 Hz), 9.54 (2H, m), 9.06 (1H, d, *J* = 8.0 Hz), 8.88 (1H, d, *J* = 8.5 Hz), 8.55 (1H, m), 8.40 (1H, d, *J* = 8.2 Hz), 8.28 (1H, m), 7.71 (2H, m), 7.45 (1H, m), 7.25 (2H, m), 7.10 (1H, s). ^{1}H NMR (CD_3OD, 600 MHz): 10.18 (1H, d, J = 16.5 Hz), 9.74 (1H, d, J = 16.2 Hz), 9.39 (1H, t, J = 6.9 Hz), 8.91 (1H, d, *J* = 7.8 Hz), 8.75 (1H, m), 8.46 (1H, m), 8.27 (1H, d, *J* = 7.8 Hz), 8.21 (1H, m), 7.66 (2H, m), 7.40 (1H, m), 7.25 (2H, m), 7.14 (1H, s). ^{13}C NMR (DMSO-*d6*, 62.5 MHz): 148.2, 145.1, 144.9, 144.7, 144.5, 142.6, 138.9, 138.3, 137.2, 136.9, 136.4, 136.0, 132.4, 132.0, 129.6, 128.8, 126.6, 126.3, 125.5, 125.2, 122.8, 122.3, 101.0, 100.8. IR (KBr, cm^{-1}): 3399 (s), 3339 (s), 3208 (s), 3080 (m), 1640 (s), 1620 (s), 1604 (s), 1586 (m), 1522 (w), 1494 (s), 1465 (m), 1435 (s), 1350 (w), 1323 (w), 1287 (w), 1226

(w), 1164 (w), 1146 (w), 1122 (w), 1087 (w), 913 (w), 851 (w), 826 (w), 802 (w), 725 (s), 665 (w), 653 (w), 427 (w). Elemental Analysis: Calcd for $C_{24}H_{18}N_6GaCl_3 \cdot H_2O$: C, 49.31%; H, 3.45%; N, 14.38%; Found: C, 49.56%; H, 3.43%; N, 14.51%.

Dichlorobis(1,2-ethanediamine)gallium(III) chloride (6). $GaCl_3$ (0.214 g, 1.22 mmol) and ethylenediamine (165 μL, 2.46 mmol) were dissolved in 10 mL of MeCN under N_2. As the reaction stirred for 2 h, a white precipitate began to form. The addition of ether deposited more solid. 0.320 g of the product was isolated as a white powder (79%). ^{1}H NMR (DMSO-*d6*, 400 MHz): 3.07 (8H, s). ^{1}H NMR (D_2O, 600 MHz): 3.14 (8H, s). ^{13}C NMR (DMSO-*d6*, 100 MHz): 36.57. ^{13}C NMR (D_2O, 150 MHz): 39.31. IR (KBr, cm^{-1}): 3420 (s), 3225 (s), 2978 (s), 2912 (s), 2804 (s), 2747 (s), 2711 (s), 2677 (s), 2634 (s), 2575 (m), 2521 (m), 2420 (m), 2280 (w), 2055 (m), 1624 (m), 1602 (m), 1504 (s), 1342 (w), 1182 (w), 1085 (m), 1034 (s), 1008 (w), 973 (w), 917 (w), 786 (w), 568 (m), 467 (m), 445 (w), 431 (w). Elemental Analysis: Calcd for $C_8H_{16}N_4GaCl_3 \cdot 2H_2O$: C, 14.46%; H, 6.07%; N, 16.86%; Found: C, 14.61%; H, 6.03%; N, 16.71%.

Reactivity Studies

All reactions were run in MeCN at 273 K under N_2, with the initial concentrations of the catalyst, alkene, and PAA_R being 5.0 mM, 500 mM, and 1.0 M, respectively. Most reactions were allowed to proceed for 1 h. At the end of each reaction, excess ether was added to precipitate the Ga(III) compound, effectively quenching the catalysis. For the studies focusing on the catalytic activity as a function of time, aliquots were taken at the indicated time points. Each portion was quenched with excess ether and filtered through a plug of silica gel to remove the remaining peracetic acid and Ga(III) salts. Control studies confirmed that this workup removed neither the olefin starting material nor the epoxide product from the solution. The remaining alkene and epoxide products were quantified relative to an internal standard of 1,2-dichlorobenzene, which is inert under the reaction conditions. All reactions were run at least three times to ensure reproducibility. All reported values are the averages of the results from these reactions. The errors represent one standard deviation.

4.3 Results

Synthesis and Characterization

The syntheses of the Ga(III) complexes proceed in a straightforward manner, and simply mixing the $GaCl_3$ salt and ligand in room temperature CH_2Cl_2 or MeCN is sufficient to ensure complexation. The compounds with the polydentate pyridylamine ligands (bispicen, trispicen, tpen) can be isolated in high purities and yields (77-85%) through precipitation from CH_2Cl_2/ether mixtures. Compounds **1**-**3** tend to be hygroscopic and noticeably moisten upon prolonged exposure to air. The compounds with the bidentate ligands (NO_2-phen, NH_2-phen, en) are prepared in moderate to high yields (51-87%) through precipitation. The en complex **6** is the least soluble of the six Ga(III) compounds in organic solvents. Complexes **4**-**6** appear to be more hygroscopic than compounds **1**-**3**, as we were unable to exclude water from the elemental analyses of the former. When the syntheses of **1**-**6** were run under air instead of N_2, much lower yields of the desired products were obtained.

The Ga(III) complexes are diamagnetic and nearly colorless, as anticipated. The 294 K ^{1}H NMR spectrum of the bispicen complex **1** has four resonances in the aromatic region, indicating that its two pyridine rings are equivalent at this temperature. The doublet at 9.41 ppm is assigned to the protons on the 6-positions of the pyridine rings. These resonances tend to be exquisitely sensitive to metal ion coordination, and their chemical shifts can be used to assess whether the affiliated pyridine rings bind to the Ga(III).[35] The resonances at 4.88 and 4.18 ppm indicate that there are two sets of methylene protons. This pattern is inconsistent with a *trans* ligand conformation, which has a sufficiently high symmetry to render all of the methylene protons equivalent. The splitting pattern is consistent with each methylene carbon bonding to two inequivalent protons and suggests a C_2 symmetry for the Ga(III) complex in solution. The ^{13}C NMR spectrum features only seven resonances, providing further evidence that the two halves of the bispicen ligand are equivalent in solution. The NMR data suggest that **1** retains the *cis*-α ligand conformation observed in its crystal structure (*vida infra*).

The ^{1}H NMR spectrum of the trispicen complex **2** has two doublets at 9.40 and 9.17 ppm that are comparable in energy to the 9.41 ppm resonance observed for **1**. We have therefore

assigned these as corresponding to the protons on the 6-positions of Ga(III)-bound pyridine rings. The integrated intensity of each of these doublets corresponds to one proton, suggesting that the two associated pyridines are inequivalent at 294 K. The resonance for the third pyridine ring's 6-position proton appears at a significantly lower chemical shift (8.45 ppm), suggesting that it does not coordinate to the Ga(III). The inequivalence of the two coordinated pyridine rings is supported by the acquired ^{13}C NMR spectrum. If the pyridines were equivalent, we would observe 14 ^{13}C resonances at most; instead, 19 resonances can be unambiguously identified. The conformation of the four coordinated N-donors cannot be assigned with certainty; Scheme 4.2 shows three possible solution structures in which the two chlorides are coordinated *cis* to each other.

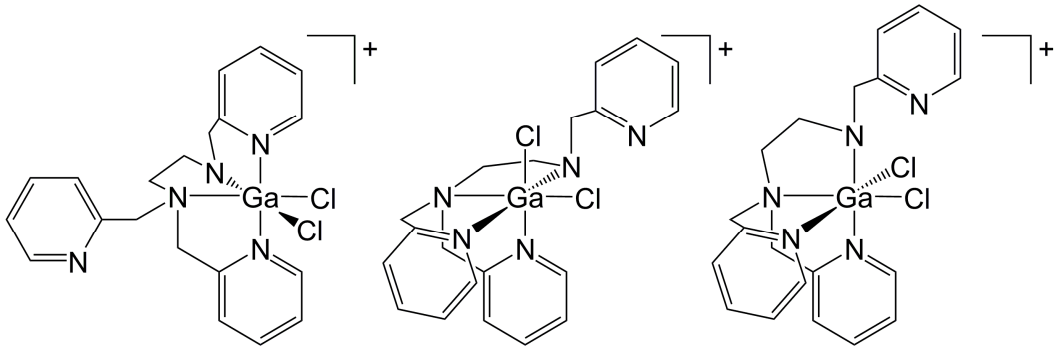

Scheme 4.2 Possible solution structures of **2**

The tpen complex **3** likewise appears to have the pyridylamine ligand coordinated to the metal in a hypodentate fashion. The ^{1}H NMR spectra in CD_3CN and $CDCl_3$ strongly resemble each other, suggesting that MeCN does not displace the chlorides to an observable degree. The NMR spectra are consistent with a structure with two pendant pyridine rings. This is again most apparent from consideration of the protons on the 6-position of the pyridine moieties, which are evenly split between doublet resonances at ~9.6 (bound) and ~8.6 ppm (unbound). There are four doublets that can be reasonably assigned to methylene protons; as with **1**, this pattern is consistent with a C_2 symmetry and a *cis*-α conformation of the N-donors. The number of resonances in the ^{13}C NMR data suggests that the two halves of the tpen ligand are equivalent in solution, supporting the assignment of a C_2 symmetric species. High-resolution mass spectrometric analysis of **3** detects a $[Ga(tpen)Cl_2]^+$ cation; consequently, we believe that the Ga(III) center in **3**, like those in **1** and **2**, is primarily

coordinated by a N_4Cl_2 set of donor atoms in solution. The mode of tpen coordination that is most consistent with the data is depicted in Scheme 4.3. The exchange between the pendant and bound pyridines appears to be slow; we observe neither broadening nor coalescing of the ^{1}H NMR signals as samples of **3** in CD_3CN are heated from 294 K to 324 K.

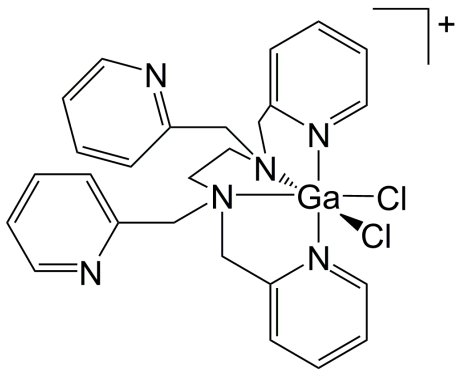

Scheme 4.3 Proposed solution structure of **3**

The solution structures of the two Ga(III) complexes with the phen derivatives are more difficult to interpret. Potentially, two 5-derivatized phen ligands could coordinate to the metal ion to form six isomers of *cis*-$[Ga(R\text{-phen})_2Cl_2]^+$; these six are comprised of three pairs of enantiomers (Scheme 4.4). Given that the *cis* conformation is present in the structures of both $[Ga(phen)_2Cl_2]^+$ and $[Ga(phen)_2Br_2]^+$,[20, 36] we suspect that additional *trans* isomers are not present in significant quantities, although the data certainly cannot preclude such a possibility. The ^{1}H and ^{13}C NMR spectra of the two Ga(III) complexes with NO_2-phen and NH_2-phen, **4** and **5**, display more resonance features than would be anticipated from the uncoordinated ligands. This demonstrates that the isomers of the Ga(III) complexes, like complex **3**, have limited fluxionality at room temperature. Rapid isomerization of **4** and **5** would result in seven and eight observable ^{1}H NMR resonances, respectively; instead, we observe ten and twelve features. As with **3**, we do not observe any ^{1}H NMR resonances broaden or shift as samples of **4** are heated to 324 K. Given the number of multiplets observed in the ^{1}H NMR spectra, we currently believe that **4** and **5** each exist as a mixture of multiple *cis* isomers in solution.

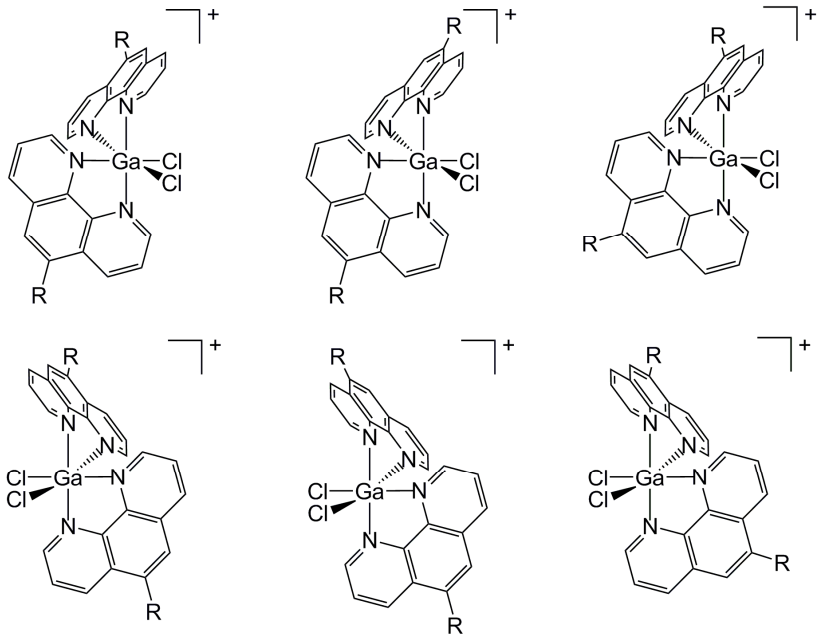

R = NO_2 (**4**), NH_2 (**5**)

Scheme 4.4 – Possible conformations of the phen ligands in complexes **4** and **5**

The ^{1}H and ^{13}C NMR spectra of the en complex **6** each contain a single resonance, consistent with the presence of a single compound with two chemically equivalent en ligands. These NMR spectra are distinct from those of free en in both DMSO-*d6* and D_2O, indicating that the ligand is indeed chelating the metal ion. The data in D_2O suggest that the Ga(III)-N bonds remain intact in solvents that can potentially ligate the Ga(III) center.

Infrared Spectroscopy

IR measurements provide support for the modes of coordination suggested by the NMR data. The IR spectrum of non-coordinated pyridine features a C-N stretch at 1578 cm^{-1}; coordination to a metal ion typically shifts this frequency to the 1590-1615 cm^{-1} range.[37] The IR spectra of complexes **1**-**3** display stronger absorbance in the 1560-1580 cm^{-1} region as the number of pyridine rings increases (Figure A5, A8, A13), with complexes **1** and **3** having weak and strong bands at 1578 cm^{-1} and 1572 cm^{-1}, respectively. The presence of this peak for **1** is unexpected and may result from either another vibrational mode or from the partial dissociation of the ligand during the preparation of the KBr pellet. Complex **2** lacks a distinct band in the 1560-1580 cm^{-1} range, but its 1611 cm^{-1} feature has a prominent shoulder that

extends into this region. All three complexes have intense bands where the C-N stretches of coordinated pyridines are expected (1612, 1611, and 1588 cm^{-1} for **1**, **2**, and **3** respectively).

X-ray Crystallography

Crystals of **1** were grown from the slow diffusion of ether into saturated MeOH solutions (Table 4.1). The X-ray diffraction data confirm that the composition of **1** is [Ga(bispicen)Cl_2]Cl (Figure 4.1). The outer-sphere chloride is 3.19 Å from one of the amine nitrogens, which may be consistent with a N-H···Cl hydrogen bond.[38] In the cation, the bispicen ligand is bound to the Ga(III) in a *cis*-α conformation, which is commonly seen in the ligand's complexes with transition metal ions,[39-43] and contributes to an overall distorted octahedral coordination geometry around the metal center. In gallium chemistry, *cis*-α conformation of four N-donors has also been observed in complexes with N_4O_2 coordination spheres.[11, 28] The Ga-N and Ga-Cl bond lengths observed for **1** are typical for a hexacoordinate Ga(III) complex with a N_4Cl_2 donor atom set.[20, 44, 45] The Ga-N bond lengths differ only slightly, and the symmetry of the cation is approximately C_2.

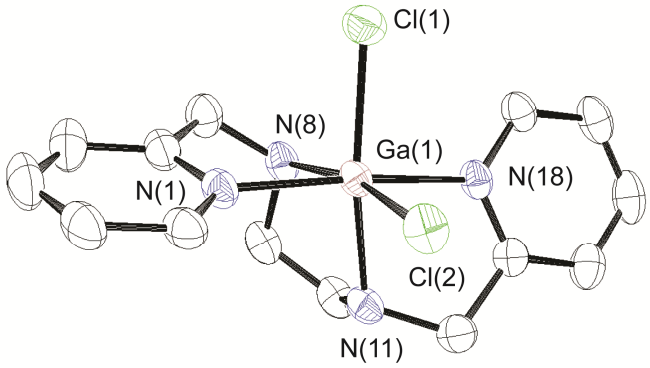

Figure 4.1. ORTEP representation of the cation [Ga(bispicen)Cl_2]$^+$. All hydrogen atoms, the Cl^- counterion, and three non-coordinated water molecules have been removed for clarity. All thermal ellipsoids are drawn at 50% probability.

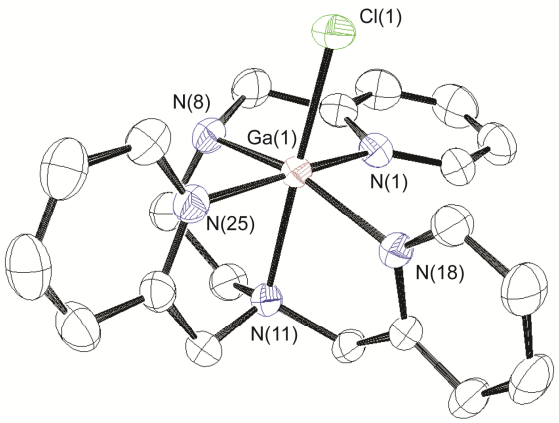

Figure 4.2. ORTEP representation of the dication $[Ga(trispicen)Cl]^{2+}$. All hydrogen atoms, the Cl^- and $[GaCl_4]^-$ counteranions, and a non-coordinated MeCN molecule have been removed for clarity. All thermal ellipsoids are drawn at 50% probability.

Table 4.1. Selected crystallographic data for $[Ga(bispicen)Cl_2]Cl$ (**1**) and $[Ga(trispicen)Cl](GaCl_4)(Cl)$ (**7**)

Parameter	$[Ga(bispicen)Cl_2]Cl•3H_2O$	$[Ga(trispicen)Cl](GaCl_4)(Cl)•MeCN$
Formula	$C_{14}H_{24}Cl_3GaN_4O$	$Ga_2H_{26}Cl_6Ga_2N_6$
M_W	472.45	727.64
Crystal system	Monoclinic	Triclinic
Space group	*$P2_1/c$(#14)*	*$P\bar{1}$ (#2)*
a (Å)	13.7249(5)	9.2381(7)
b (Å)	7.3885(3)	12.0453(9)
c (Å)	20.7913(8)	14.7889(11)
α (deg)	90	88.9220(10)
β (deg)	105.600(1)	79.7160(10)
γ (deg)	90	69.0670(10)
V ($Å^3$)	2030.70(14)	1510.5(2)
Z	4	2
Cryst color	Colorless	Colorless
T (K)	296	296
Reflns collected	63556	59468
Unique reflns	4194	7113
R1 (F, $I > 2\sigma(I)$)	0.0302	0.0327
wR2 (F^2, all data)	0.0828	0.0728

$R1 = \Sigma \| |F_o| - |F_c| \| / \Sigma |F_o|$; $wR2 = [\Sigma w(F_o^2 - F_c^2)^2 / \Sigma w(F_o^2)^2]^{1/2}$.

Crystals were also grown from saturated solutions of **2** in mixtures of MeOH and MeCN (Table 4.1). The structural data, however, correspond to the formula [Ga(trispicen)Cl](GaCl$_4$)(Cl) (**7**, Figure 4.2), as opposed to [Ga(trispicen)Cl$_2$]Cl. Given that only the latter composition is consistent with the NMR, IR, and elemental analysis data for freshly isolated solid samples of **2**, we believe that **2** converts to **7** over the prolonged period of time required for crystal growth. In the structure of **7**, the bound trispicen is κ-5 rather than κ-4. Two different counteranions are in the outer sphere: [GaCl$_4$]$^-$ and Cl$^-$. The presence of the tetrachlorogallate(III) anion indicates that some of the Ga(III) in the sample had dissociated from the trispicen ligand over the time required for crystallization.

Crystals that grew from saturated solutions of **3** were likewise consistent with decomposition products rather than the formula anticipated from the NMR and elemental analysis of the freshly precipitated product. In some cases, the Ga(III) centers in the crystals were coordinated by bispicen, with unit cell parameters that were identical to those of the aforementioned crystals of **1**. In other cases, Ga(III) complexes with trispicen were isolated from the solutions. Both degradation products contain ligands that are missing picolyl arms. Water molecules are present in these crystal structures, which may suggest that these portions are being lost through hydrolytic processes. Attempts to grow the crystals in the strict absence of air and moisture were unsuccessful.

Short-Term Reactivity

The six Ga(III) compounds were tested for their ability to catalyze the epoxidation of alkenes by PAA$_R$ (Table 4.2). A 1% loading of catalyst and two equiv of PAA$_R$ per equiv of substrate were used, primarily to facilitate comparison to our previous results with [Ga(phen)$_2$Cl$_2$]Cl.[20] For each catalyzed oxidation reaction, the epoxide is the sole organic product observed at 1 h; no allylic oxidation or dihydroxylation is observed with the 1% mol catalytic loading. In all cases, the percentage of the alkene substrate that has been consumed is equal within error to the yield of the epoxide product, suggesting that the GC analysis has accounted for all organic products. As anticipated, the more electron-deficient terminal alkenes react less readily, as evidenced by the lower yields of epoxides.

Table 4.2. Alkene Conversions/Yields of Epoxides (%) of Reactions Catalyzed by **1-6**[a]

Substrate	Product	$[Ga(phen)_2Cl_2]Cl$[b]	**1**	**2**	**3**	**4**	**5**	**6**
		*46 (±5)* 46 (±8)	*31 (±4)* 32 (±4)	*27 (±2)* 25 (±2)	*14 (±1)* 15 (±1)	*56 (±4)* 56 (±7)	*43 (±2)* 40 (±3)	*41 (±2)* 40 (±3)
	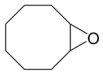	*90 (±3)* 87 (±4)	*80 (±3)* 82 (±2)	*66 (±4)* 68 (±5)	*32 (±2)* 31 (±3)	*93 (±3)* 94 (±2)	*87 (±3)* 84 (±2)	*85 (±5)* 83 (±5)
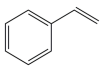	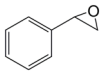	*10 (±1)* 11 (±2)	*7 (±0.4)* 7 (±0.6)	*3 (±0.2)* 3 (±0.2)	*0* 0	*13 (±1)* 13 (±1)	*10 (±1)* 9 (±1)	*10 (±1)* 9 (±1)
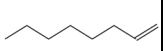	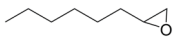	*38 (±4)* 41 (±3)	*2 (±0.2)* 2 (±0.3)	*2 (±0.2)* 2 (±0.2)	*0* 0	*51 (±3)* 47 (±3)	*34 (±3)* 35 (±3)	*2 (±0.2)* 2 (±0.2)
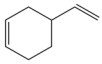	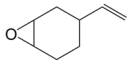	*59 (±8)* 61 (±6)	*40 (±4)* 37 (±3)	*26 (±4)* 28 (±4)	*17 (±2)* 17 (±2)	*70 (±6)* 72 (±4)	*52 (±5)* 50 (±5)	*38 (±2)* 39 (±3)

[a]Standard reaction conditions: MeCN, 273 K, N_2, [Ga(III)] = 5.0 mM, $[alkene]_o$ = 500 mM, $[PAA_R]_o$ = 1.0 M. The alkene conversion, defined as the percentage of alkene that has been consumed by the reaction, was measured at 1 h via GC. The alkene conversions are italicized in the above table. The yield of epoxide, defined as the percentage of alkene converted to the epoxide, was measured at 1 h via GC. Since the substrate is in a 100-fold excess relative to the catalyst, the above yield of epoxides also serve as turnover numbers. [b]From reference 20.

Three trends can be observed in the epoxidation activities. First, the Ga(III) complexes with phen derivatives promote alkene epoxidation to much greater extents. In particular, compounds **4** and **5** promote the oxidation of 1-octene to 1-octene oxide to much higher degrees than any of the other four newly reported Ga(III) complexes. The increases in the yields of the other epoxide products are much less pronounced. Second, the use of more electron-deficient ligands tends to result in more epoxidation. Comparison of the activities of $[Ga(phen)_2Cl_2]Cl$, **4**, and **5** reveals that the installation of a more electron-withdrawing NO_2 group on the 5-position of the phen ligands increases the turnover rate; the addition of an electron-donating NH_2 group reduces the yield of the epoxide at 1 h. Third, as the maximum denticity of the ligand increases past κ-4, the Ga(III) complexes become less able to quickly catalyze olefin epoxidation. Within the series of complexes with pyridylamine ligands, the catalytic activity associated with the tetradentate ligand bispicen is fastest; conversely, the complex with the potentially hexadentate tpen, **3**, is the worst at promoting olefin epoxidation.

In the previously studied alkene oxidation catalyzed by $[Ga(phen)_2Cl_2]Cl$, the selectivity for the epoxide product is lost upon switching to a lower catalyst loading. With a 0.1% catalyst loading of the phen complex, the most heavily represented products result from allylic C-H oxidation and bishydroxylation.[20] A loss of selectivity for the epoxide is also observed for the oxidation of cyclohexene catalyzed by **1**, but with a substantially different product distribution. With a 0.1% loading of **1**, 3.0 M cyclohexene is oxidized by 6.0 M PAA_R to predominantly *trans*-1,2-cyclohexanediol (49%), with cyclohexene oxide as a minor product (6%) and the remainder of the substrate failing to react (45%). Unexpectedly, 2-cyclohexenol is not observed. Another potential product of allylic C-H oxidation, 2-cyclohexenone, is not formed in the olefin oxidations catalyzed by low concentrations of either **1** or $[Ga(phen)_2Cl_2]Cl$.[20]

Time-Scale of Reactivity

The ability of the Ga(III) complexes to catalyze the epoxidation of olefins by peracetic acid was monitored beyond 1 h in order to assess whether a more highly chelating ligand could extend the lifetime of the reactivity. Figure 4.3 shows the yields as a function of time for the epoxidations of five olefins catalyzed by the bispicen complex **1**. There is no noticeable initiation period, although this may occur on a much shorter timescale. The data show that the catalytic activity of **1** is maintained past 1 h; the observed increases in the yields beyond this time point are too large to be attributed to the uncatalyzed reactions between the olefins and terminal oxidant.[20] The most reactive substrate, cyclooctene, is fully converted to cyclooctene oxide by 2 h. Beyond 5 h, diol products consistent with the subsequent opening of the epoxide are observed. With cyclohexene as the substrate, cyclohexene oxide is the sole organic product until 5 h, forming in 75% yield from the alkene. By 6 h, noticeable amounts of *trans*-1,2-cyclohexanediol are observed in addition to the epoxide.

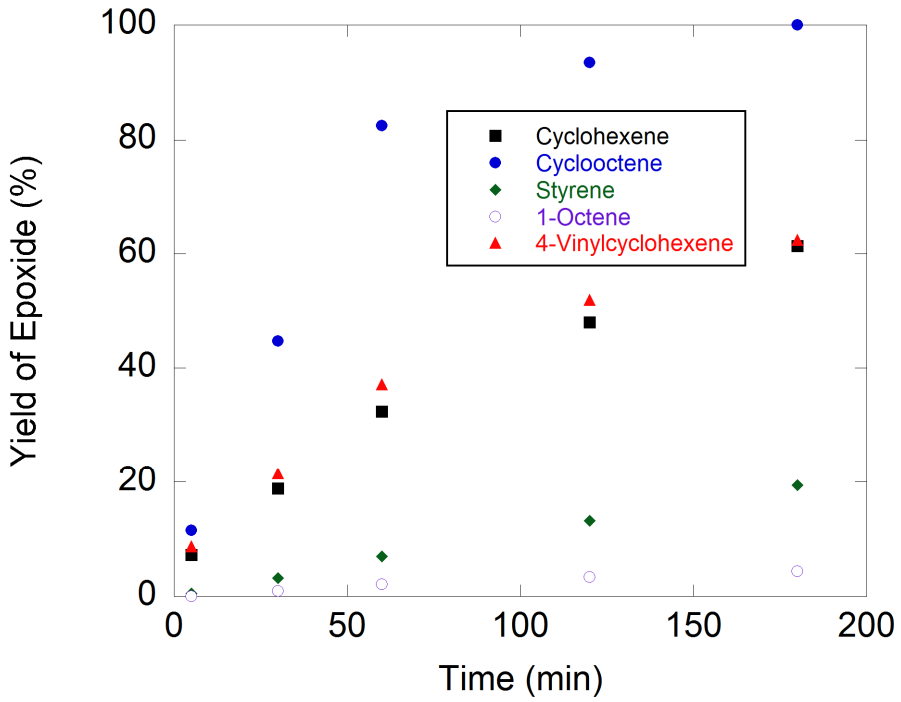

Figure 4.3. Yields of alkene epoxidations by PAA_R catalyzed by the bispicen complex **1** as a function of time. The reaction conditions are identical to those listed for Table 4.2.

Mass spectrometry (MS) of the cyclohexene epoxidation at 3 h reveals that the bispicen-Ga(III) adduct is still intact. At both 5 min and 3 h, the most intense feature has a m/z of 369.0817, consistent with $[Ga(bispicen\text{-}H)(CH_3CO_2)]^+$ (predicted m/z = 369.0842). This suggests that the two chlorides in **1** are displaced by acetate shortly after the beginning of the reaction. Under the ionization conditions, one of the amine protons is likely lost, explaining both the reduced mass and the +1 charge of the observed ion.

The trispicen and tpen complexes **2** and **3** likewise appear to retain their catalytic activity for longer periods of time than $[Ga(phen)_2Cl_2]Cl$, as assessed by their abilities to catalyze the oxidation of cyclohexene by PAA_R. Figure 4.4A compares the longer term reactivities of compounds **1**-**6** and $[Ga(phen)_2Cl_2]Cl$, using the oxidation of cyclohexene to cyclohexene oxide as a standard.[20] The plot shows that the activities of the complexes with the bidentate ligands have decreased substantially by 3 h. Catalysts **1**-**3**, though slower, appear to retain more of their activity, with the overall catalytic activity of **1** becoming approximately equivalent to those of **5** and $[Ga(phen)_2Cl_2]Cl$ by 3 h. As anticipated, compounds **2** and **3** are much less active than **1** throughout the 3 h. MS analyses of **2** and **3** at 3 h do not reveal any

peaks consistent with the ligand hydrolysis observed in the crystals grown from solutions of **3**. Although **3**, for instance, eventually decomposes to **1** and **2** (Figure 4.2), we did not observe m/z features for either of these compounds in the 3 h data for reactions using **3** as a catalyst. As with **1**, the peaks observed at 3 h are consistent with acetate adducts.

The plots of the cyclohexene oxide yields versus time for catalysts **4**-**6** are more curved than those observed for compounds **1**-**3**, suggesting that the former set is less durable under the reaction conditions. Despite this, catalyst **4** remains the best catalyst of the six at the 3 h timepoint. Losses of activity for **4** and **5** are also observed over time when 1-octene is used as the standard (Figure 4.4B), but with this particular substrate, the durabilities of **1**-**3** do not come close to compensating for their slower activity.

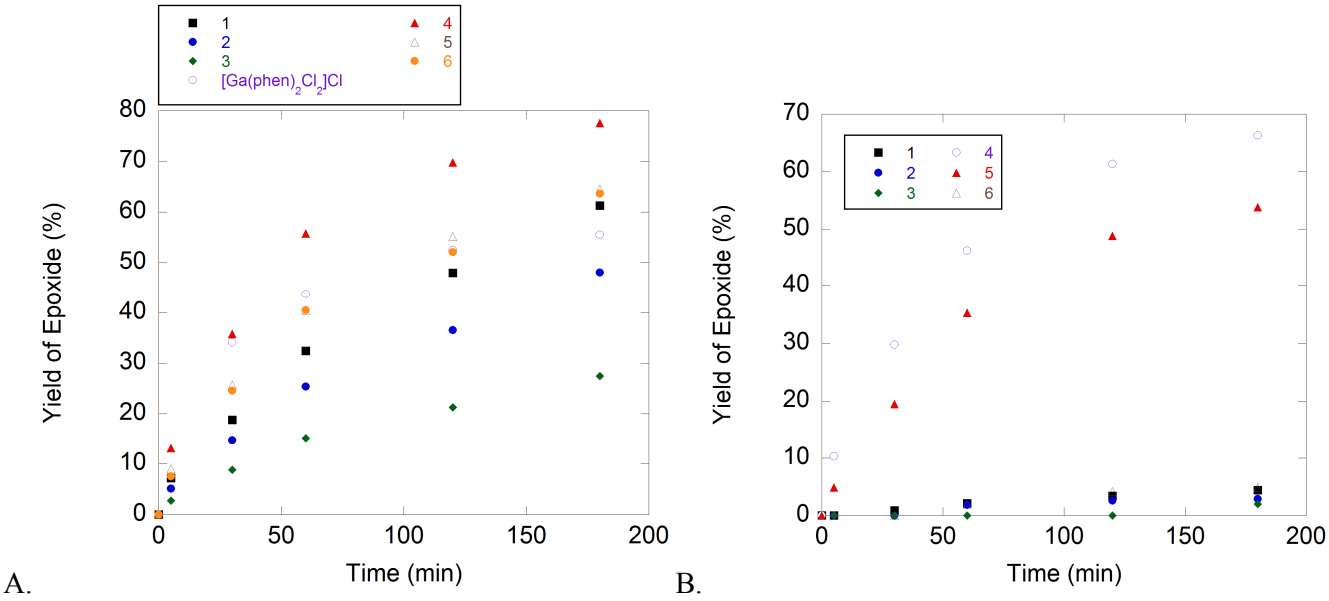

Figure 4.4. Yields of alkene epoxidation by PAA_R catalyzed by the **1**-**6** and $[Ga(phen)_2Cl_2]Cl$ as a function of time. Panel A shows the oxidation of cyclohexene; whereas, B shows the oxidation of 1-octene. The reaction conditions are identical to those listed for Table 4.2. The data for $[Ga(phen)_2Cl_2]Cl$ are from Reference 20.

4.4 Discussion

The syntheses of the Ga(III) complexes are generally straightforward, in that no special measures are necessary to form adducts between the N-donor ligands and the metal ion and that pure products can be isolated without chromatography. The obtained yields range from

moderate (51%) to high (85%). One complication with the syntheses is that the compounds are hygroscopic, and prolonged exposure to moisture appears to degrade the pyridylamine ligands, as evidenced by the crystallized decomposition products of **3**. The complexes with the phen derivatives are likely isolated as mixtures of *cis* isomers (Scheme 4.4).

Three pyridylamine ligands were investigated: bispicen, trispicen, and tpen (Scheme 4.1). The bispicen molecule is a well-established tetradentate ligand.[32, 46-48] The tpen ligand typically coordinates metal ions in a hexadentate fashion, although tetra- and pentadentate modes of coordination have been observed.[49-53] With respect to previously reported Group 13 chemistry, there exists a heptacoordinate complex of tpen with In(III), with the tpen itself providing six of the donor atoms in the inner sphere.[54] The coordination chemistry of trispicen is much less established, but a singly methylated derivative, *N'*-methyl-*N,N,N'*-tris(2-pyridylmethyl)-1,2-ethanediamine, is pentadentate in its structurally characterized complexes with Mn(II) and Fe(II).[34, 55] NMR analysis of **1**, **2**, and **3** suggests that all three ligands predominantly coordinate Ga(III) through four N-donors, with one or two pyridine rings failing to ligate the metal in **2** and **3**, respectively. This is supported by IR analysis of freshly precipitated powder samples of these compounds.

Although the crystal structure of **1** (Figure 4.1) is consistent with its NMR spectra and elemental analysis, crystals grown from solutions of **2** are not consistent with the initially obtained [Ga(trispicen)Cl_2]Cl. The crystal structure of the isolated **7** (Figure 4.2) demonstrates that the coordination of trispicen to Ga(III) is not limited to the hypodentate mode supported by the NMR data. In one of the complex ions within the asymmetric unit, $[Ga(trispicen)Cl]^{2+}$, the ligand is pentacoordinate; whereas, in the other complex ion, $[GaCl_4]^-$, the trispicen is entirely absent from the gallium. The $[Ga(trispicen)Cl]^{2+}$ dication represents only the second example of a structurally characterized Ga(III) ion with a N_5X coordination sphere (X = F, Cl, Br, I).[56]

The capability of the trispicen and tpen ligands to more fully coordinate the Ga(III) may explain the decreased epoxidation activities exhibited by **2** and **3** (Table 4.2, Figure 4.4). Focusing the analysis on the complexes with the three pyridylamine ligands, the bispicen complex **1** promotes the most extensive epoxidation of all substrates except 1-octene, which

essentially doesn't react with either **1**, **2**, or **3** present as the catalyst. The tpen-containing **3** is the worst catalyst of the three compounds, with 1 h yields that are less than half of those measured for **1**. Based on the results, we speculate that the pendant pyridine rings in **2** and **3** may compete with the terminal oxidant for the coordination sites vacated by the initially bound chloride anions. Previous work suggests that the affinities of pyridine rings to Ga(III) are comparable to those of carboxylate ligands.[28] Reducing the number of pendant pyridine donors would alleviate the competition between intramolecular and intermolecular binding and facilitate the coordination of PAA to the Ga(III) center necessary for catalysis. Alternatively, the steric bulk provided by the additional binding arms in **2** and **3** may hinder coordination of the terminal oxidant and/or limit the accessibility of the alkene substrate to the reactive portion of the active oxidant.

The results may suggest that two available coordination sites are needed to activate the PAA most efficiently, which is reminiscent of the Sharpless type mechanism proposed for the epoxidation of alkenes by mixtures of $[Al(H_2O)_6]^{3+}$ and H_2O_2.[27, 57] In the mechanistic scheme proposed by Shul'pin et al for this Al(III) catalysis, coordination of both oxygen atoms of the H_2O_2 to the metal center precedes a concerted oxygen atom transfer from the bound oxidant to an uncoordinated alkene.[27] If two coordination sites are likewise needed for the activation of PAA by the Ga(III) centers of the current catalysts, **2** would be anticipated to be an inferior catalyst to **1**, in accordance with our results (Table 4.2). Scheme 4.5 illustrates a possible mechanism for the epoxidation reactions that highlights the potential benefit of a second coordination site for the PAA. The illustrated mechanism assumes that the N-donor ligands remain fully bound during the reaction; this assumption has not been experimentally confirmed. We are currently assessing the feasibility of various mechanistic pathways through computational analysis and experiments involving Ga(III) complexes with sterically encumbered bispicen derivatives.

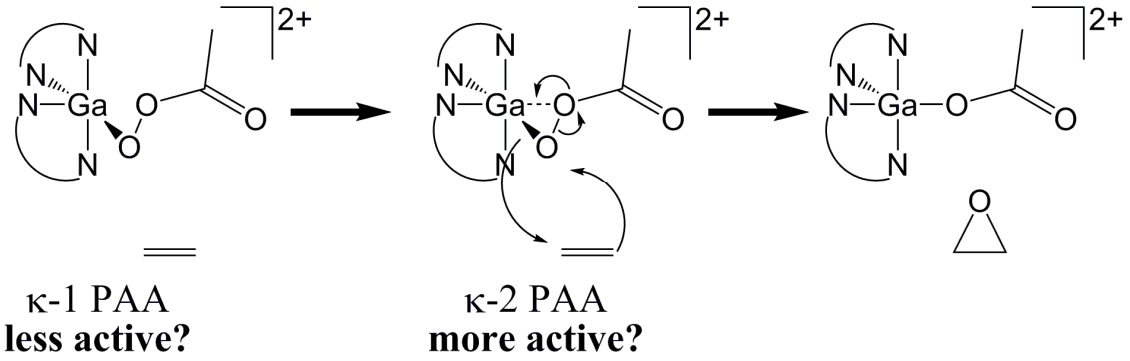

Scheme 4.5 Illustration of possible mechanism for the epoxidation reactions

The higher catalytic activities of the complexes with the phen derivatives suggest that the Ga(III) centers enable catalysis through their abilities to act as Lewis acids. That more electron-rich alkenes tend to react more readily would suggest an electrophilic oxidant, which would be stabilized and rendered less active by more electron-rich ligands. The electrophilicity of the oxidant in the Ga(III) catalysis is also consistent with the inability of H_2O_2 and *t*-BuOOH to serve as terminal oxidants for the epoxidation reactions. Carbonyl groups are widely considered to be electron-withdrawing functional groups. When PAA is used as the terminal oxidant, its carbonyl group may reduce the electron density on the transferred oxygen atom sufficiently to allow oxygen atom transfer to the alkene substrate. The acetate produced upon oxygen atom transfer would also be a better leaving group than the hydroxide or *t*-butyloxide resulting from H_2O_2 or *t*-BuOOH.

1,10-Phenanthroline is widely viewed as being electron-poor relative to amine N-donor ligands and should render chelated metal ions more electron-deficient. Complexes **4** and **5** are notable for their ability to catalyze the oxidation of 1-octene; the other four Ga(III) compounds reported here, conversely, cannot promote this reaction to a significant degree. The addition of electron-withdrawing nitro groups onto the phen ligands improves the yields of the epoxidation reactions; conversely, the installation of electron-donating amino groups decreases the yields (Table 4.1).

Although the complexes with the phen ligands are more active over shorter durations, the compounds with the pyridylamine ligands can potentially achieve superior turnover numbers over longer periods of time due to the greater stability provided by chelate effects. One noted shortcoming with the $[Ga(phen)_2Cl_2]Cl$ catalyst is that it decomposed to unreactive Ga(III)

salts and free phen within approximately the first hour of the epoxidation reactions.[20] The phen appears to slowly dissociate from the Ga(III) center under acidic conditions. The stability of the Ga(III) catalyst can be increased by using a single tetradentate ligand in the place of two bidentate ligands. The ability of bispicen, trispicen, and tpen to sustain the catalysis over longer periods of time confirms that this is a viable strategy for Ga(III)-catalyzed olefin epoxidations (Figures 4.3 and 4.4). Compound **1** is an equivalent catalyst to $[Ga(phen)_2Cl_2]Cl$ when the yields of cyclohexene epoxidation are measured at 3 h (Figure 4.4). Unlike the phen compound, the Ga(III)-bispicen adduct remains intact at 3 h. The observed decomposition of **2** and **3** (Figure 4.2, Figure A1), however, suggest that the pyridylamine-containing complexes do have finite catalytic lifetimes. Compounds **1**-**3** appear to retain their intact polydentate ligands through the 3 h necessary for the alkene epoxidation, however, suggesting that the ligand degradation is slow relative to the alkene epoxidation.

The reactivity with the 1% catalyst loading is selective for the epoxide product for short durations, with the epoxide accounting for the entirety of the observed organic product. The reactions using **1** as the catalyst do start to produce *trans*-1,2-cyclohexanediol between 5 and 6 h after the start of the reaction. As with the olefin oxidation catalyzed by $[Ga(phen)_2Cl_2]Cl$,[20] the selectivity for the epoxide product is lost when the catalyst loading of **1** is reduced to 0.1%. Oddly, the chemistry associated with **1** differs from that promoted by the phen compound in that the lower concentration of **1** does not promote allylic C-H activation. Instead, bishydroxylation is overwhelmingly favored under such circumstances. When cyclohexene oxide is used as a substrate with the standard reaction conditions and a 1% mol loading of gallium (3.0 mM **1**, 6.0 M PAA_R, 0 °C, 7 h), no diol is observed, suggesting that cyclohexene may be converted directly to *trans*-1,2-cyclohexanediol as opposed to a two-step reaction involving epoxidation followed by ring-opening. We speculate that another Ga(III)-based oxidant is responsible and are continuing to investigate this side-reactivity through experimental and computational methods. The mechanism displayed on Scheme 4.5 certainly doesn't explain all of the observed oxidative activity of the Ga(III) complexes.

4.5 Conclusions

Six new gallium(III) complexes with N-donor ligands have been prepared and tested as catalysts for the epoxidation of alkenes by peracetic acid. Comparison of the compounds' activities provides three major insights into Ga(III)-catalyzed alkene epoxidation. First, more electron-deficient ligands are found to support more rapid catalytic turnover, with phen derivatives leading to superior initial activity over ligands with amine and pyridine chelating groups. The Ga(III) complexes with phen derivatives are markedly better at activating the electron-deficient substrate 1-octene, and $[Ga(NO_2\text{-phen})_2Cl_2]Cl$ is the best catalyst of the six under all characterized reaction conditions. Second, more highly coordinating ligands, such as the tetradentate bispicen, can prolong the catalytic activity by stabilizing the ligand-metal adduct. Third, it is found that the more highly chelating N-donor ligands, trispicen and tpen, decrease the catalytic activity. The additional binding arms may compete with terminal oxidant for the coordination sites, or they may impede the reactivity through steric effects.

Appendix

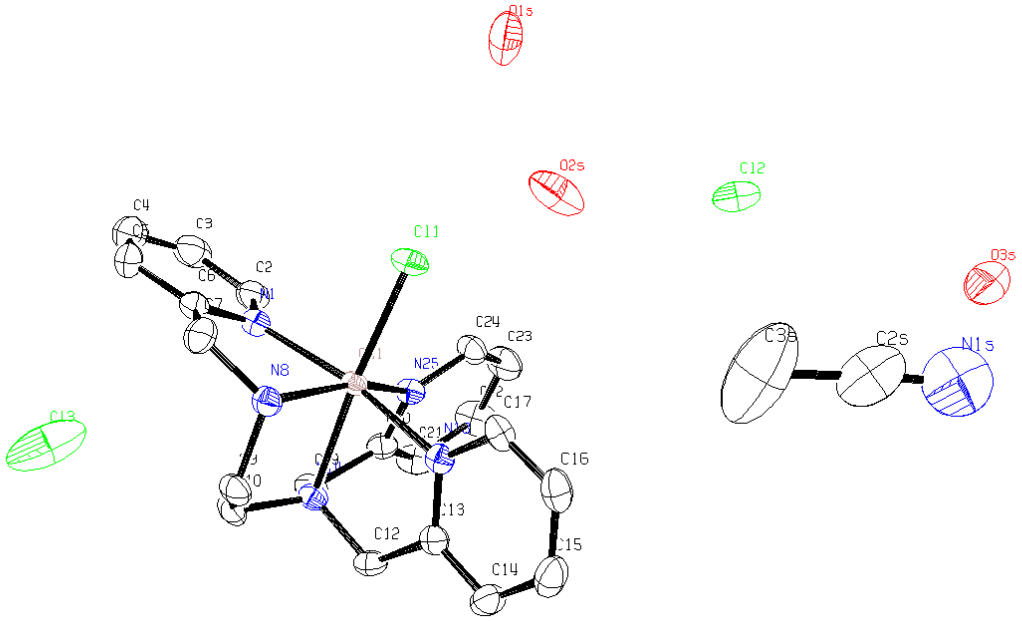

Figure A1. ORTEP representation of $[Ga(trispicen)Cl]Cl_2 \bullet MeCN \bullet 3H_2O$ grown from a solution of $[Ga(tpen)Cl_2]Cl$ in MeCN. All hydrogen atoms are omitted for clarity. All thermal ellipsoids are drawn at 50% probability.

Table A1. Selected crystallographic data for $[Ga(trispicen)Cl]Cl_2$.

Parameter	$[Ga(trispicen)Cl]Cl_2 \bullet MeCN \bullet$
Formula	$C_{22}H_{32}Cl_3GaN_6O_3$
MW	602.61
Crystal system	Triclinic
Space group	$P\bar{1}$ *(#2)*
a (Å)	9.1540(3)
b (Å)	11.9245(4)
c (Å)	12.8632(4)
α (deg)	80.3060(10)
β (deg)	81.8800(10)
γ (deg)	88.0630(10)
V ($Å^3$)	1370.11(8)
Z	2
Cryst color	Colorless
T (K)	198
Reflns	36681
Unique reflns	3770
R1 (F, I > 2σ(I))	0.0364
wR2 (F^2, all	0.0943

$R1 = \Sigma \left| \left| F_o \right| - \left| F_c \right| \right| / \Sigma \left| F_o \right|$; $wR2 = [\Sigma w(F_o^2 - F_c^2)^2 / \Sigma w(F_o^2)^2]^{1/2}$.

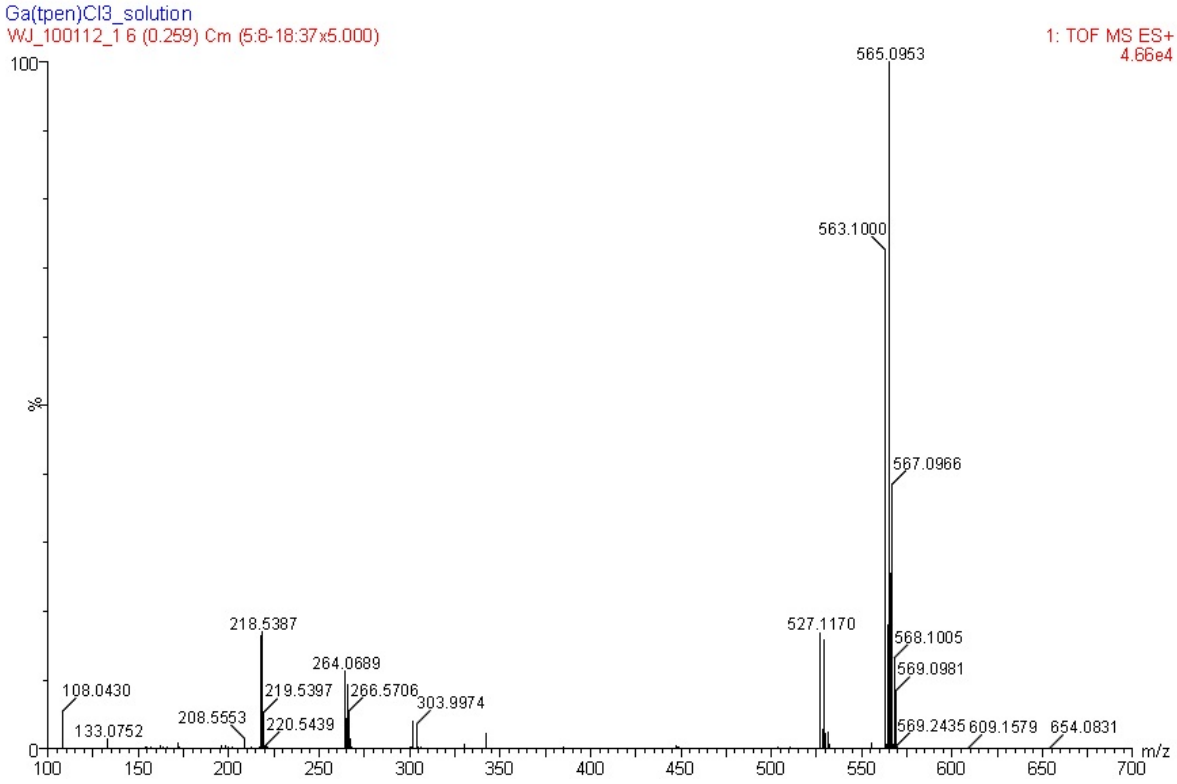

Figure A2. Mass spectrum (ESI) of $[Ga(tpen)Cl_2]Cl$. The m/z features at 563.1000 and 565.0953 are assigned to $[Ga(tpen)Cl_2]^+$ (calcd m/z = 563.1008 and 565.0979). The m/z feature at 264.0689 is assigned to $[Ga(tpen)Cl]^{2+}$ (calcd m/z = 264.0650).

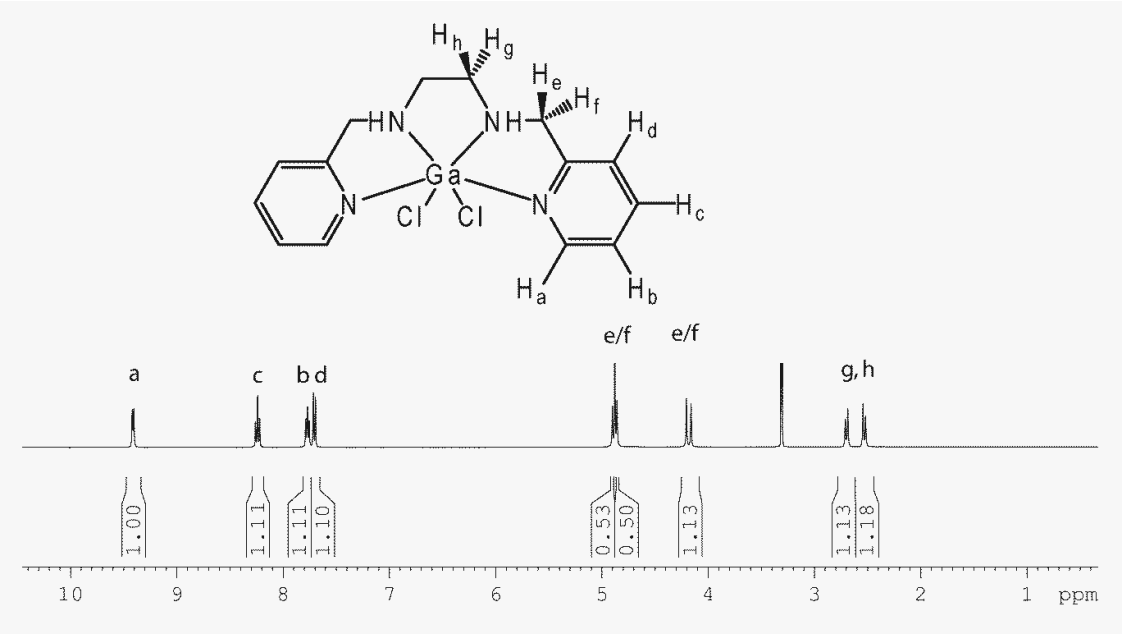

Figure A3. ^{1}H NMR spectrum of **1** in CD_3OD at 294 K. The data were acquired on a 400 MHz instrument. Solvent peaks are present at 4.87 (water) and 3.31 (methanol) ppm; these have been truncated for clarity. The doublet centered at 4.88 ppm overlaps with the water peak.

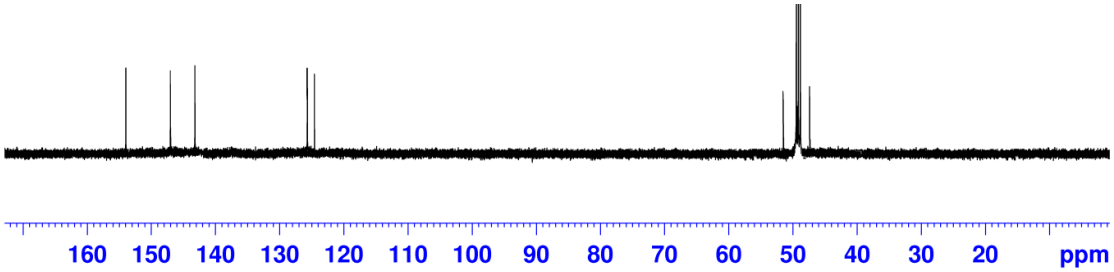

Figure A4. ^{13}C NMR spectrum of **1** in CD_3OD at 294 K. The solvent peak at 49.86 ppm (methanol) has been truncated for clarity.

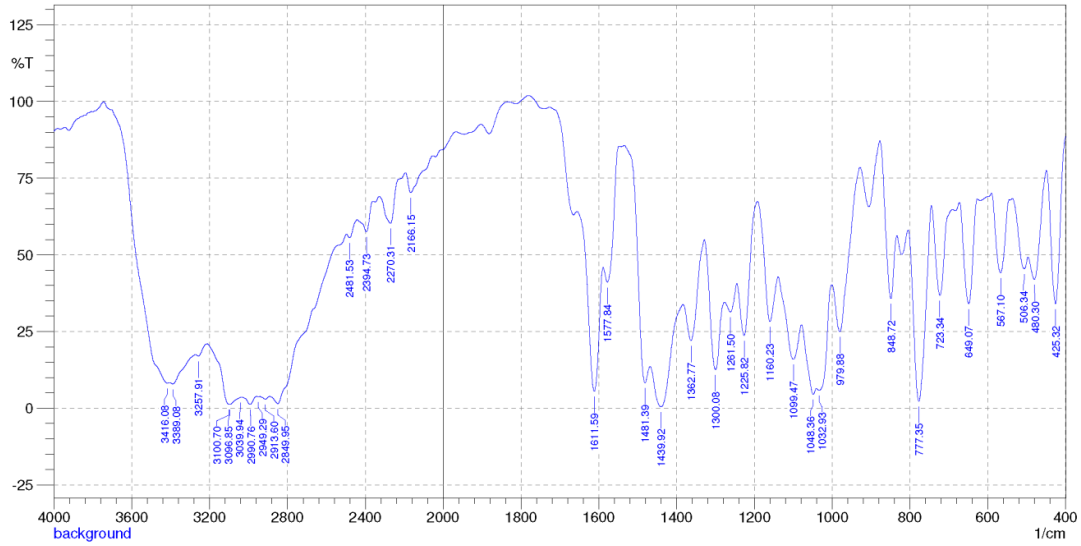

Figure A5. IR spectrum of **1**. The sample was prepared as a KBr pellet. The full listing of peak frequencies in cm^{-1} is as follows: 3416 (s), 3389 (s), 3100 (s), 3040 (s), 2991 (s), 2914 (s), 2850 (s), 2482 (w), 2395 (w), 2270 (w), 2166 (w), 1665 (w), 1612 (s), 1578 (m), 1481 (s), 1440 (s), 1363 (s), 1300 (s) 1262 (m), 1226 (s), 1160 (m), 1099 (s), 1048 (s), 1033 (s), 980 (m), 906 (w), 849 (m), 821 (w), 777 (s), 723 (m), 649 (m), 567 (m), 506 (m), 480 (m), 425 (m).

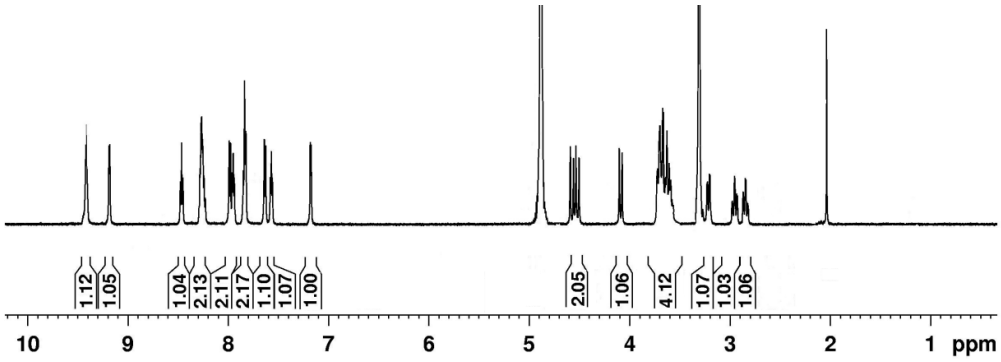

Figure A6. ^{1}H NMR spectrum of **2** in CD_3OD at 294 K. The data were acquired on a 400 MHz instrument. The solvent peaks present at 4.87 (water) and 3.31 (methanol) ppm have been truncated for clarity.

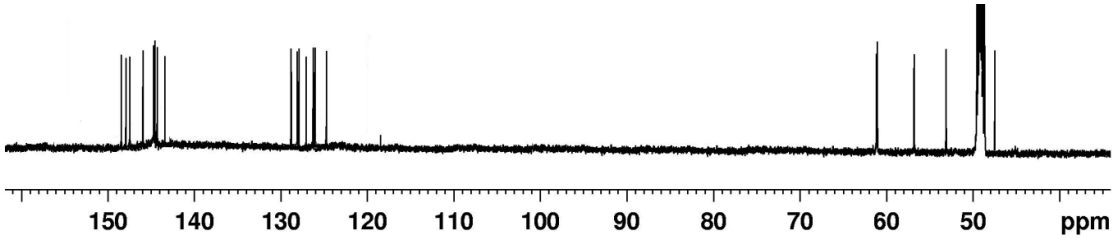

Figure A7. ^{13}C NMR spectrum of **2** in CD_3OD at 294 K. The solvent peak at 49.86 ppm (methanol) has been truncated for clarity.

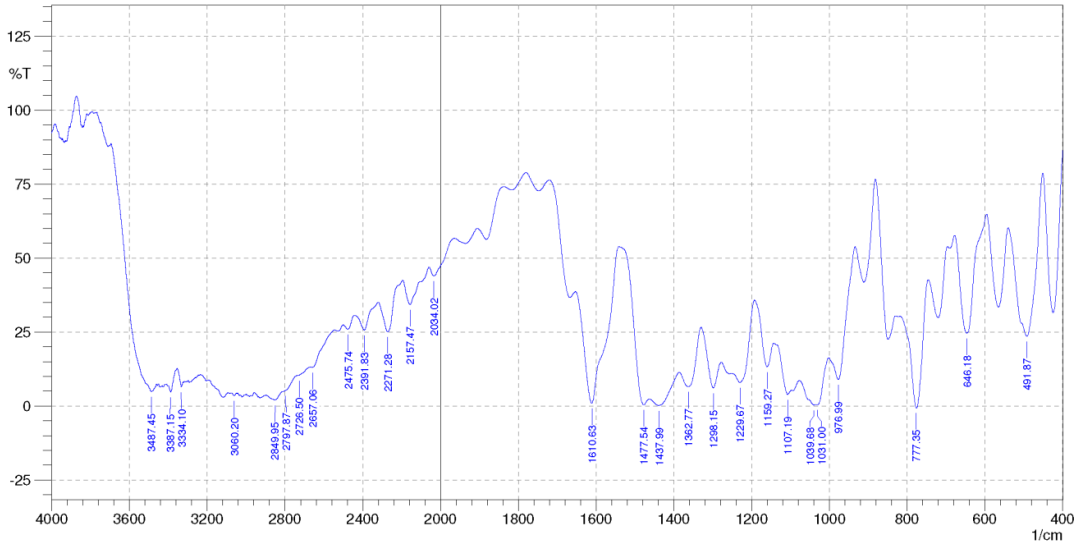

Figure A8. IR spectrum of a powder sample of **2**. The sample was prepared as a KBr pellet. The full listing of peak frequencies in cm^{-1} is as follows: 3487 (s), 3387 (s), 3334 (s), 3115 (s), 2850 (s), 2657 (s), 2476 (m), 2392 (m), 2271 (m), 2157 (m), 2034 (w), 1936 (w), 1882 (w), 1815 (w), 1747 (w), 1611 (s), 1478 (s), 1438 (s), 1363 (s), 1298 (s), 1230 (s), 1159 (s), 1107 (s), 1040 (s), 1031 (s), 977 (s), 910 (w), 849 (m), 777 (s), 720 (m), 646 (m), 565 (m), 492 (m), 424 (m). Note the shoulder on the feature at 1611 cm^{-1}.

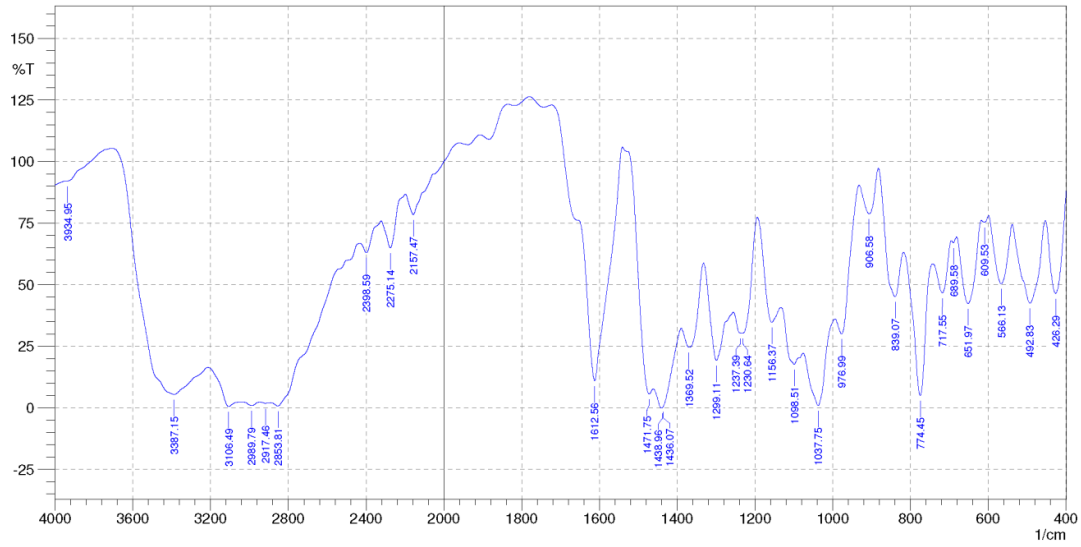

Figure A9. IR spectrum of a crystalline sample of **7**, which was grown from a saturated solution of **2**. The sample was prepared as a KBr pellet.Note that the peak at 1613 cm^{-1} lacks the shoulder found for the powder sample of **2**, which would be consistent with the lack of non-coordinated pyridine rings in the solid.

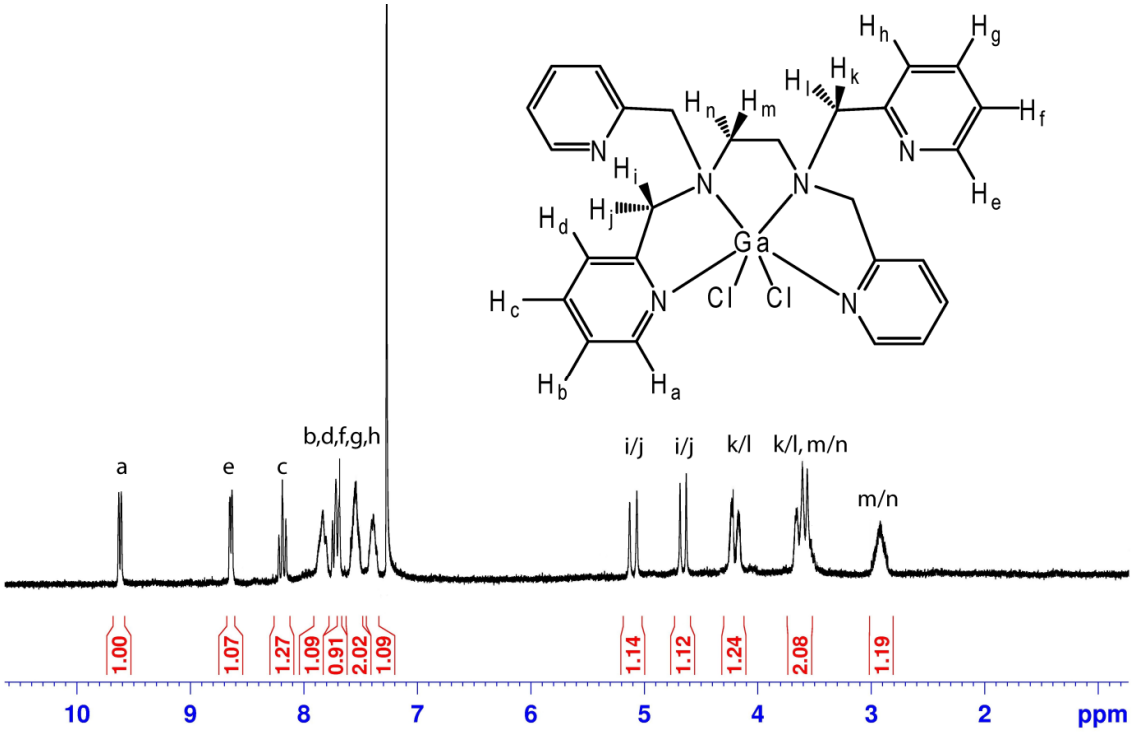

Figure A10.[1]H NMR spectrum of **3** in $CDCl_3$ at 294 K. The data were acquired on a 250 MHz instrument. The solvent peak present at 7.26 (chloroform) has been truncated for clarity.

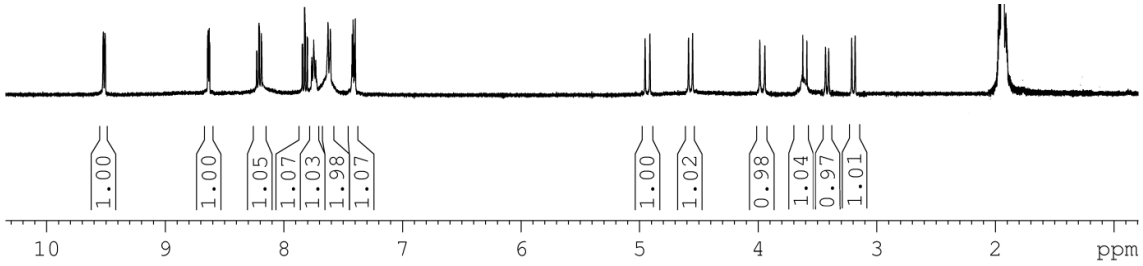

Figure A11.[1]H NMR spectrum of **3** in CD_3CN at 294 K. The data were acquired on a 400 MHz instrument. The solvent peak present at 1.94 (acetonitrile) has been truncated for clarity.

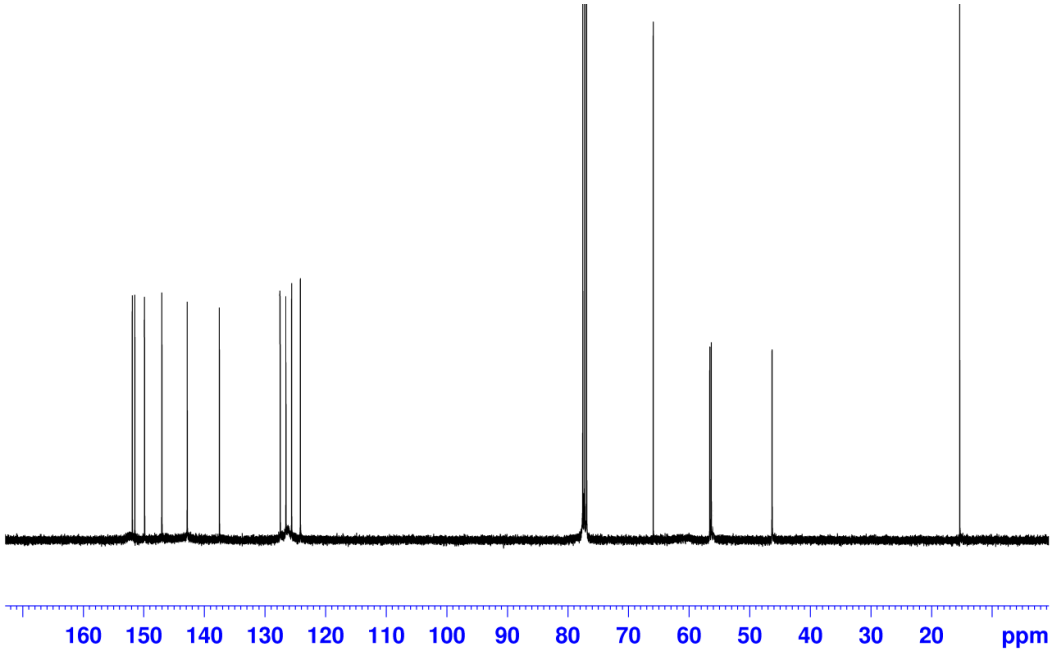

Figure A12. [13]C NMR spectrum of **3** in $CDCl_3$ at 294 K. The solvent peak at 77.16 (chloroform) has been truncated for clarity.

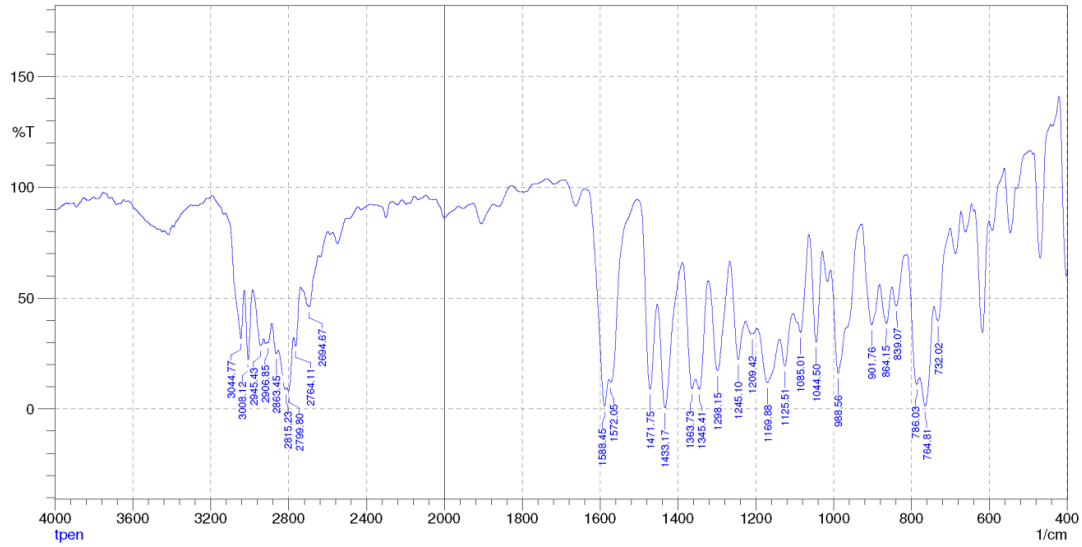

Figure A13. IR spectrum of a powder sample of **3**. The sample was prepared as a KBr pellet. The full listing of peak frequencies in cm^{-1} is as follows: 3045 (m), 3008 (s), 2945 (s), 2907 (s), 2863 (s), 2815 (s), 2800 (s), 2764 (s), 2695 (m), 2550 (w), 2300 (w), 1905 (w), 1859 (w), 1796 (w), 1662 (w), 1588 (s), 1572 (s), 1472 (s), 1433 (s), 1364 (s), 1345 (s), 1298 (s), 1245 (s), 1209 (m), 1170 (s), 1126 (s), 1085 (m), 1045 (m), 1016 (w), 989 (s), 902 (m), 864 (m), 839 (m), 786 (s), 765 (s), 732 (m), 687 (w), 662 (w), 617 (m), 593 (w), 546 (w), 470 (w).Note the intense feature at 1588 cm^{-1}, which is consistent with the presence of two non-coordinated pyridine rings in the solid.

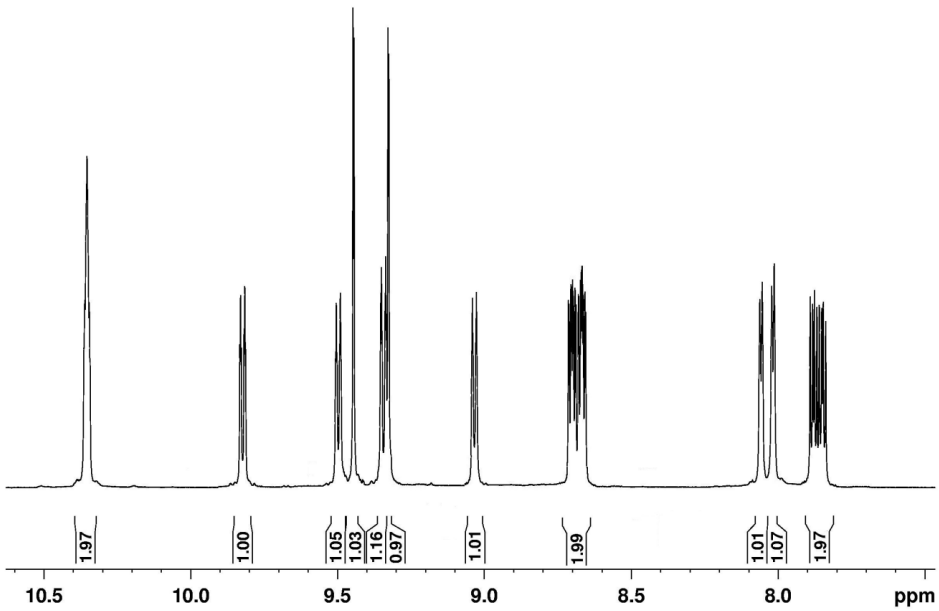

Figure A14. ^{1}H NMR spectrum of **4** in CD_3OD at 294 K. The data were acquired on a 600 MHz instrument. Only solvent resonances were observed outside the shown 7.0-10.5 ppm range.

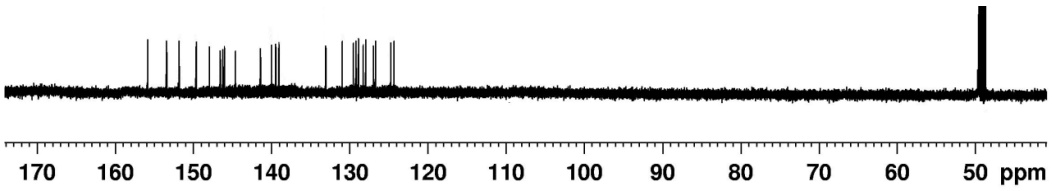

Figure A15. ^{13}C NMR spectrum of **4** in CD_3OD at 294 K. The feature at 49.00 ppm corresponds to solvent and has been truncated for clarity.

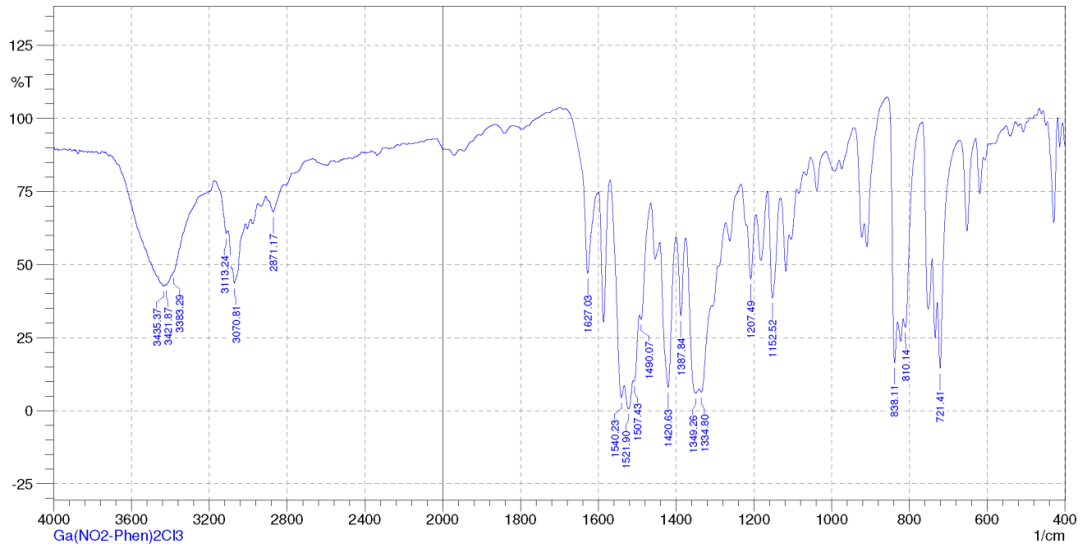

Figure A16. IR spectrum of a powder sample of **4**. The sample was prepared as a KBr pellet. The full listing of peak frequencies in cm^{-1} is as follows: 3422 (m), 3113 (w), 3071 (m), 3004 (w), 2970 (w), 2934 (w), 2871 (w), 2337 (w), 1970 (w), 1946 (w), 1841 (w), 1627 (m), 1586 (m), 1540 (s), 1522 (s), 1507 (s), 1490 (m), 1453 (m), 1421 (s), 1388 (m), 1349 (s), 1335 (s), 1261 (w), 1207 (m), 1181 (m), 1153 (m), 1117 (m), 1104 (m), 1038 (w), 992 (w), 974 (w), 920 (m), 838 (s), 823 (s), 810 (m), 751 (m), 734 (s), 721 (s), 652 (m), 619 (w), 541 (w), 507 (w), 429 (w).

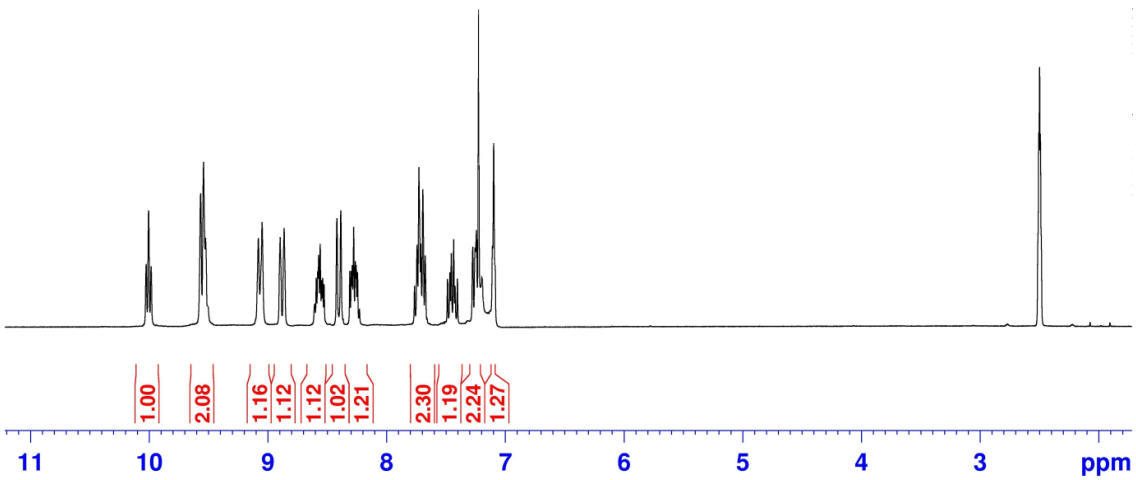

Figure A17. ^{1}H NMR spectrum of **5** in DMSO-*d6* at 294 K. The data were acquired on a 250 MHz instrument. The solvent contributes a resonance feature at 2.50 ppm.

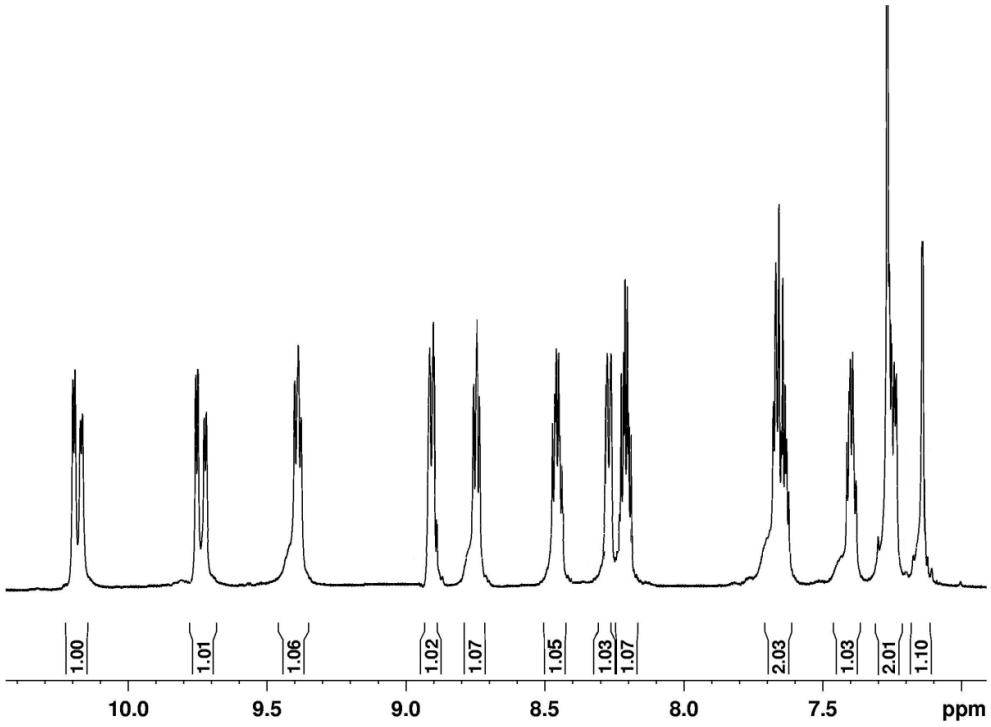

Figure A18. ^{1}H NMR spectrum of **5** in CD_3OD at 294 K. The data were acquired on a 600 MHz instrument. Only solvent resonances were observed outside the shown 7.0-10.5 ppm range.

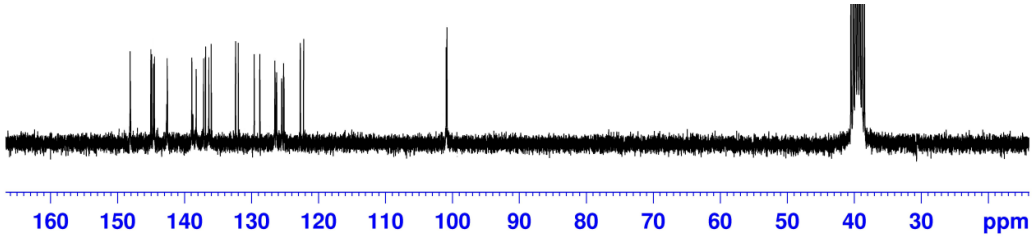

Figure A19. ^{13}C NMR spectrum of **5** in DMSO-*d6* at 294 K. The feature at 39.51 ppm corresponds to solvent and has been truncated for clarity.

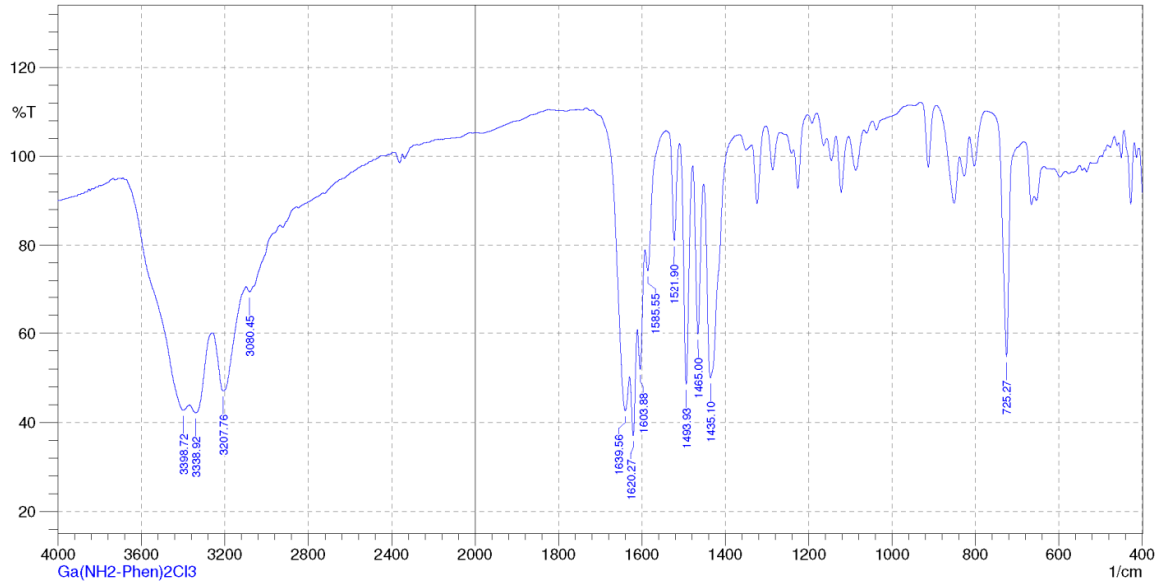

Figure A20. IR spectrum of a powder sample of **5**. The sample was prepared as a KBr pellet. The full listing of peak frequencies in cm^{-1} is as follows: 3399 (s), 3339 (s), 3208 (s), 3080 (m), 1640 (s), 1620 (s), 1604 (s), 1586 (m), 1522 (w), 1494 (s), 1465 (m), 1435 (s), 1350 (w), 1323 (w), 1287 (w), 1226 (w), 1164 (w), 1146 (w), 1122 (w), 1087 (w), 913 (w), 851 (w), 826 (w), 802 (w), 725 (s), 665 (w), 653 (w), 427 (w).

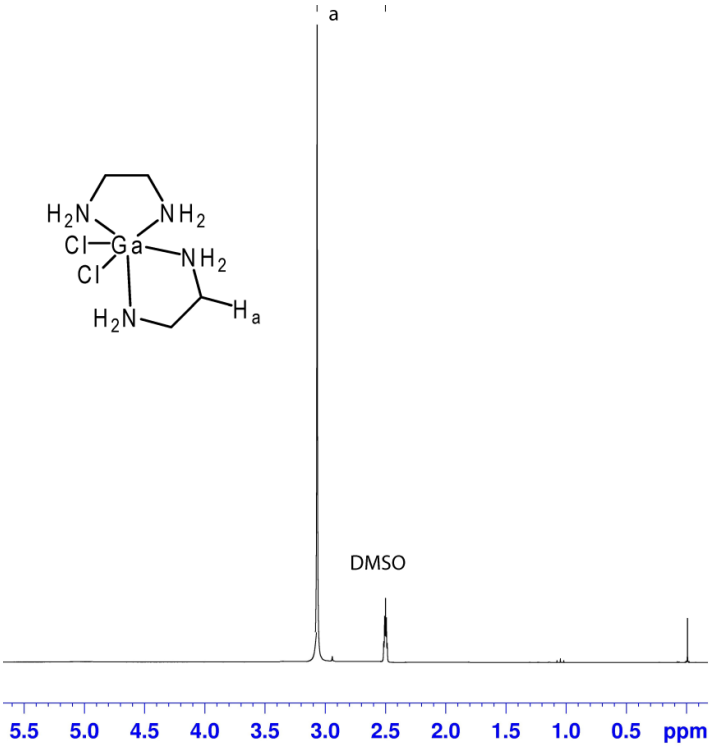

Figure A21. ^{1}H NMR spectrum of **6** in DMSO-*d6* at 294 K. The data were acquired on a 400 MHz instrument. A solvent peak is present at 2.50 ppm.

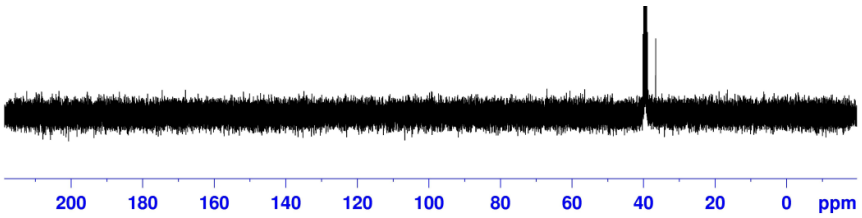

Figure A22. ^{13}C NMR spectrum of **6** in DMSO-*d6* at 294 K. The solvent peak at 39.51 ppm has been truncated for clarity.

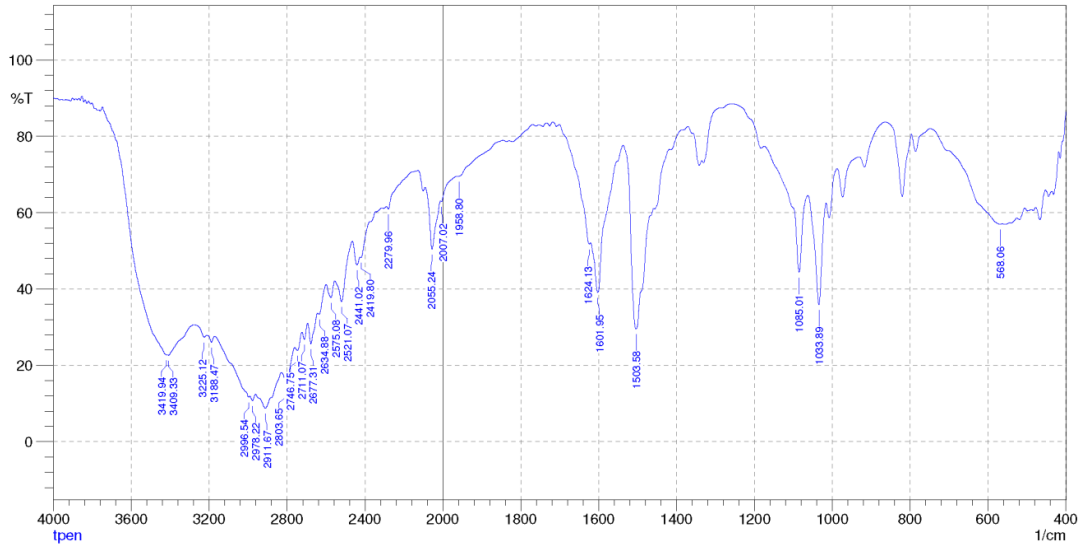

Figure A23. IR spectrum of a powder sample of **6**. The sample was prepared as a KBr pellet. The full listing of peak frequencies in cm^{-1} is as follows: 3420 (s), 3225 (s), 2978 (s), 2912 (s), 2804 (s), 2747 (s), 2711 (s), 2677 (s), 2634 (s), 2575 (m), 2521 (m), 2420 (m), 2280 (w), 2055 (m), 1624 (m), 1602 (m), 1504 (s), 1342 (w), 1182 (w), 1085 (m), 1034 (s), 1008 (w), 973 (w), 917 (w), 786 (w), 568 (m), 467 (m), 445 (w), 431 (w).

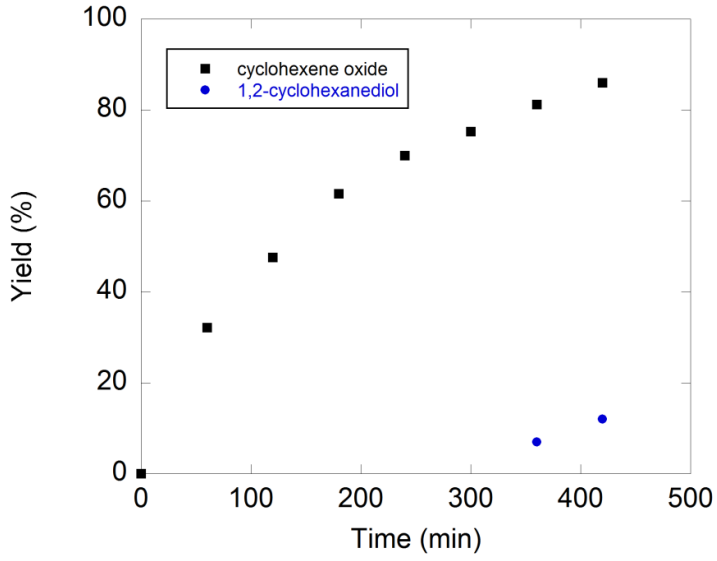

Figure A24. The yields of the organic products of [Ga(bispicen)Cl_2]Cl-catalyzed cyclohexene oxidation by PAA_R over time. The reaction was run at 0 °C in MeCN with initial concentrations of 5.0 mM Ga(III) catalyst, 500 mM cyclohexene, and 1000 mM PAA_R.The points on the plot are the averages of three separate reactions, with errors of ±2% for the yields of cyclohexene oxide and ±1% for the yields of 1,2-cyclohexanediol. The diol is not observed until the 6 h time point.

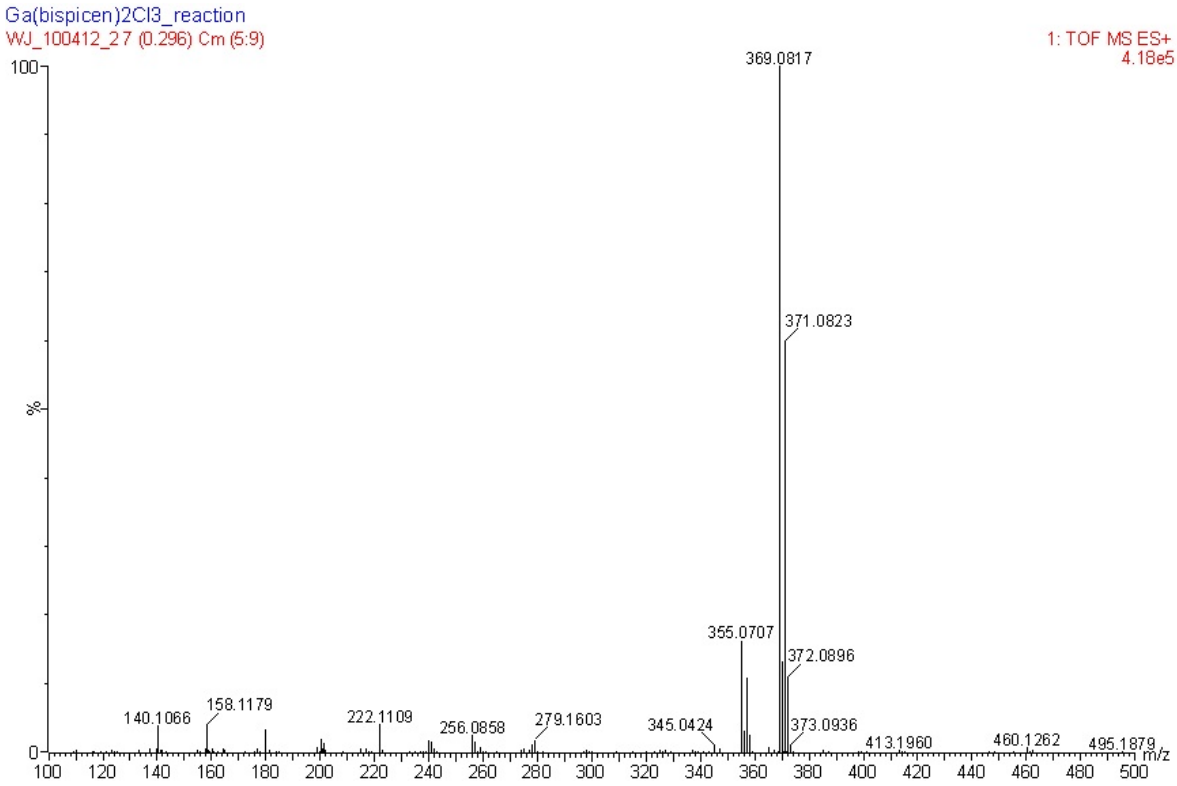

Figure A25. Mass spectrum (ESI) of the gallium species present in solution 3 h after the beginning of the cyclohexene epoxidation reaction catalyzed by **1**. 500 mM cyclohexene, 1000 mM peracetic acid, and 5.0 mM $[Ga(bispicen)Cl_2]Cl$ were mixed in MeCN and allowed to stir at 0 °C for 3 h. The m/z features at 369.0817 and 371.0823 are assigned to $[Ga(bispicen\text{-}H)(CH_3CO_2)]^+$ (calcd m/z = 369.0842 and 371.0833).

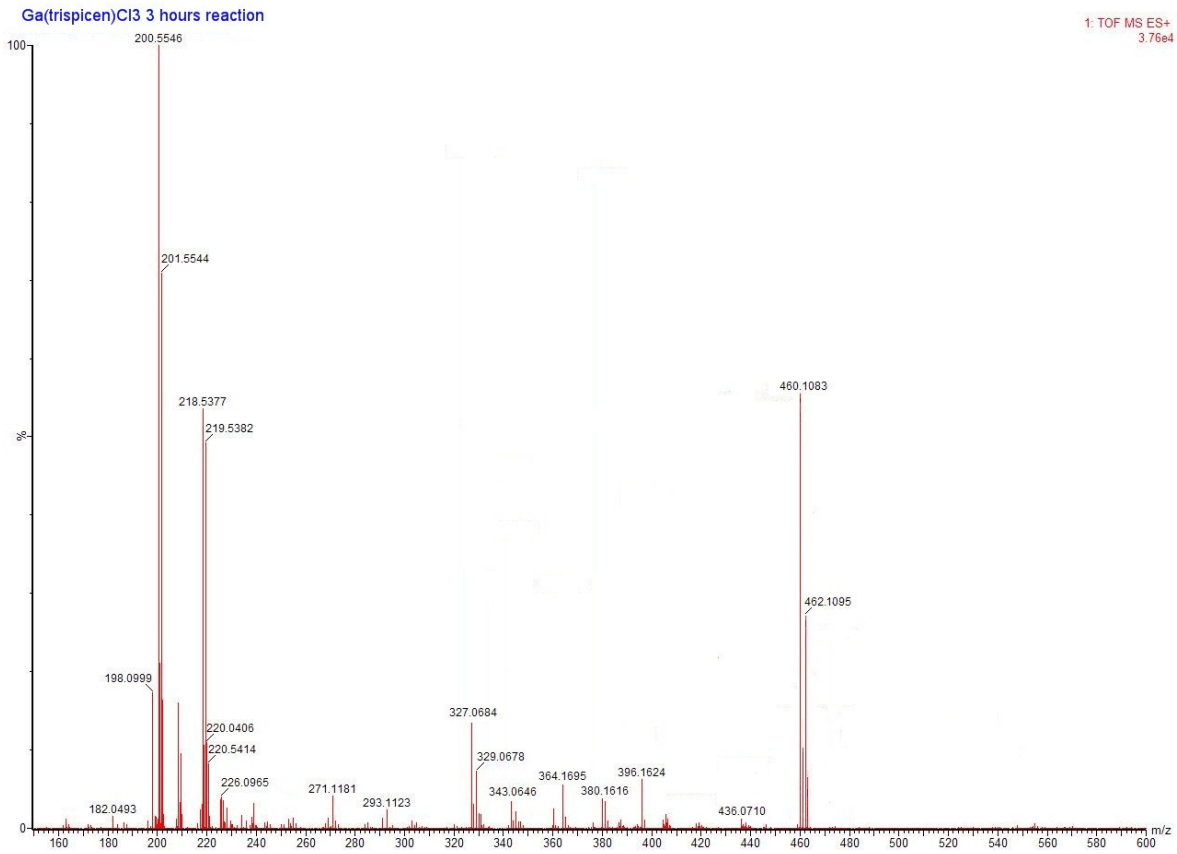

Figure A26. Mass spectrum (ESI) of the gallium species present in solution 3 h after the beginning of the cyclohexene epoxidation reaction catalyzed by **2**. 500 mM cyclohexene, 1000 mM peracetic acid, and 5.0 mM [Ga(trispicen)Cl_2]Cl were mixed in MeCN and allowed to stir at 0 °C for 3 h. The m/z features at 460.1083 and 462.1095 are assigned to [Ga(trispicen-H)(CH_3CO_2)]$^+$ (calcd m/z = 460.1264 and 462.1255). The peaks at 281.5377 and 219.5382 are assigned to [Ga(trispicen)Cl]$^{2+}$ (calcd m/z = 218.5445 and 219.5445). The peaks at 200.5546 and 201.5544 are assigned to [Ga(trispicen-H)]$^{2+}$ (calcd m/z = 200.5566 and 201.5561).

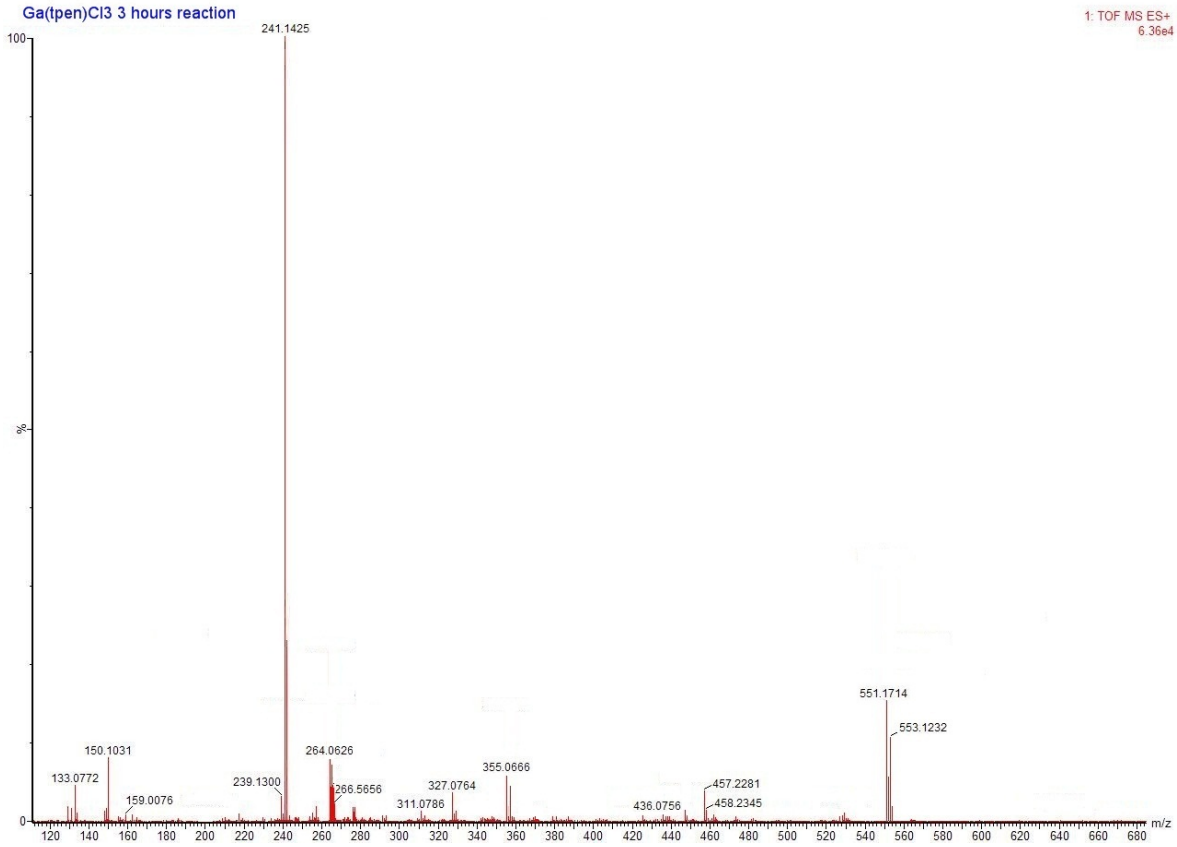

Figure A27. Mass spectrum (ESI) of the gallium species present in solution 3 h after the beginning of the cyclohexene epoxidation reaction catalyzed by **3**. 500 mM cyclohexene, 1000 mM peracetic acid, and 5.0 mM $[Ga(tpen)Cl_2]Cl$ were mixed in MeCN and allowed to stir at 0 °C for 3 h. The m/z features at 551.1714 and 553.1232 are assigned to $[Ga(tpen\text{-}H)(CH_3CO_2)]^+$ (calcd m/z = 551.1686 and 553.1677).

References

(1) Chi, Y.; Chou, T.-Y.; Wang, Y.-J.; Huang, S.-F.; Carty, A. J.; Scoles, L.; Udachin, K. A.; Peng, S.-M.; Lee, G.-H. *Organometallics* **2003**, *23*, 95-103.

(2) Park, J.-H.; Afzaal, M.; Helliwell, M.; Malik, M. A.; O'Brien, P.; Raftery, J. *Chem. Mater.* **2003**, *15*, 4205-4210.

(3) Valet, M.; Hoffman, D. M. *Chem. Mater.* **2001**, *13*, 2135-2143.

(4) Suh, S.; Hoffman, D. M. *Chem. Mater.* **2000**, *12*, 2794-2797.

(5) MacInnes, A. N.; Power, M. B.; Barron, A. R. *Chem. Mater.* **1993**, *5*, 1344-1351.

(6) Kouvetakis, J.; Beach, D. B. *Chem. Mater.* **1989**, *1*, 476-478.

(7) Cowley, A. H. *J. Organomet. Chem.* **2000**, *600*, 168-173.

(8) Bartholomä, M. D. *Inorg. Chim. Acta* **2012**, *389*, 36-51.

(9) Wadas, T. J.; Wong, E. H.; Weisman, G. R.; Anderson, C. J. *Chem. Rev.* **2010**, *110*, 2858-2902.

(10) Bartholomä, M. D.; Louie, A. S.; Valliant, J. F.; Zubieta, J. *Chem. Rev.* **2010**, *110*, 2903-2920.

(11) Boros, E.; Ferreira, C. L.; Cawthray, J. F.; Price, E. W.; Patrick, B. O.; Wester, D. W.; Adam, M. J.; Orvig, C. *J. Am. Chem. Soc.* **2010**, *132*, 15726-15733.

(12) Dagorne, S.; Atwood, D. A. *Chem. Rev.* **2008**, *108*, 4037-4071.

(13) Yamaguchi, M.; Nishimura, Y. *Chem. Commun.* **2008**, 35-48.

(14) Wehmschulte, R. J.; Steele, J. M.; Young, J. D.; Khan, M. A. *J. Am. Chem. Soc.* **2003**, *125*, 1470-1471.

(15) Lichtenberg, C.; Spaniol, T. P.; Okuda, J. *Inorg. Chem.* **2012**, *51*, 2254-2262.

(16) Tang, S.; Monot, J.; El-Hellani, A.; Michelet, B.; Guillot, R.; Bour, C.; Gandon, V. *Chem. Eur. J.* **2012**, *18*, 10239-10243.

(17) Carty, A. J.; Dymock, K. R.; Boorman, P. M. *Can. J. Chem.* **1970**, *48*, 3524-3529.

(18) Ivanov-Emin, B. N.; Nisel'son, L. A.; Rabovik, Y. I.; Larionova, L. E. *Russ. J. Inorg. Chem.* **1961**, *6*, 1142-1146.

(19) McPhail, A. T.; Miller, R. W.; Pitt, C. G.; Gupta, G.; Srivastava, S. C. *J. Chem. Soc., Dalton Trans.* **1976**, 1657-1661.

(20) Jiang, W.; Gorden, J. D.; Goldsmith, C. R. *Inorg. Chem.* **2012**, *51*, 2725-2727.

(21) Fricke, R.; Kosslick, H.; Lischke, G.; Richter, M. *Chem. Rev.* **2000**, *100*, 2303-2405.

(22) Pescarmona, P. P.; Janssen, K. P. F.; Jacobs, P. A. *Chem. Eur. J.* **2007**, *13*, 6562-6572.

(23) Stoica, G.; Santiago, M.; Jacobs, P. A.; Pérez-Ramírez, J.; Pescarmona, P. P. *Appl. Catal. A* **2009**, *371*, 43-53.

(24) Cates, C. D.; Myers, T. W.; Berben, L. A. *Inorg. Chem.* **2012**, *51*, 11891-11897.

(25) Nam, W.; Valentine, J. S. *J. Am. Chem. Soc.* **1990**, *112*, 4977-4979.

(26) Rinaldi, R.; de Oliveira, H. F. N.; Schumann, H.; Schuchardt, U. *J. Mol. Catal. A* **2009**, *307*, 1-8.

(27) Kuznetsov, M. L.; Kozlov, Y. N.; Mandelli, D.; Pombeiro, A. J. L.; Shul'pin, G. B. *Inorg. Chem.* **2011**, *50*, 3996-4005.

(28) Caravan, P.; Rettig, S. J.; Orvig, C. *Inorg. Chem.* **1997**, *36*, 1306-1315.

(29) Murphy, A.; Pace, A.; Stack, T. D. P. *Org. Lett.* **2004**, *6*, 3119-3122.

(30) Sheldrick, G. M., 6.12 ed.; Siemens Analytical X-ray Instruments, Inc.: Madison, WI, 2001.

(31) Sheldrick, G. M.; Bruker Analytical X-ray Systems: Madison, WI, 1996.

(32) Toftlund, H.; Pedersen, E.; Yde-Andersen, S. *Acta. Chem. Scand. A* **1984**, *38*, 693-697.

(33) Anderegg, G.; Wenk, F. *Helv. Chim. Acta* **1967**, *50*, 2330-2332.

(34) Mialane, P.; Nivorojkine, A.; Pratviel, G.; Azéma, L.; Slany, M.; Godde, F.; Simaan, A.; Banse, F.; Kargar-Grisel, T.; Bouchoux, G.; Sainton, J.; Horner, O.; Guilhem, J.; Tchertanova, L.; Meunier, B.; Girerd, J.-J. *Inorg. Chem.* **1999**, *38*, 1085-1092.

(35) Goldsmith, C. R.; Jonas, R. T.; Cole, A. P.; Stack, T. D. P. *Inorg. Chem.* **2002**, *41*, 4642-4652.

(36) Junk, P. C.; Skelton, B. W.; White, A. H. *Aust. J. Chem.* **2006**, *59*, 147-154.

(37) Gill, N. S.; Nuttall, R. H.; Scaife, D. E.; Sharp, D. W. A. *J. Inorg. Nucl. Chem.* **1961**, *18*, 79-87.

(38) Willett, R. D.; Gómez-García, C. J.; Twamley, B.; Gómez-Coca, S.; Ruiz, E. *Inorg. Chem.* **2012**, *51*, 5487-5493.

(39) Goodson, P. A.; Glerup, J.; Hodgson, D. J.; Michelsen, K.; Pedersen, E. *Inorg. Chem.* **1990**, *29*, 503-508.

(40) Coates, C. M.; Fiedler, S. R.; McCullough, T. L.; Albrecht-Schmitt, T. E.; Shores, M. P.; Goldsmith, C. R. *Inorg. Chem.* **2010**, *49*, 1481-1486.

(41) Collins, M. A.; Hodgson, D. J.; Michelsen, K.; Towle, D. K. *J. Chem. Soc., Chem. Commun.* **1987**, 1659-1660.

(42) Arulsamy, N.; Hodgson, D. J.; Glerup, J. *Inorg. Chim. Acta* **1993**, *209*, 61-69.

(43) Ardon, M.; Bino, A.; Michelsen, K.; Pedersen, E.; Thompson, R. C. *Inorg. Chem.* **1997**, *36*, 4147-4150.

(44) Restivo, R.; Palenik, G. J. *J. Chem. Soc., Dalton Trans.* **1972**, 341-344.

(45) Sofetis, A.; Raptopoulou, C. P.; Terzis, A.; Zafiropoulos, T. F. *Inorg. Chim. Acta* **2006**, *359*, 3389-3395.

(46) Glerup, J.; Goodson, P. A.; Hazell, A.; Hazell, R.; Hodgson, D. J.; McKenzie, C. J.; Michelsen, K.; Rychlewska, U.; Toftlund, H. *Inorg. Chem.* **1994**, *33*, 4105-4111.

(47) Arulsamy, N.; Goodson, P. A.; Hodgson, D. J.; Glerup, J.; Michelsen, K. *Inorg. Chim. Acta* **1994**, *216*, 21-29.

(48) Heinrichs, M. A.; Hodgson, D. J.; Michelsen, K.; Pedersen, E. *Inorg. Chem.* **1984**, *23*, 3174-3180.

(49) Hureau, C.; Blanchard, S.; Nierlich, M.; Blain, G.; Rivière, E.; Girerd, J.-J.; Anxolabéhère-Mallart, E.; Blondin, G. *Inorg. Chem.* **2004**, *43*, 4415-4426.

(50) Musso, S.; Anderegg, G.; Ruegger, H.; Schläpfer, C. W.; Gramlich, V. *Inorg. Chem.* **1995**, *34*, 3329-3338.

(51) Chang, H. R.; McCusker, J. K.; Toftlund, H.; Wilson, S. R.; Trautwein, A. X.; Winkler, H.; Hendrickson, D. N. *J. Am. Chem. Soc.* **1990**, *112*, 6814-6827.

(52) Yoon, D. C.; Lee, U.; Oh, C. E. *Bull. Korean Chem. Soc.* **2004**, *25*, 796-800.

(53) Dueland, L.; Hazell, R.; McKenzie, C. J.; Nielsen, L. P.; Toftlund, H. *J. Chem. Soc., Dalton Trans.* **2001**, 152-156.

(54) Harrington, J. M.; Oscarson, K. A.; Jones, S. B.; Reibenspies, J. H.; Bartolotti, L. J.; Hancock, R. D. *Z. Naturforsch.* **2007**, *62b*, 386-396.

(55) Hureau, C.; Groni, S.; Guillot, R.; Blondin, G.; Duboc, C.; Anxolabéhère-Mallart, E. *Inorg. Chem.* **2008**, *47*, 9238-9247.

(56) Radish, K. M.; Cornillon, J. L.; Korp, J. D.; Guilard, R. *J. Heterocycl. Chem.* **1989**, *26*, 1101-1104.

(57) Sharpless, K. B.; Townsend, J. M.; Williams, D. R. *J. Am. Chem. Soc.* **1972**, *94*, 295-296.